

**PROCESS STUDY, THE DEVELOPMENT AND
APPLICATION OF NOVEL LOW-FOULING
MEMBRANES FOR FISH PROCESSING WASTEWATER
TREATMENT THROUGH MEMBRANE BIOREACTOR
(MBR) TECHNOLOGY**

JANE NJOKI MBURU

**DOCTOR OF PHILOSOPHY
(Environmental Technology)**

**JOMO KENYATTA UNIVERSITY OF
AGRICULTURE AND TECHNOLOG**

2021

**Process Study, the Development and application of Novel Low-Fouling
Membranes for Fish Processing Wastewater Treatment through
Membrane Bioreactor (MBR) Technology**

Jane Njoki Mburu

**A Thesis Submitted in Fulfillment of the Requirements for the Degree
of Doctor of Philosophy in Environmental Technology of the Jomo
Kenyatta University of Agriculture and Technology**

2021

DECLARATION

This thesis is my original work and has not been presented for a degree in any other university.

Signature.....Date.....

Mburu, Jane Njoki

This thesis has been submitted for examination with our approval as university supervisors

Signature..........Date...06-10-2021.....

Prof. Jan. Hoinkis, PhD
Karlsruhe University of Applied Sciences, Germany

Signature.....Date.....

Dr. Paul. Njogu, PhD
JKUAT, Kenya

Signature.....Date.....

Prof. Robert Kinyua, PhD
JKUAT, Kenya

DEDICATION

This work is dedicated to my Dad, Mum and to all my brothers and sisters. Their love, support and effort throughout my studies gave me the strength to persevere and proceed even when it seemed hard.

ACKNOWLEDGEMENTS

I sincerely offer my appreciation to my supervisors; Prof. Jan Hoinkis a research scientist in the Department of Sensor Systems Technology, Faculty of Electrical Engineering and Electronics, Karlsruhe University of Applied Sciences, Germany. I am grateful for the invitation to carry out my PhD research work under his supervision in the Centre of Applied Research (CAR), Karlsruhe University of Applied Sciences, Germany. I acknowledge the valuable time he supervised and gave technical directions to see my lab work successful. I am grateful to Prof. Robert Kinyua a research scientist of Jomo Kenyatta University of Agriculture and Technology for the opportunity he offered to carry out my PhD research work under the VicInAqua project. I highly appreciate the endless effort he offered by ensuring that all the financial support I required for publication, purchase of lab reagents, conference participation, travel to Germany, upkeep, and other needs were met. I am grateful for his guidance and contributions to my research work in JKUAT – IEET Labs and for ensuring my PhD Thesis writing was successful. I give my sincere appreciation to my supervisor Dr. Paul Njogu a research scientist in the Institute of Energy and Environmental Technology (IEET) at Jomo Kenyatta University of Agriculture and Technology. His great support, technical guidance and dedication from the start of this work lead to a successful completion of this study. I appreciate his guidance, valuable suggestions, and comments he made to facilitate in the writing of my papers and my PhD Thesis. I offer my special thanks to Ephraim Gukelberger a PhD student and Talha Atiye Msc. student of Karlsruhe University, Germany for facilitating the installation of the Membrane bioreactor equipment in our JKUAT-IEET Lab and for the enormous assistance, technical support they offered as I carried out my lab work. I appreciate Dr. Saadia Ilhem Bouhadjar a researcher in the area of membrane bioreactor technology, for the support and contribution she offered at the start of my lab work at the Centre of Applied Research (CAR) at Karlsruhe University. I am grateful to Dr. Francesco Galiano and Dr. Alberto Figoli of the Institute on Membrane Technology (ITM-CNR), Italy for their contribution and guidance in the writing of my paper on the application of novel low fouling membranes. This made my publication a success. I give

my special thanks to my colleague Ms. Purity Njeru, a research scientist, and Mr. Kidego a PhD student, at the Institute of Energy and Environmental Technology (IEET) at Jomo Kenyatta University of Agriculture and Technology JKUAT for the much-needed support they offered during the period of my study. I am grateful to all the VicInAqua project team members for all the support they offered as I carried out my research work, in JKUAT and in Karlsruhe University, Germany. I express my special thanks to the VicInAqua (grant agreement number 689427) European Union's Horizon 2020 research, and innovation program for financial support to carry out my PhD thesis work. I am grateful to the Division of Research, Production and Extensions (RPE-JKUAT) for their support, and contribution to the success of this study. I appreciate my dad and mum, James Mburu, and Albin Mburu, my sisters, Judy, and Joan Mburu and my brothers, Anthony and Samuel Mburu for the moral, material and financial support they have tirelessly offered during my study period. Above all, I give thanks to the Almighty God to whom all glory belongs. This research has received funding from the European Union's Horizon 2020 research and innovation program under grant agreement number 689427 for the project VicInAqua

TABLE OF CONTENT

DECLARATION.....	ii
DEDICATION.....	iii
ACKNOWLEDGEMENTS.....	iv
TABLE OF CONTENT	vi
LIST OF TABLES	xii
LIST OF FIGURES	xiv
LIST OF PLATES	xviii
SCHEME	xix
ABBREVIATIONS AND ACRONYMS.....	xx
LIST OF APPENDICES	xx
ABSTRACT.....	xxiii
CHAPTER ONE	1
INTRODUCTION.....	1
1.1 Background to the study.....	1
1.2 Statement of problem	12
1.3 Hypothesis.....	13
1.4 Study Objectives	14

1.4.1 Main Objective	14
1.4.2 Specific objectives	14
1.5 Justification of the study	14
1.6 Research questions	15
1.7 Scope of study	15
CHAPTER TWO	17
LITERATURE REVIEW.....	17
2.1 Fish processing.....	17
2.1.1 Fish processing wastewater	17
2.1.2. Convectional wastewater treatment method	20
2.1.3. Non-convectional wastewater treatment method.....	21
2.1.4 Membrane Bioreactor (MBR) Technology.....	22
2.2 Working principles of MBR	23
2.2.1 Membranes.....	23
2.2.2 Membrane module	26
2.3 Fundamentals of membrane bioreactor (MBR) technology	30
2.3.1 Drawbacks of MBR systems.....	32
2.3.2 Theory of membrane fouling	33

2.3.3 Factors that determine severity of membrane fouling	34
2.3.4 Techniques used to control fouling in MBRs	37
2.4 Membrane surface modification techniques	40
2.4.1 Surface grafting and coating	40
2.4.2 Polymerisable bicontinuous microemulsion technique	41
2.4.3 Polymerization and initiation techniques.....	44
CHAPTER THREE	51
MATERIALS AND METHODS	51
3.1 Study Area.....	51
3.2 Sampling of raw fish processing wastewater	53
3.3 Research design.....	54
3.4 Experimental design.....	56
3.4.1 Membrane Bioreactor specifications and operations.....	56
3.4.2 Membrane Bioreactor operation	59
3.4.3 Critical flux determination.....	63
3.4.4 Analytical methods	64
3.5. Optimization of commercial PES membrane modules	66
3.6. Performance of Microdyn-Nadir and CUBE Mini Martin module.....	67

3.7 Development of low fouling PBM-oated membrane	68
3.7.1 Materials and methods	68
3.7.2 Characterization of PES and PBM- coated membranes	74
3.7.3 Comparative study of PBM-coated and commercial PES membrane modules	79
3.8 Cost analysis methodology	82
3.8.1 The cost-benefit analysis for a containerized MBR system	82
3.8.2 Calculation of CAPEX.....	84
3.8.3 Operation expenditure.....	84
3.8.4 Calculation of the total output	87
3.8.5 Comparative analysis of ASP, WSP and MBR treatment systems.....	88
CHAPTER FOUR.....	91
RESULTS AND DISCUSSIONS	91
4.1 Fish processing wastewater quality parameters	91
4.2 Process performance of PES membranes and optimization results	93
4.2.1 Rate of water permeability, flux and transmembrane Pressure	93
4.2.2 COD removal efficiency for commercial PES membrane modules	100
4.2.3 Nitrogenous compounds removal efficiency for commercial PES membrane modules	106

4.2.4 Phosphates compounds removal efficiency for commercial PES membrane modules	111
4.3 Performance of Microdyn-Nadir module and CUBE Mini module of Martin systems	114
4.3.1 Rate of water permeability, flux and transmembrane pressure	114
4.3.2 Results for comparison of COD removal efficiency for Microdyn-Nadir module and CUBE Mini module of Martin systems	117
4.3.3 Comparison of nitrogenous compounds removal in permeate for Microdyn-Nadir and CUBE Mini module	121
4.3.4 Comparison of phosphate ($\text{PO}_4^{3-}\text{-P}$) removal in permeate for Microdyn-Nadir and Cube Mini module	124
4.4 Characterization of PES and low fouling PBM- coated membranes	126
4.4.1 Chemical characterization.....	127
4.4.2 Contact angle measurement for PES and PBM membranes.....	128
4.4.3 Comparison of fouling for PES and PBM-coated membrane.....	129
4.4.4 Cross-flow water permeability for PES and PBM coated membranes.....	130
4.5 Performance of commercial PES and PBM coated membrane modules	131
4.5.1. Comparison of water permeability, flux and transmembrane pressure for PES commercial and PBM coated membrane modules	132
4.5.2 Critical flux for PBM coated membrane module and PES membrane module.	136

4.5.3 Comparison of COD removal efficiency for PES module and PBM-coated PES module	137
4.4.4 Comparison of nitrogenous compounds removal in permeate using PES and PBM coated membrane.....	142
4.5 Cost-benefit analysis for a containerized MBR system	148
4.5.1 Calculation of CAPEX.....	148
4.5.2 Calculation of OPEX	151
4.5.3 Calculation of the total output	151
4.5.4 Comparative analysis for MBR, activated sludge process and wastewater stabilization ponds	152
CHAPTER FIVE.....	155
CONCLUSIONS AND RECOMMENDATIONS.....	155
5.1 Conclusions	155
5.2 Recommendations	157
5.2 .1 Recommendations for further research.....	157
REFERENCES.....	158
APPENDICES	174

LIST OF TABLES

Table 2.1: Maximum permissible limits of water quality parameters discharge into environment and used for irrigation	19
Table 2.2: Quality guidelines for organic polymers and their properties.....	25
Table 2.3: Surface tension values for different polymeric materials	35
Table 3.1: Technical specifications for the PES membrane modules	59
Table 3.2: Operating conditions of the MBR.....	64
Table 3.3: Chemicals used for photo initiated PBM preparation.....	69
Table 3.4: Chemical composition of PBM coating solution	70
Table 3.5: MBR components and equipment specification	83
Table 3.6: MBR operational expenditure.....	86
Table 3.7: A cost model of MBR, ASP, and WSP treatment systems.....	89
Table 4.1: Fish processing wastewater quality for lab scale MBR tests for PES membrane modules	91
Table 4.2: Fish processing wastewater quality for MBR lab scale test for PES Microdyn-Nadir, and CUBE Mini modules	92
Table 4.3: Fish processing wastewater quality for MBR lab scale test for PES and PBM-coated CUBE Mini modules.....	92
Table 4.4: Comparison of water permeability for the two tested PES UF membrane modules	96

Table 4.5: Optimal operating parameters for MBR unit installed with PES/UF membrane modules	99
Tables 4.6: Comparison of COD removal efficiency in permeate for two commercial PES membranes.	102
Table 4.7: Comparison of COD removal efficiency in permeate for commercial PES membrane modules in a follow-up experiment.....	104
Table 4.8: Comparison of COD removal efficiency in permeate for Microdyn-Nadir and CUBE Mini module	119
Table 4.9: Comparison of NH ₄ ⁺ -N concentration in permeate for Microdyn-Nadir and Cube Mini module	124
Table 4.10: Comparison of PO ₄ ³⁻ - P concentration in permeate for Microdyn-Nadir and Martin Membrane module	126
Table 4.11: Comparison of contact angle measurement (CAM) for the PES and PBM coated membrane surface at t =0-8 seconds).....	129
Table 4.12: Comparison of TMP, flux and WP for PBM-coated and PES membrane module	135
Table 4.13: Comparison of COD concentration in permeate for PES module and PBM module	139
Table 4.14: Comparison of NH ₄ ⁺ -N and NO ₃ ⁻ -N in permeate for PES module and PBM module	145
Table 4.15: Total cost for MBR components and equipment	149

LIST OF FIGURES

Figure 1.2: Density evolutions around Lake Victoria Basin.....	2
Figure 2.1: A flow chart for a fish processing factory	17
Figure 2.2: Membrane filtration ranges and contaminants rejection	24
Figure 2.3: A sample of a hollow fiber membrane module structure	27
Figure 2.4: A schematic diagram of a tubular membrane module.....	28
Figure 2.5: Schematic diagram of a spiral wound membrane module.....	29
Figure 2.6: Schematic diagram of a flat sheet membrane module.....	30
Figure 2.7: Immersed membrane bioreactor	31
Figure 2.8: Side stream membrane bioreactor	31
Figure 2.9: Photo initiated reaction.....	47
Figure 2.10: Reaction of free radical species with monomer methyl methacrylate.....	47
Figure 2.11: Formation of micelles and monomer-swollen micelle	48
Figure 2.12: UV initiated PBM polymerization process	49
Figure 3.1: Map of the Lake Victoria Basin showing.....	52
Plate 3.2: Fish processing unit in Makindi fish farm	53
Plate 3.1: Sample collection point along the wastewater drainage system	53
Figure 3.2: A schematic overview of the study	55

Figure 3.3: Schematic diagram for the immersed membrane bioreactor	57
Plate 3.3: Photo of the immersed membrane bioreactor pilot plant	58
Figure 3.4: Schematic diagram for contact angle measurement	76
Figure 3.5: Schematic diagram of an auto-controlled cross-flow testing cell	78
Figure 3.6: Schematic diagram for the immersed membrane bioreactor	81
Figure 4.1: Water permeability (WP), flux and transmembrane pressure	94
Figure 4.2: WP, flux and TMP with operation time (days) in a follow-up experiment.....	97
Figure 4.3: COD removal rate during Experiment 1(start-up experiment).....	101
Figure 4.4: COD in feed, in permeate and COD removal efficiency in Experiment 1(in a follow-up experiment)	103
Figure 4.5: Comparison of HRT, F/M ratio and COD removal rate for commercial PES membrane modules	105
Figure 4.6: Comparison of concentration of NO_3^- -N and NH_4^+ -N in feed and in permeate during Experiment 1	107
Figure 4.7: Comparison of concentration of NO_3^- -N and NH_4^+ -N in the feed and in permeate in a follow-up experiment	109
Figure 4.8: Comparison of phosphate (PO_4^{3-} -P) concentration in feed and permeate during Experiment 1	111
Figure 4.9: Comparison of phosphate (PO_4^{3-} -P) concentration in feed and permeate during a follow-up experiment	113

Figure 4.10: WP, flux and TMP for Microdyn-Nadir and CUBE Mini module	115
Figure 4.11: Comparison of COD removal efficiency for Microdyn-Nadir and CUBE Mini module.....	118
Figure 4.12: Comparison of HRT, F/M ratio and COD removal efficiency for Microdyn-Nadir and CUBE Mini module	120
Figure 4.13: Comparison of NH_4^+ -N and NO_3^- -N concentration in the feed and in permeate for Microdyn-Nadir module.....	122
Figure 4.14: Comparison of NH_4^+ -N and NO_3^- -N concentration in the feed and in permeate for Cube Mini module	123
Figure 4.15: Comparison of PO_4^{3-} -P) concentration in feed and permeate for Microdyn-Nadir module and Cube Mini module.....	125
Figure 4.16: IR spectra of PES commercial and PBM-coated membrane.....	127
Figure 4.17: Color intensity deposited on PES and PBM-coated membrane after treatment with humic acid.....	130
Figure 4.18: Cross-flow water permeability for PES and PBM membranes	131
Figure 4.19: WP, flux and TMP for PES module and PBM module.....	133
Figure 4.20: Critical flux measurements for PES module and PBM module	136
Figure 4.21: Comparison of COD removal efficiency for PES module and PBM module.....	138
Figure 4.22: Comparison of HRT, F/M ratio and COD removal efficiency with operation time for PES and PBM membrane module	141

Figure 4.23: Comparison of NH_4^+ -N and NO_3^- -N in the feed and in permeate for the PES module 143

Figure 4.24: Comparison of NH_4^+ -N and NO_3^- -N in the feed and in permeate for the PBM-coated module 144

Figure 4.25: Comparison of PO_4^{3-} -P concentration in the feed and in permeate for PES and PBM-coated membrane modules 147

Figure 4.26: Correlation of CAPEX for ASP, WSP and MBR treatment systems with similar flow capacity 153

Figure 4.27: Correlation of OPEX for ASP, WS and MBR treatment systems with similar flow capacity (treatment volume)..... 154

LIST OF PLATES

Plate 1.1: Invasion of water hyacinth plant along shores of Lake Victoria.....	6
Plate 1.2: Parts of Lake Victoria covered by aquatic vegetation	7
Plate 1.3: Lake Victoria.....	6
Plate 1.4: Trickling filter in Kisumu wastewater treatment plant	9
Plate 1.5: Wastewater stabilization ponds at Nyalenda in Kisumu.....	9
Plate 3.1: Sample collection point along the wastewater drainage system	58
Plate 3.2: Fish processing plant in Makindi fish farm.....	61
Plate 3.3: Photo of the immersed membrane bioreactor (iMBR) pilot plant	67
Plate 3.4: Preparation process for PBM microemulsion	83
Plate 3.5: Photo of membrane casting chamber	84
Plate 3.6: Coating of membrane and irradiated with UV light.....	73
Plate 3.7: Measurement of contact angel for PES and PBM membrane surface	73
Plate 3.8: Schematic diagram of the cross-flow testing cell	91

SCHEME

Scheme 6.1: Acryloyloxyundecyltriethylammonium bromide	43
---	----

LIST OF APPENDICES

Appendix I: Water Quality At The Vicinaqua Pilot Plant 174

ABBREVIATIONS AND ACRONYMS

APHA:	American Public Health Association
ASP:	Activated Sludge Process
BOD:	Biochemical oxygen Demand
BOD₅:	Five days Biochemical oxygen Demand
COD:	Chemical Oxygen Demand
DAFLD:	Department of Agriculture, Fisheries and Livestock Development
RAS:	Recirculating Aquaculture Systems (RAS)
EMCA:	Environmental Management and Coordination Act
EPA:	Environmental Protection Agency
EU:	European Union
GDP:	Gross Domestic Product
IUPAC:	International Union of Pure and Applied Chemistry
JICA:	Japan International Cooperation Agency
LVBC:	Lake Victoria Basin Commission
LVEMP:	Lake Victoria Environmental Management Program
KIWASCO:	Kisumu Water and Sewerage Company
MoH:	Ministry of Health

MWCO:	Molecular Weight Cut Off
MoWI:	Ministry of Water and Irrigation
N.E.P:	National Environment Policy
NGV:	No guideline value
NTDAs:	National Trans-boundary Diagnostic Analysis
UNEP:	United Nations Environment Programme
WSBs:	Water Services Boards
WASREB:	Water Services Regulatory Board
WSP:	Water service provider
WHO:	World Health Organization

ABSTRACT

Management of wastewater from industries is a challenge in many urban centers in developing countries due to scarcity of space as lagoons and maturation ponds (with large footprint) are largely used for wastewater treatment. A typical example is Kisumu City, a major fish source to the Kenya economy and a host of fish processing companies. The sewerage system coverage in the city is poor with most of the industries lacking proper connection. The fish processing industries are intensive consumers of high volumes of clean water and later release huge amounts of wastewater (effluent) on daily basis. Most of these industries lack proper wastewater treatment facilities and discharge effluent on open drainage systems. The huge investment required to construct proper wastewater treatment facilities is a challenge that fish industries have to overcome. In view of the high land prices and scarcity of space in urban centers, the need to install wastewater treatment facilities that are cost effective, efficient and of low footprint has been realized. In the present work, application of membrane bioreactor (MBR) technology for treatment of fish processing wastewater in fish industries was studied. The study investigated the efficiency of commercial polyethersulfone (PES) membrane, the development and application of novel low-fouling membrane for treatment of fish processing wastewater through MBR Technology. The physicochemical parameters of fish processing wastewater were determined. Process optimization for the performance of commercial UF/PES membrane modules was done at a laboratory scale in JKUAT using the immersed membrane bioreactor (iMBR) unit. A novel low fouling membrane was developed through surface modification of commercial PES membrane via the polymerizable bicontinuous microemulsion (PBM) technique. Tests for the fouling characteristics of commercial UF/PES membrane and PBM-coated membrane were done using the automated cross-flow testing cell and the lab-scale MBR unit. The cost-benefit for a containerized MBR system was determined. The studied UF/PES membrane modules showed good performance for water permeability during pilot testing but were found to be susceptible to fouling. A novel low-fouling membrane was successfully developed through a successful coating process. This was demonstrated using IR spectrums that confirmed the presence of PBM coating and, by the low contact angle (CA) of $31.6 \pm 2.2^\circ$ - $34.1 \pm 2.8^\circ$ thus indicating that hydrophilic property was achieved for the modified membrane. The PBM-coated module showed improved ability to resist fouling with no critical flux achieved at TMP of up to 340mbar relative to the PES module whose critical flux was observed at $7.3 \text{L/m}^2 \cdot \text{h}$ with TMP of 230mbar. PBM module had higher removal efficiency for COD, (NO_3^- -N and NH_4^+ -N) and PO_4^{3-} -P in the range of $96 \pm 1\%$, $88 \pm 1\%$, and $84 \pm 1\%$ in comparison to $92 \pm 2\%$, $80 \pm 3\%$, and $64 \pm 1\%$ for the PES module respectively with mean values significantly different ($t_{\text{observed}} > t_{\text{critical}}$) for paired T-test (at 95 % confidence level). The MBR system had a cost benefit of 82.8% per m^3 of treated water. The correlation cost curves demonstrated that, small-scale MBR systems with a volume flow of $10 \text{m}^3/\text{d}$ to $30 \text{m}^3/\text{d}$ are cost-effective in terms of capital expenditure (CAPEX) in comparison to activated sludge process (ASP) systems, where investment cost is driven higher by the cost of land and site redesign requirements. However, MBR systems have high operation expenditure (OPEX) due to the high energy requirements. Nonetheless, MBR systems encourage the reuse of high-quality treated water (for washing, irrigation etc.) which

makes them economical during the course of the plant life. In conclusion, the analysis showed that small-scale MBR containerized systems could become an economic solution for small industries, (such as fish processing industries) in the urban centers in Kenya, where land scarcity and high costs are a major challenge.

CHAPTER ONE

INTRODUCTION

1.1 Background to the study

Lake Victoria is a trans-boundary resource situated in East Africa, mainly between Kenya, Uganda, and Tanzania with a catchment area that extends to Rwanda and Burundi (Kevin *et al.*, 2015). It is the largest tropical lake and the world's second largest freshwater lake covering a surface area of approximately 68,800 square kilometers (Awange *et al.*, 2019). The Lake has a maximum depth ranging between 80-84meters and an average depth of 40meters (Inne *et al.*, 2018). It has a volume of about 2,760 cubic kilometers of water and serves as a major reservoir for water supply for domestic, commercial, and industrial use (Awangea *et al.*, 2019). The Lake's basin has the largest freshwater inland fisheries in Africa that yields over 1million metric tonnes per annum worth over the US 590 million dollars annually (Kolding *et al.*, 2014). The lake receives its water supply from the rain, several rivers, and streams while River Nile is its main outlet (LVBC, 2017). The map of the lake is presented in Figure 1.1.

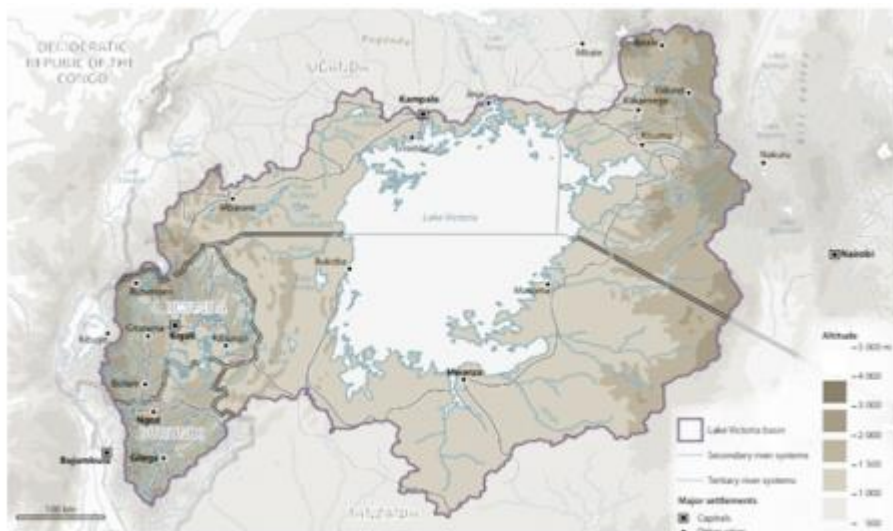


Figure 1.1: Map of the Lake Victoria Basin showing secondary and tertiary river systems (Lake Victoria Basin Commission, 2017)

The Lake Victoria basin constitutes a wide range of biodiversity-rich in fisheries, good agricultural soils, minerals, forests and wildlife resources (Dauglas *et al.*, 2014). As a result, the shores and its watersheds are a major attraction to human settlement and a host for over 40 million people living in the urban and peri-urban centers and with a high population growth rate of about 3.5% per year (Awangea *et al.*, 2019). Figure 1.2 presents the density evolution around the surrounding areas of Lake Victoria basin from 1960 to 2015 (LVBC, 2017).

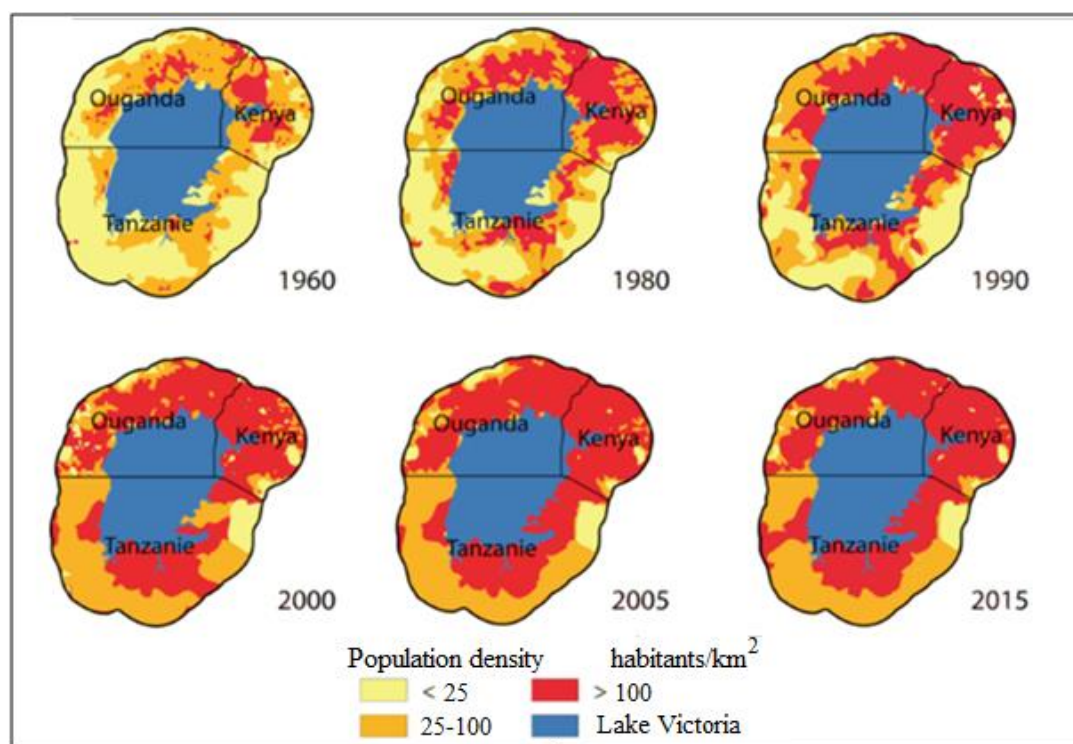


Figure 1.2: Density evolutions around Lake Victoria Basin (Source: Lake Victoria Basin Commission, 2017)

The various social-economic activities in the Lake Victoria basin include agricultural production, fisheries, industrialization, regional trade, wildlife, and tourism management (Yanda, 2015). However, fisheries are the main source of livelihood both for a domestic and commercial purpose within the Lake region (Kolding *et al.*, 2014). The fish farming and processing sector have directly or indirectly employed over 500,000 people within the Lake region (Tim *et al.*, 2015). Agricultural production is

generally carried out for food security and income generation (Awangea *et al.*, 2019). Food crops commonly grown include maize, wheat, millet, sorghum, groundnuts, beans, and vegetables among others (Sayer *et al.*, 2018). Major cash crops are sugar canes, coffee, cotton and pyrethrum (Yanda, 2015). Small and medium scale irrigation schemes within the lake basin are common practice (Kevin *et al.*, 2015). The pastoralist communities within the basin region mainly depend on livestock keeping (Charles *et al.*, 2011).

The Lake has attracted much attention in recent years following severe ecological changes observed in the last 3 decades triggered by the declining quality of its waters (Matindi *et al.*, 2014). A study conducted on water quality for Lake Victoria showed an increase of nitrate-nitrogen (NO_3^- -N) and soluble phosphorus (P-PO_4^{3-}) from (10 $\mu\text{g/L}$ to 98 $\mu\text{g/L}$) and from (4 $\mu\text{g/L}$ to 57 $\mu\text{g/L}$) respectively for data collected in a period of 20 years (Dauglas *et al.*, 2014). These findings confirmed continued nutrients loading as a major cause of increased eutrophication of the Lake (Salome & Samwel, 2018). In the present years, the problem has been aggravated by increasing deforestation, urbanization and industrialization among other factors (Martin *et al.*, 2016). In Kenya for example, there has been extensive destruction of the Mau Forest which is the main source of Sondu and Mara Rivers (Aloyce *et al.*, 2018). The catchment areas have been subjected to over-cultivation on steep slopes while wetlands have been used as grazing fields (Gichuru *et al.*, 2017). This has exposed the land to soil erosion and progressive enrichment of the lake with nutrients (Gichuru *et al.*, 2017).

The informal settlements in the city of Kisumu for example, are largely characterized by poverty, high population, poorly planned infrastructure and lack basic sanitation facilities (Martin *et al.*, 2016). In most cases, wastewater from pit latrines and septic tanks, agricultural runoff, storm-water, urban municipal sewerage, and industrial effluent get improperly disposed off to the Lake without any treatment (Rodrick *et al.*, 2017). Several industries that include manufacturing industries, sugarcane factories, fish factories, leather, and paper mill have for a long time contributed directly to the rising pollution caused by discharge of raw effluent to the Lake through open drainage systems (Kabenge *et al.*, 2016).

According to an audit conducted on waste generation for the fish processing industries along the Lake Victoria, an annual wastewater generation of 1,838,000 m³ was estimated (Robert *et al.*, 2018). Further, the fish processing wastewater generated from the fish industries was found to have high chemical oxygen demand (COD) of 12,400 mg/l with high nutrient content of about 20 mg/l of total phosphorous, 61 mg/l of ammonia nitrogen and 340 mg/l organic nitrogen (Robert *et al.*, 2018). The fish industries were mainly in urban centers and with limited land area for construction of wastewater management systems (Matindi *et al.*, 2014). The wastewater was largely managed using small sized waste stabilization ponds or by use of wetlands (Hongtao *et al.*, 2014). These types of wastewater management systems were found to be neither efficient nor profitable options (Robert *et al.*, 2018). According to the report, the annual nutrient load from industries to the Lake Victoria was estimated at 5,606 tones per year of BOD, 414 tones per year of total nitrogen and 342 tones per year of total phosphates (LVEMP, 2017). Discharge from fish industries was considered as a point source for nutrient generation. Consequently, it has been recommended that nutrient loading into the Lake be controlled by reducing discharge of raw effluent to the Lake (LVEMP, 2017).

Increasing eutrophic conditions in Lake Victoria is largely attributed to the growth and flourishing of water hyacinth plant (*Eichhornia crassipes*) and the spread of other aquatic weeds (Gidudu *et al.*, 2018). In the present time, large parts of the Lake are heavily covered by the invasive water hyacinth plant (Kabenge *et al.*, 2016). Plate 1.1 presents a photo of the aquatic plant floating along the shores of Lake Victoria.



Plate 1.1: Invasion of water hyacinth plant along shores of Lake Victoria

As was reported in previous study, the invasive alien aquatic species was first introduced in Lake Victoria in the 1990s and quickly flourished with increased nutrients levels (Gidudu *et al.*, 2018). This was confirmed through a comparison of moderate resolution imaging spectroradiometer (MODIS) images collected between 2000 and 2015 (Gidudu *et al.*, 2018). The findings showed that a mean area of 543.12 square kilometers was covered with aquatic vegetation in 2007 and increased throughout the years with the highest value noted at 6,357.31 square kilometers in April 2010 (Gidudu *et al.*, 2018; Cheruiyot *et al.*, 2014). Plate 1.2 represents a satellite image of aquatic vegetation (illustrated as green areas) covering the Lake Victoria while the light green part represents the area covered with dense aquatic vegetation.

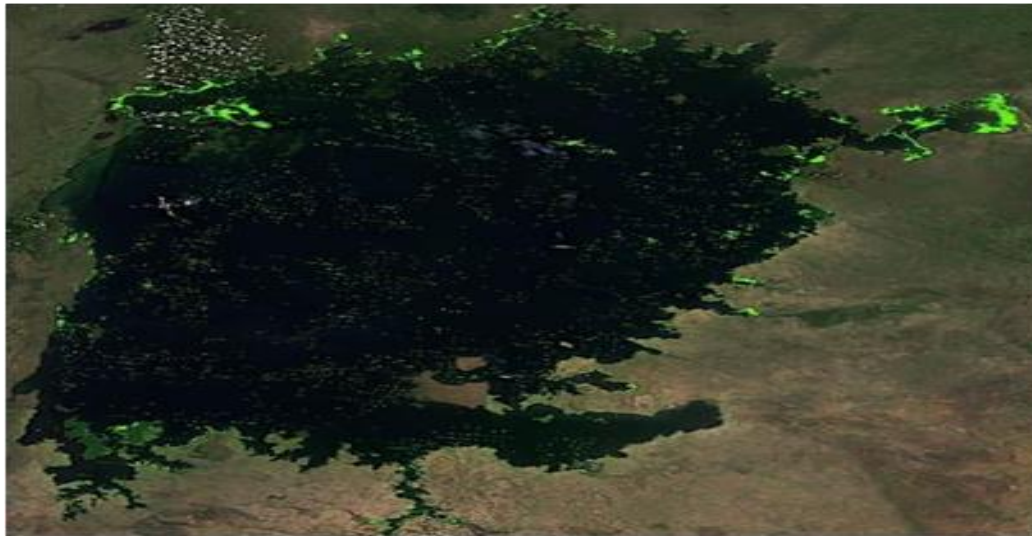


Plate 1.2: Parts of Lake Victoria covered by aquatic vegetation (Cheruiyot *et al.*, 2014)

Plate 1.3 represents a recent satellite image of Lake Victoria.

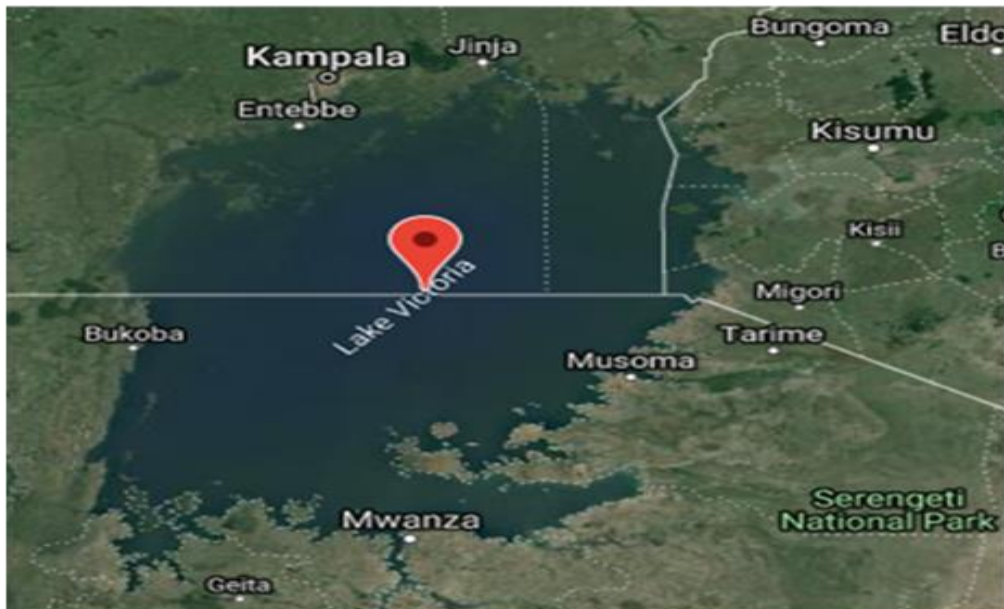


Plate 1.3: Lake Victoria (Satellite image retrieved, 21-12-2019)

The infestation of aquatic vegetation in Lake Victoria has serious environmental and socioeconomic impacts attributed to anoxic conditions, fish kills, obstruction of transport for fishing boats and difficulties in fishing (Tim *et al.*, 2015). In the early

1990s, fish industry in Kenya was doing well with about 15 fully functional fish processing plants mostly located in Kisumu (Kevin *et al.*, 2015). In the present time, most of the industries have closed down with only about three remaining and with insufficient resource to sustain their operations (Gichuru *et al.*, 2017).

An early effort made to control rapid growth and spread of water hyacinth in Lake Victoria was by the use of hands (manual method) (Sayer *et al.*, 2018). However, the weed grew at a high rate and the manual method was not effectively sufficient (David *et al.*, 2015). Other measures put in place were biological and mechanical methods (David *et al.*, 2015). In biological methods, insects were introduced to the Lake to feed on the aquatic weed while in mechanical methods, large harvesting and chopping boats were introduced to harvest the weed for use as fertilizer and for production of biogas (Goyal & Ananthakrishnan, 2013; Njogu *et al.*, 2014). Presently, programs worth millions of dollars have been implemented in eradication and control of water hyacinth in Lake Victoria without sustainable results (Sayer *et al.*, 2018). This calls for a change of method from eradication to having a new focus on sustainable utilization of the lake's resource (Awangea *et al.*, 2019).

The Kenya Government is making effort towards management of the Lake Victoria ecosystem. This is mainly by creating public awareness and participation in the implementation of national environmental policies for sustainable management of the environment and natural resources (NEP, 2013). This has been achieved through the Ministry of Environment, Water and Natural resources. As stipulated in Section 3.1 (c) of the National Environment Policy 2013, one of their objectives is to protect terrestrial and aquatic ecosystems by ensuring sustainable management of the environment and natural resources thus promote national economic growth and improved livelihoods (NEP, 2013).

Proper disposal of wastewater remains a challenge in Kenya's densely populated urban settlements that mostly lack coverage of sewerage systems with the existing ones poorly maintained and unable to serve the growing population (Paul *et al.*, 2011; Rodrick *et al.*, 2017). In Kisumu, for example, the Kisumu wastewater treatment plant operated by the Kisumu Water and Sanitation Company (KIWASCO) is responsible

for water supply and sanitation. The plant sewer lines were constructed between the years 1965 to 1985 to serve a smaller town with a population of fewer than 968,909 persons (LVEMP, 2017). Since then, the population has dramatically increased in the last 2 decades to over 1,145,747 persons, according to the 2017 population and housing Census. Consequently, it is approximated that only 26% of the city has sewerage system connection (LVEMP, 2017). KIWASCO mainly uses trickling filters and stabilization ponds for the treatment of wastewater. The sewerage treatment system has a design capacity of approximately 17800m³ when operating in full capacity against a total dairy inlet volume flow of about 34000m³, but is currently operating at a lower capacity with about 4000m³-5000m³ per day (LVEMP, 2017). This capacity is low and does not fully meet the demand for water and sanitation services in the region (Hongtao *et al.*, 2014). The facility is however earmarked for expansion to enable it to cover a wider part of Kisumu (LVEMP, 2017). Further Nyalenda Sewage treatment lagoons are in constant rehabilitation and are also used for the treatment of sewage before discharging to the Lake (Ibrahim *et al.*, 2015). Nonetheless, lagoons or pond treatment systems have limited performance in terms of low pathogen removal efficiency. They are used for treatment of wastewater only to some extent before releasing it to the Lake (Charles *et al.*, 2014). Plates 1.4 and 1.5 illustrate a trickling filter at Kisumu wastewater treatment plant (KIWASCO) and Nyalenda Sewage treatment lagoons.



Plate 1.4: Trickling filter in Kisumu wastewater treatment plant (KIWASCO)



Plate 1.5: Wastewater stabilization ponds at Nyalenda in Kisumu

Fish processing industries in Kisumu are a major consumer of water and release huge amounts of wastewater on daily bases (Gichuru *et al.*, 2017). However, the existing sewerage and wastewater treatment facilities in Kisumu are overloaded and cannot therefore effectively serve the industries (Kevin *et al.*, 2015). This has resulted in cases of sewage overflows and open drainage systems that drain raw effluent from industrial discharge into the Lake without proper treatment (LVEMP, 2017). In response to this

menace, the government through NEMA has prompted to closing down several fish processing industries for lack of proper wastewater treatment facilities and for noncompliance with the water quality standards for discharge in aquatic environment as set out in the third schedule of EMCA (Water Quality) regulations, 2006 (EMCA, 2006). Section 74 (2) of the Environmental Management and Co-ordination Act EMCA (1999) stipulates that: “The owner of a trade or an industrial undertaking shall be granted a license to discharge effluent into the environment upon installation of an appropriate treatment plant for its resultant effluent” (EMCA, 1999).

Stabilization ponds are commonly used in Kenya for the treatment of wastewater (Ramadan & Ponce, 2016). These are natural wastewater treatment reservoirs with cheap construction, low energy demand and low operation costs (Eckenfelder *et al.*, 2014). However, the technology has low pathogen removal efficiency and requires large land areas for constructing ponds which is expensive and not readily available in urban areas thus results in high capital costs (Hongtao *et al.*, 2014). Membrane bioreactor (MBR) technology is an immersing wastewater treatment technique with a small footprint (requires less space for installation) and could become a potential immediate solution if adopted by fish processing industries in Kenya’s urban centers (Luong *et al.*, 2016). Small-scale containerized MBR equipment requires less space and can be installed as an indoor facility in tandem to the production line for treatment of wastewater and reuse in fish processing industries with no need for sedimentation or clarification tanks (Galiano *et al.*, 2015).

Membrane bioreactor (MBR) technology is a more recent technological innovation that combines the use of an activated sludge (ASP) process for biological treatment of wastewater and a filtration process for separation of the treated effluent from the biomass (Saadia *et al.*, 2015). The technology has presently been adopted for treatment of various wastewaters in several countries of the Middle East, North Africa and Europe (Tan *et al.*, 2016). It has become a method of choice over the activated sludge process (ASP) commonly used in African countries mainly because of its small footprint and better quality effluent (Tan *et al.*, 2016).

As discussed in the literature review of the past studies MBR technology was first developed as a side stream system in the late 1960s by the author Dorr-Oliver (Deowan *et al.*, 2013). However, the Dorr-Oliver system had major drawbacks and process limitations that included high energy demand required to attain high fluxes, membrane fouling problems and high cost of operation attributed to the cost of membranes (Bouhadjar *et al.*, 2016). Nonetheless, the technology obtained its breakthrough in 1989 when Yamamoto and coworkers developed the MBR system with membranes directly submerged in the bioreactor (Deowan *et al.*, 2013). The system had lower energy demand and better resistance for fouling attributed to a coarse bubble aeration system that produced cross flow current thus limit fouling (Deowan *et al.*, 2013). The submerged MBR system was therefore accepted and has now been adopted in many countries for treatment and reuse of domestic and industrial wastewaters (Saadia *et al.*, 2015; Tan *et al.*, 2016).

According to a study carried out to test the efficiency of a submerged MBR system used for treatment of model textile dye wastewater, a COD removal efficiency of 95% to 97% was obtained (Deowan *et al.*, 2013). The study used commercial flat sheet membrane modules submerged in an aerated reactor tank of the MBR unit. A similar study was conducted on treatment of textile dye wastewater using a tubular membrane module (pore size 0.4 μm) immersed in a 60 L aerated reactor tank. The results showed COD removal efficiency ranging between 89% to 94% and therefore confirmed again the ability of MBR systems to produce effluent of high-quality (Deowan *et al.*, 2016). The MBR technology is, therefore an effective method with the potential to become an alternative technique for wastewater treatment in the present and future industries (Tan *et al.*, 2016). The technology has however not been tested or adapted for use in fish processing industries in any country and is yet to be implemented as an alternative method for treatment and reuse of fish processing wastewater.

The diverse application of MBR technology for wastewater treatment is however challenged by membrane fouling problem that has for a long time limited its use (Bokhary *et al.*, 2018). According to the definition given by the International Union of Pure and Applied Chemistry (IUPAC), membrane fouling is the process that leads to loss of performance as solutes or suspended particles are deposited on the surface or

into the pores of the membrane during filtration process (Oliver *et al.*, 2016). These may occur as reversible or irreversible depending on the physical and chemical interactions that occur between the foulants on the surface of the membrane (Iorhemen *et al.*, 2016).

Irreversible membrane fouling is caused by adsorption of foulants in the membrane pores and is mainly responsible for severe fouling of membranes. Severe fouling of membranes leads to flux losses and eventually affects the system's efficiency (Saadia *et al.*, 2015). When chemical cleaning does not help to regain the flux, membranes have to be replaced frequently. This makes the technology expensive as the cost of membrane replacement may account for approximately 30–50% of the operational expenditure (Deowan *et al.*, 2016). The need to mitigate severe fouling of the membranes is thus realized for the purpose of making the technology commercially viable for field application (Galiano *et al.*, 2015).

In recent studies, researchers have come up with membrane modification techniques that help to improve on surface properties of the membranes thus overcome fouling problems. Galiano *et al.*, (2018) conducted a study on preparation of a novel antifouling coating material used for surface modification of commercial membranes. The study was carried out in the Institute of Membrane Technology (ITM), Italy within an EU funded project BioNexGen (BioNexGen, 2010). The coating material was used for modifying an ultrafiltration (UF) commercial membrane that was then tested for the first time in the aerobic membrane bioreactor (MBR) using artificial model textile dye wastewater (Deowan *et al.*, 2016). The performance of the modified membranes was compared with that of unmodified commercial membranes. The results showed a significant improvement in fouling resistance ability for the modified membrane as compared to the commercial membrane that was not modified (Galiano *et al.*, 2018).

1.2 Statement of problem

The City of Kisumu is one of the most industrialized cities in the Lake Victoria basin and hosts many industries that specialize in fish processing and exporters. Most of these industries are however intensive consumers of freshwater with inadequate facilities for wastewater treatment and reuse. The sewerage system coverage in

Kisumu is low with only 26% of the population living within areas connected to the sewer lines. The existing sewerage system has a designed capacity of approximately 17,800m³ but currently receives over 34,000m³ of sewerage generated from industrial effluent, domestic sewage and other sources connected to the sewer lines. The system is overloaded and is characterized by over flow of sewage through open drainage systems that discharge huge amounts into the Lake. Subsequently the effluent suffers from incomplete removal of contaminants during treatment process and is a major cause of pollution and eutrophication of the Lake's waters. The impact has been infestation and rapid growth of water hyacinth and other invasive aquatic species that cause anoxic conditions. This has led to poor quality of water and loss of aquatic life. The Kenya Government has however laid plans for expansion of the Kisumu sewerage system along with rehabilitation of Nyalenda lagoons and construction of artificial wetlands that will increase the capacity of the wastewater treatment systems. Alongside the already proposed solutions, this study proposes the introduction of membrane bioreactor (MBR) technology as an innovative alternative technology for treatment of fish processing wastewater by fish industries. These will in return alleviate the strain on the already overloaded sewerage system and contribute in mitigating serious environmental and socio-economic impacts resulting from pollution and eutrophication of the lake's waters. However, MBRs though efficient are prone to membrane fouling problems. Due to the fouling problem this technology has not been adopted for use in the treatment of fish processing wastewater. There is, therefore, a need to develop low fouling membrane modules for effective implementation of MBR technology for treatment of fish processing wastewater.

1.3 Hypothesis

1. There is no significant difference in removal efficiency of COD, NO₃⁻-N , NH₄⁺-N and PO₄³⁻-P between polyethersulfone (PES) and polymerizable bicontinuous microemulsion (PBM)-coated membrane modules immersed in Membrane Bioreactor (iMBR) for treatment of fish processing wastewater
2. A change of membrane module construction design does not improve resistance to fouling during fish processing wastewater treatment in iMBR

3. There is no significant difference between fouling characteristics of PES and PBM-coated membrane
4. The use of MBR technology is not economically viable for fish processing industries in urban centers

1.4 Study Objectives

1.4.1 Main Objective

To determine the efficiency of commercial flat ultrafiltration polyethersulfone (UF/PES) membrane and comparison with modified novel low-fouling membrane for fish processing wastewater treatment through Membrane Bioreactor (MBR) Technology, and determination of the cost efficiency of a containerized system.

1.4.2 Specific objectives

1. To determine the physicochemical parameters of fish processing wastewater
2. To optimize the performance of commercial UF/PES membrane modules immersed in Membrane Bioreactor (iMBR) for treatment of fish processing wastewater
3. To determine the improved resistance to fouling for UF/PES membrane when fitted in Microdyn-Nadir, and CUBE Mini modules of different construction design for treatment of fisheries wastewater
4. To modify commercial UF/PES membrane through biocontinuous microemulsion polymerization technique and test the fouling characteristics when used for treatment of fish processing wastewater
5. To conduct a cost-benefit and comparative analysis of a containerized MBR system for treatment of fish processing wastewater

1.5 Justification of the study

Improper management of wastewater in fish processing industries have largely been attributed to continued pollution and eutrophication of natural water resources and, hygiene and sanitation issues. The problem is mainly attributed to lack of proper effluent treatment plants due to the huge investment that would be required for their

construction. Consequently, with an increasing demand for cost effective wastewater treatment plant and with raising scarcity of space in urban settlements, the need to introduce Membrane bioreactor (MBR) treatment systems with small foot print and at a manageable cost has been realized. Membrane bioreactor (MBR) technology is considered a promising and useful technique for treatment and reuse of various industrial wastewaters. The technique requires minimum space for installation (no need for sedimentation and clarification tanks), offers high quality effluent and has attractive investment life cycle cost. However, despite the advantages that come along with MBR technology, it has not been tested or used for the treatment of fish processing wastewater in any country. The main obstacle to the implementation of MBR technology is membrane fouling problem. Severe fouling of membranes leads to flux losses and frequent replacement makes the technology expensive. This presents the need to develop low fouling membranes that can be used for a longer time thus make MBR technology more commercially viable.

1.6 Research questions

1. What is the quality of wastewater used for the lab-scale membrane bioreactor (MBR) experiments?
2. What procedure offers optimal conditions for treatment of fish processing wastewater in membrane bioreactor (MBR) treatment system using immersed commercial flat ultra filtration Polyethersulfone (UF/PES) membranes?
3. What are the effects on improved resistance to fouling when using Microdyn-Nadir and Martin membrane modules of different construction design but made of the same UF/PES material?
4. What are the significant differences between the fouling characteristics and hydrophilic surface properties of PES and PBM-coated membrane?
5. What is the economic viability for a containerized MBR system used for treatment of wastewater in fish processing industries in urban centers?

1.7 Scope of study

The study investigated on treatment of fish processing wastewater using Membrane Bioreactor (MBR) only. Not all types of treatment systems were studied. A novel low

fouling membrane was developed through a polymerizable bicontinuous microemulsion (PBM) technique for surface modification of commercial PES membrane only. Fouling characteristics for PES and PBM-coated membranes were determined at lab-scale only and by use of fish processing wastewater of high strength only. The cost benefit analysis was conducted for a containerized MBR treatment system with a volume flow capacity of $10\text{m}^3/\text{d}$ only. The comparative analysis was conducted for ASP, WSP and MBR treatment systems only, all with similar flow capacity of $(10-100\text{ m}^3/\text{d})$.

CHAPTER TWO

LITERATURE REVIEW

2.1 Fish processing

Fish is a highly nutritious food and an important source of protein (Muthukumaran & Baskaran, 2013). It is however highly perishable and needs to be processed to deliver to the market safely and in fresh condition (Fábio & Liliana, 2019). Fish processing, therefore, refers to the preparation of fish right from the time it is harvested to the time the final product is delivered to the market for human consumption (Tim *et al.*, 2015). This entails loading and handling of raw material (fish), primary and secondary processing, consumer packaging and storage. An adequate supply of water is required for use during processing and for cleaning storage tanks and sinks and other working space (Rodrick *et al.*, 2017). In the Lake Victoria region, fish processing industries specialize in the production of freshwater fish (Kolding *et al.*, 2014). Figure 2.1 illustrates a flow chart for a fish processing factory.

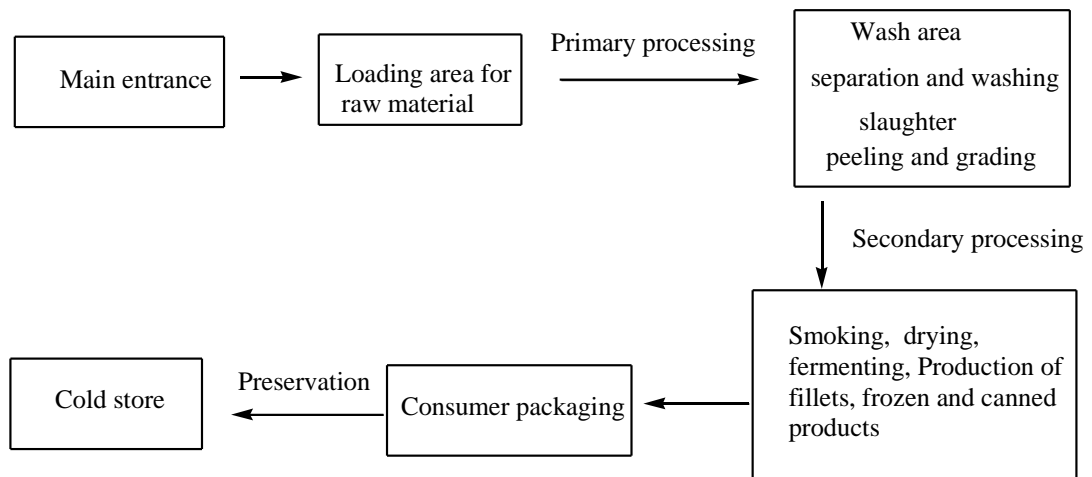


Figure 2.1: A flow chart for a fish processing factory

2.1.1 Fish processing wastewater

Fish processing industries utilize high volumes of water and equally release huge amounts of wastewater (effluent) characterized by high organic load received from the various production stages (Fábio & Liliana, 2019). This may constitute a mixture of

blood waste from fish storage tanks, solid waste from fish slaughter, nutrients, fats and oil waste (Muthukumaran & Baskaran, 2013). Depending on the effluent strength and the period of continuous discharge, it may cause serious pollution problems and therefore requires biological treatment before releasing to natural water bodies (Rahayu & Hady, 2018). As stipulated in Part III of the Environmental Management and Coordination Act, (EMCA) (Waste Management) Regulations 2006, 17(1) “it is the obligation of any trade or industrial sector to install at its premises anti-pollution technology for treatment of resultant waste generated from the various trade or industrial activities” Table 2.1 illustrates the standards and quality guidelines for effluent discharge into aquatic environment and water used for irrigation purpose as set out in the 3rd and 8th schedule to (water quality) regulations, 2006 (EMCA, 2006) and by the world health organization (WHO, 2006).

Table 2.1: Maximum permissible limits of water quality parameters discharge into environment and used for irrigation

Water quality parameters	Maximum permissible limit	Organization	
		Treated effluent in discharge environment	Water for irrigation
Total nitrogen (mg/L)	100	NGV	EMCA
Ammonia Nitrogen (mg/L)	NGV	<5	WHO
Nitrates (mg/L)	NGV	5-30	EMCA
Phosphorus (mg/L)	≤5	≤5	WHO
pH	6-9	6.9-8.5	EMCA
Biological Demand (mg/L)	Oxygen 30	< 30	EMCA/WHO
Chemical Demand (mg/L)	Oxygen 50	100	EMCA/WHO
Total Suspended Solids, (mg/L)	30	150	EMCA/WHO
Total Dissolved solids (mg/L)	1200	1200	EMCA
Oil and grease	Nil	NGV	EMCA
Phenols (mg/L)	0.001	NGV	EMCA

Source: (WHO, 2006) and (EMCA, 2006)

Where NGV means no guideline value and, where standard values are given as daily average discharge values.

Fish industries face challenges related to hygiene and sanitation issues mainly because of inadequate and inefficient methods used for handling and disposal of wastewater (Rodrick *et al.*, 2017). In most cases, they lack proper wastewater treatment facilities due to the high investment costs required for construction and land requirements, which is a challenge for most industries in developing and middle-income countries in Africa (Hongtao *et al.*, 2014). The various techniques used for the treatment of fish processing industrial effluent include biological treatment methods (conventional and non-convectional) and physical-chemical treatment processes (Mara, 2013).

2.1.2. Convectional wastewater treatment method

Convectional wastewater treatment method entails the use of preliminary, primary(physical), secondary (biological) and tertiary (chemical) treatment processes (Ugya & Fidelis, 2016). During preliminary treatment, screening is conducted to remove big debris from the wastewater (Hongtao *et al.*, 2014). Primary or physical treatment process entails the removal of floating matter, small particles, and medium-sized particles by trapping them in screens (Mara, 2013). Sedimentation process further removes settling suspended solids from the wastewater through the action of gravity thus generating primary sludge (Geoffrey, 2015).

Secondary treatment is a biological treatment process that uses a bacteria-rich activated sludge (bacterial floc) to remove dissolved organic matter from wastewater (Muthukumaran & Baskaran, 2013). In this process, primary wastewater is mixed with bacteria-rich activated sludge and air is injected into the mixed liquor contained in the aeration tank (Eckenfelder *et al.*, 2014). Aerobic microorganisms in the aeration tank assimilate or breakdown organic impurities and convert them into carbon dioxide, water and biomass (Corominas *et al.*, 2013). The resulting effluent is drained into a secondary clarifier where a gravity settling process separates biological sludge from the clear treated water (Iffat *et al.*, 2015). The resulting clear effluent goes through to clarification tanks as some bacteria-rich activated sludge gets back to the secondary treatment tank all over again. The tertiary treatment process is conducted in a clarification tank through chemical treatment, ozonolysis or ultraviolet radiation to disinfect the water (Ugya & Fidelis, 2016). Generally, the conventional wastewater treatment method has low energy demand, low operating and maintenance cost. However, the system requires huge areas of land for constructing ponds and takes long periods of time to complete the treatment process. This makes it inappropriate for application in urban areas where land is scarce and expensive. Despite the limitations, this technology is commonly used in developing countries for the treatment of sewage and industrial effluent (Hongtao *et al.*, 2014).

2.1.3. Non-convectonal wastewater treatment method

Non-conventional treatment methods are decentralized wastewater treatment systems mainly of low cost and preferably used in urban and peri-urban areas due to their affordability (Ronald, 2018). Such facilities include the use of trickling filters, waste stabilization ponds (lagoons), septic tanks, constructed wetlands, and sand filters among others (Neena & Lekha, 2013). Trickling filters are fixed film systems made of plastic medium or fixed bed of rocks (covered with bacteria-rich biofilm) (Carolynne et al., 2020). In these systems, wastewater is spread and passes through filters where microbes decompose organic waste under aerobic conditions to release water, carbon dioxide and biomass (Iffat *et al.*, 2015). The effluent from trickling filters requires further treatment in a sedimentation tank and clarification tank to reduce BOD and pathogen to an acceptable level before discharge to the environment.

Sand filters are equally useful for the primary treatment of wastewater (Neena & Lekha, 2013). These are shallow beds filled with sand and fitted with pipes for the distribution of wastewater and have a depth of approximately 0.6 to 1.1m (Halis *et al.*, 2013). The wastewater passes through the sand layers to the bottom of the filtering bed where treated effluent is collected through drainage pipes. The systems treat wastewater through filtration, adsorption and biological oxidation processes (Iffat *et al.*, 2015).

Septic tanks are underground chambers commonly made of materials such as plastic, concrete or fiberglass (Meena *et al.*, 2015). They are mainly used for the primary treatment of black-water and grey-water through settling and anaerobic processes. Septic tanks have a (five days biological oxygen demand) BOD₅ removal rate of about 30-40% and provide only partial treatment (Nitin *et al.*, 2015). They, however, have low operating costs and a small footprint as they occupy a small land area (Meena *et al.*, 2015).

Waste stabilization ponds are open man-made basins that cover large areas of land and are a few meters deep (Njenga *et al.*, 2013). The system uses a series of three or more ponds for removal of pollutants and for improved levels of treatment (Khalid *et al.*, 2014). Wastewater is fed into an anaerobic stabilization pond (approximately 2-5m

deep) for about 1-7 days to allow anaerobic microorganisms to assimilate or breakdown organic impurities in the absence of air thus produce methane, carbon dioxide gas and biomass (Ramadan & Ponce, 2016). The anaerobic ponds can achieve a BOD₅ removal rate of about 60-70% at between 20°C to 25°C (Halis *et al.*, 2013). The resultant anaerobic pond effluent is drained into facultative ponds (approximately 1-2.5m deep) for 5-30 days, the time when most of the remaining organic matter is removed mainly by heterotrophic bacteria (Khalid *et al.*, 2014). Facultative ponds have a BOD₅ removal efficiency of about 70-90% (Mara, 2013). The resulting facultative pond effluent ends up in maturation ponds (approximately 0.5-1.5m deep) where removal of pathogens and nutrients reduction takes place. Stabilization ponds generally have nitrogen and ammonia removal rate of about 80 and 90% respectively while phosphorus removal is about 50% (Ramadan & Ponce, 2016). In most cases, additional steps are needed for the treatment of the effluent where higher quality effluent is needed (Ramadan & Ponce, 2016). The system takes long periods of time to complete the process and requires large areas for constructing ponds, which is not appropriate for urban areas due to scarcity of land (Njenga *et al.*, 2013). Despite the limitations, this technology is widely used for the treatment of sewage and industrial wastewater in many third world countries since it does not require highly skilled labor to operate and has low costs of maintenance and operation (Njenga *et al.*, 2013).

2.1.4 Membrane Bioreactor (MBR) Technology

Despite the extensive discussion of wastewater treatment methods here, the current study was narrowed down to membrane bioreactor (MBR) technology as an innovation that integrates the use of biological activated sludge process (ASP) with membrane filtration (Saadia *et al.*, 2015). The systems contain a bioreactor (aeration tank) where effluent is mixed with bacteria-rich activated sludge. Air is injected in to the aeration tank in order to supply to the microorganisms that simultaneously break down organic carbon and nitrogen pollutants in the wastewater. The treated water is separated from the biomass as clarified effluent through the process of filtration conducted using microfiltration or ultrafiltration membranes (Bokhary *et al.*, 2018). Unlike the activated sludge process (ASP), MBR technology has a smaller footprint as it does not require a sedimentation tank or a clarifier (Saadia *et al.*, 2015). The system has a high

effluent quality that exceeds the capacity of stabilization ponds and conventional activated sludge process (ASP) (Bouhadjar *et al.*, 2016). Therefore, the methodology is an upgrade of the conventional ASP and has recently been applied for the treatment of domestic sewage and textile industrial wastewater in southern European countries, in China, Japan among others (Serdarevic *et al.*, 2019).

2.2 Working principles of MBR

2.2.1 Membranes

Membranes are physical barriers with billions of microscopic holes on their surface (Deowan *et al.*, 2013). Their working principle is by the process of size exclusion as the microscopic holes provide selective filtration of impurities, contaminants, ions, and molecules to produce a clarified effluent also referred to as permeate (Bouhadjar *et al.*, 2016). The rest of the liquid is retained back as a concentrate (retentate) (Saadia *et al.*, 2015). Membranes are classified according to their pore size (filtration ranges) as microfiltration (MF), ultrafiltration (UF), nanofiltration (NF) and reverse osmosis (RO) (Zhu *et al.*, 2012). Membranes used for MBR are in the MF and UF range and have pore size 0.1–1.0 μm for MF and from 5nm to 0.01 μm for the UF membrane (Nagy, 2019). At MF range, the membranes can reject the suspended solids, organic colloids and bacteria (David *et al.*, 2016). At UF range they eliminate all suspended solids, organic matter, viruses, coliform bacteria and protozoa cysts among other pathogens from the filtrate (David *et al.*, 2016).

Membranes are commonly made from ceramic, organic polymer or composite materials (Amanmyrat *et al.*, 2019). However, the organic polymer is the most widely used material for making water purification membranes (Shao *et al.*, 2014). Some of these include polyethylene (PE), polypropylene (PP), polysulfone (PS) and polyethersulphone (PES) (Oliver *et al.*, 2016). These materials are the most preferred due to their desirable properties that include reasonable mechanical strength, high resistance to thermal and chemical attack (Shao *et al.*, 2014). At the same time, they are easy to blend and to fabricate into the desired pore size that helps to attain a high throughput with the required selective degree of rejection (Sarah *et al.*, 2018). Figure

2.2 presents the spectrum for rejection of pathogenic microorganisms for membranes with different pore size (Tan *et al.*, 2016).

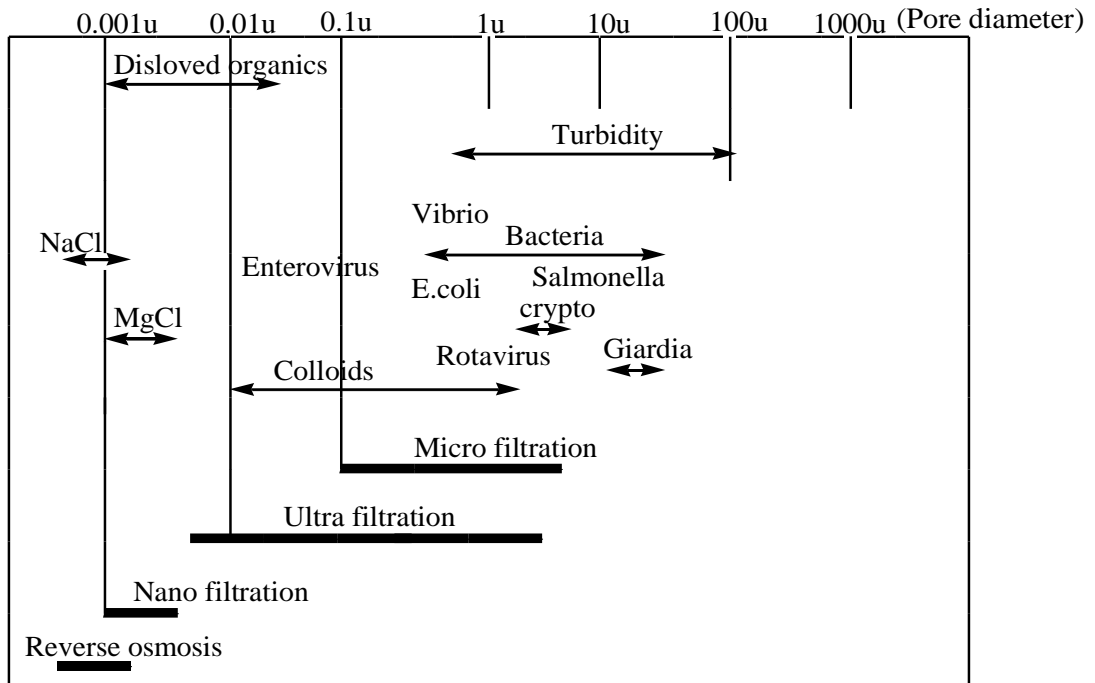
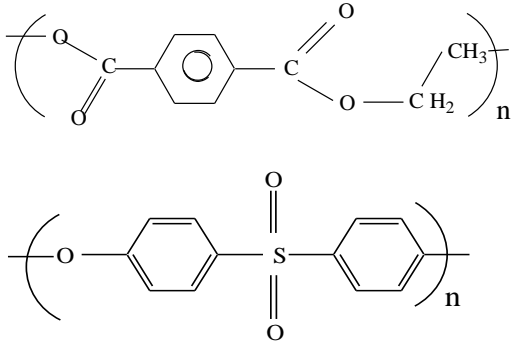
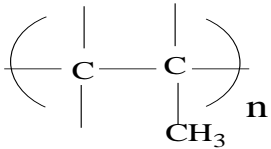
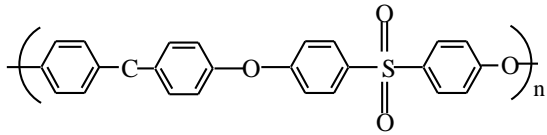


Figure 2.2: Membrane filtration ranges and contaminants rejection

Table 2.2 illustrates the various organic polymers used for making water purification membranes and their properties.

Table 2.2: Quality guidelines for organic polymers and their properties

Organic polymer	Chemical structure	Material properties
Polyethersulphone (PES)	 <p>The structure shows a repeating unit in brackets with a subscript 'n'. It consists of an oxygen atom connected to a para-phenylene ring, which is connected to a sulfonyl group (S=O)₂, which is then connected to another para-phenylene ring, and finally to another oxygen atom. The oxygen atoms are also connected to the next repeating unit.</p>	<p>Stiff, high strength attributed to the strong oxygen and aromatic bonds</p> <p>Transparent, thermodynamically stable with phenyl and biphenyl groups linked alternatively by ether and sulphone groups that make it rigid and tough</p>
Polypropylene (PP)	 <p>The structure shows a repeating unit in brackets with a subscript 'n'. It consists of two carbon atoms connected by a single bond. One carbon has two generic bonds (represented by vertical lines), and the other carbon has a methyl group (CH₃) attached to it.</p>	<p>Tough and rigid with a liner hydrocarbon resin constituting the monomer propylene. Easy to blend and to fabricate to the desired pore size and shape</p>
Polysulphone (PS)	 <p>The structure shows a repeating unit in brackets with a subscript 'n'. It consists of a phenyl ring connected to a methylene group (-CH₂-), which is connected to an ether linkage (-O-), which is connected to another phenyl ring, which is then connected to a sulfonyl group (S=O)₂, which is finally connected to another phenyl ring. The ether linkages are also connected to the next repeating unit.</p>	<p>Thermodynamically stable, has good chemical resistance, clear polymer chain made of monomer styrene with phenyl group attached to a back born of carbon chains thus make it hard, and brittle</p>

On the other hand, membranes made from ceramic material are fragile (Oliver *et al.*, 2016). This makes them economically unfeasible due to the high cost of maintenance (Amanmyrat *et al.*, 2019). Composite membranes are generally made from a combination of one or two materials constituting an active surface and a support layer (Deowan *et al.*, 2016).

2.2.2 Membrane module

Membranes are housed in a complete unit known as a module that constitutes a feed inlet, permeate outlet and concentrate outlet (Nagy, 2019). The modules come in different configurations and may contain several membranes. This helps to create a larger surface area and optimize the membrane's process performance (Norfamilabinti *et al.*, 2014). The four types of module configurations commercially available include hollow fiber, spiral wound, tubular modules and flat sheet (plate-and-frame) (Oliver *et al.*, 2016).

2.2.2.1 Hollow fiber modules

These are modules that constitute hundreds or thousands of hollow fibers in a bundle that is mounted into a large tube shell (pressure vessel) having an inlet and outlet line (Norfamilabinti *et al.*, 2014). The feed is supplied to the membrane module and gets distributed in the hollow fibers while permeate passes through the porous walls and out of the fibers, and is collected at the outlet line (Zhang, 2014). Hollow fiber modules have the advantage of having a high membrane packaging density that increases the contact for the surface to volume ratio. However, they are narrow and have tight fiber packing that makes them highly susceptible to fouling caused by suspended particles and also suffer from fiber breakage (Amanmyrat *et al.*, 2019). However, they are relatively easy to clean by applying back pressure (Norfamilabinti *et al.*, 2014). They are used in wastewater treatment in MBR and in food processing industries among other applications. Figure 2.3 illustrates a schematic diagram of the hollow fiber membrane module structure (Zhang, 2014).

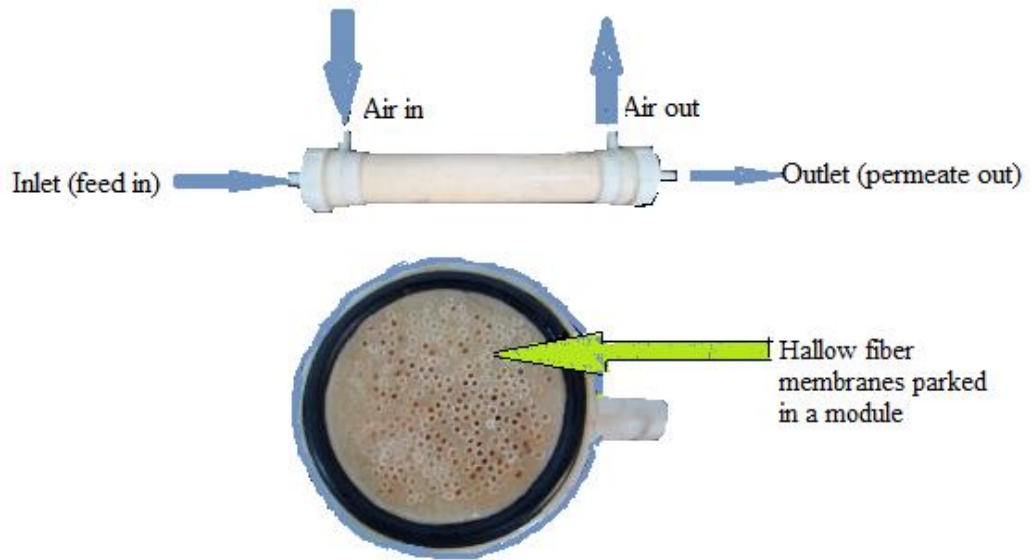


Figure 2.3: A sample of a hollow fiber membrane module structure (Zhang, 2014)

2.2.2.2 Tubular membrane modules

Tubular membrane modules are made by placing UF membranes inside the water-permeable tubes that are then packed together in polyvinyl chloride (PVC) shell (Kumar *et al.*, 2016). During operation, the feed water is pumped into the membrane tubes where separation occurs as permeate penetrates through the semi-permeable membrane walls and gets collected in the outer shell (Guirgis *et al.*, 2015). At the same time, the concentrate is discharged from the membrane tubes at the far end as illustrated in Figure 2.4. Tubular membrane modules have less fouling problems and are easy to clean using mechanical methods, chemical method and back flashing (Nagy, 2019). They are therefore used in MBR for treatment of oily wastewater, gray water and desalinization of dye among other uses (Kumar *et al.*, 2016). However, they require more energy (high operation cost) to pump the feed through the membrane tubes due to their large size (Guirgis *et al.*, 2015). They have a large footprint in comparison to hollow fiber modules and require a bigger space for installation (Kumar *et al.*, 2016). They also have low packaging density thus low contact for the surface to volume ratio in comparison to hollow fiber membrane modules (Nagy, 2019). Figure

2.4 illustrates a schematic diagram showing the configuration of a tubular membrane module.

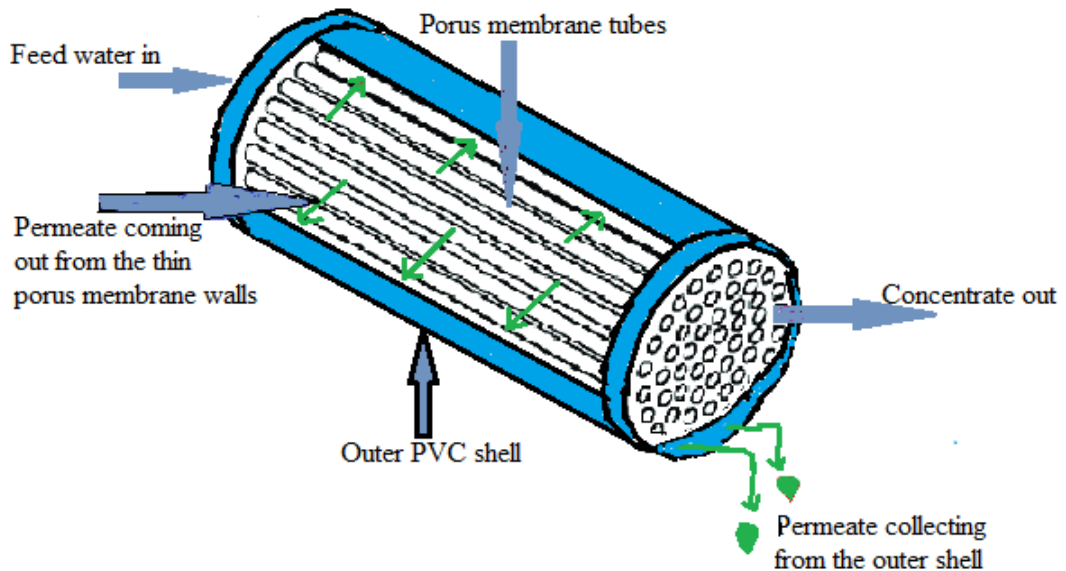


Figure 2.4: A schematic diagram of a tubular membrane module (Nagy, 2019)

2.2.2.3 Spiral wound modules

The spiral wound membrane modules are made of multiple layers that constitute two or more UF flat sheet membranes separated by a plastic mesh and polar plastic sheets inserted between the two sides of membranes (Balster, 2015). The multiple layers are rolled around a perforated tube and the ends sealed to prevent mixing of the feed and permeate. The spiral wound layers are then housed in a metal cylindrical tube (metallic shell) that is resistant to high pressure (Siddiqui *et al.*, 2016). During operation, the feed is pumped through perforated tubes and gets into the plastic mesh as permeate spirals through the membrane and collects in the central collector tube where it gets discharged (Kim *et al.*, 2013). The modules have a simple structure with a bigger surface membrane area per unit volume in comparison to the tubular modules and are relatively easy to clean through backflush (Siddiqui *et al.*, 2016). However, spiral wound membrane modules are tightly packed and are highly susceptible to fouling thus not suitable for the treatment of wastewater with high levels of fouling agents

(Balster, 2015). Their application is in MBR wastewater treatment, purification of pharmaceutical and medical products, and enzyme preparation among other applications. Figure 2.5 shows a sample of a spiral wound membrane module (David *et al.*, 2016).

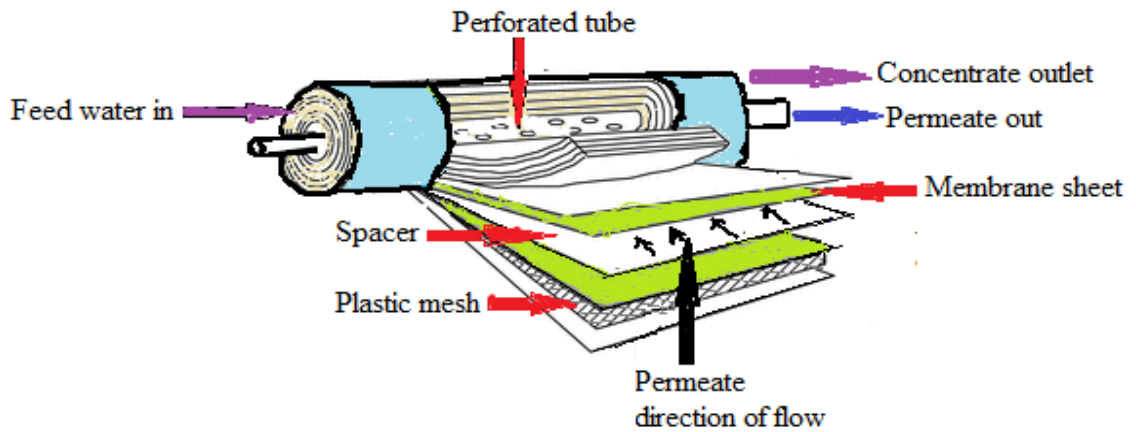


Figure 2.5: Schematic diagram of a spiral wound membrane module (David *et al.*, 2016)

2.2.2.4 Flame and plate membrane modules

The flame and plate or flat sheet (FS) membrane modules are made of a flame-like structure where the membrane flat sheets are packed together and separated with a separation distance of approximately 0.5 to 2.0 mm between sheets by porous plastic spacers (Alkudhiri *et al.*, 2018). The modules have two types of configurations that include the cross-flow and dead-end. The cross-flow configuration systems are made to allow a tangential flow of the feed to the membrane wall, while in dead-end systems the feed-water flow's perpendicular into the membrane (Oliver *et al.*, 2016). Both module configurations have an inlet for feed-water, an outlet for permeate and for an immersed process the concentrate remains in the tank (Alkudhiri *et al.*, 2018). The flat sheet modules have a smaller surface membrane area per unit volume in comparison to the hollow fiber membrane and spiral wound modules (David *et al.*, 2016). However, they have a greater advantage over other modules due to the simplicity of their structure that permits easy physical cleaning through backflash (Nagy, 2019). The flat sheet (FS) membrane modules are the most commonly used for

biomass separation in membrane bioreactor (MBR) technology and find application in the treatment of industrial wastewater and domestic sewage (Shao *et al.*, 2014). Figure 2.6 illustrates a schematic diagram of a flat sheet membrane module.

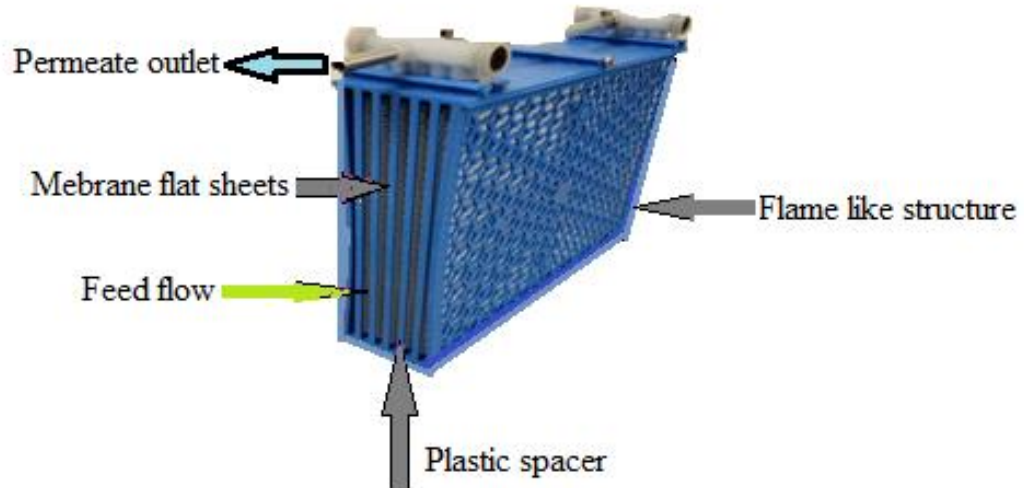


Figure 2.6: Schematic diagram of a flat sheet membrane module (www.martin-membrane.de)

2.3 Fundamentals of membrane bioreactor (MBR) technology

Membrane bioreactors (MBR) are wastewater treatment systems that combine a biological treatment process with a membrane filtration process to produce high-quality effluent (Luong *et al.*, 2016). The systems constitute a biological reactor tank that holds the activated sludge and a membrane module (Oliver *et al.*, 2016). The microbial community in the MBR activated sludge constitutes a wide range of microorganisms (Eckenfelder *et al.*, 2014). This may include the autotrophic bacteria (nitrifiers) that convert ammonia to nitrates, heterotrophic bacteria (denitrifiers) that reduce nitrate or nitrite to gaseous nitrogen, actinobacteria (actinomycetales) that help to decompose organic matter, and proteobacteria (Gammaproteo-bacteria, alphaproteo-bacteria) among others (Kochkodan *et al.*, 2014). During the treatment process microorganisms in the biological reactor assimilate or breakdown organic impurities and convert them into carbon dioxide, water, and biomass (Tan *et al.*, 2016).

The biomass is then separated from the clarified effluent through a process of filtration at ultra and microfiltration (MF) range (Zhang *et al.*, 2014).

There are mainly two types of MBR systems; aerobic (aMBR) and anaerobic (AnMBR) (Deowan *et al.*, 2013). In aerobic (aMBR) systems air is injected into the activated sludge in the reactor and the biomass is simultaneously separated from the clarified effluent through a selective filtration process (Bouhadjar *et al.*, 2016). On the other hand, anaerobic MBRs are operated without oxygen supply to the activated sludge and by using a membrane for separation of the biomass from the clarified effluent (Kochkodan *et al.*, 2014). MBR systems are also classified into two configurations; these are submerged/immersed (iMBR) and side-stream (sMBR) units depending on the way the modules are mounted to the unit (Saadia *et al.*, 2015). In (iMBR) the membrane module is completely submerged or immersed in the reactor tank while in (sMBR) it is placed outside the reactor tank (Deowan *et al.*, 2013). Figure 2.7 and 2.8 illustrate the two types of MBR configurations (Saadia *et al.*, 2015).

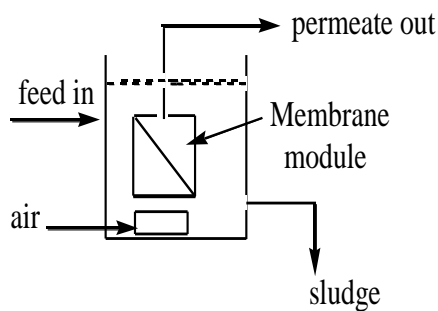


Figure 2.7: Immersed membrane bioreactor (iMBR)

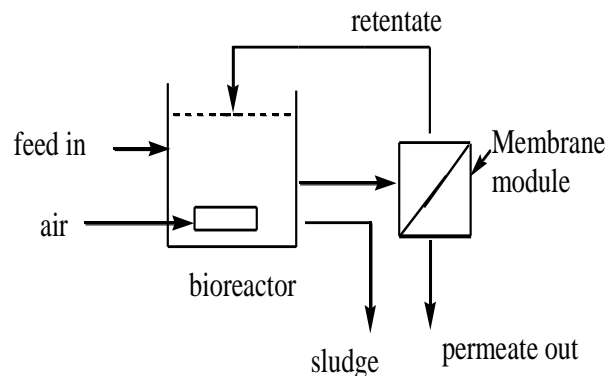


Figure 2.8: Side stream membrane bioreactor (sMBR)

Side-stream (sMBR) systems require a recirculation pump to push bioreactor effluent into the membrane chamber where permeate is drained out and the concentrate returned into the tank (Saadia *et al.*, 2015). The recirculation pump is therefore operated at high pressure to create high cross-flow velocity for mitigating membrane fouling (Bouhadjar *et al.*, 2016). As a result, cross-flow systems require more energy

and the overall demand for energy in sMBR systems is therefore high (Bouhadjar *et al.*, 2016). On the other hand, immersed iMBR systems have membrane modules submerged in the reactor with an airlift pump to create vacuum used to pull the permeate through the membranes (Serdarevic *et al.*, 2016). An air bubbler is installed in the bioreactor to supply oxygen and in the process create a cross-flow velocity that helps to control membrane fouling (Liu *et al.*, 2018). Membrane fouling is further reduced through backwash process as the effluent gets pumped back through the membrane. The iMBR systems are therefore low energy consuming and the most preferred (Saadia *et al.*, 2015).

2.3.1 Drawbacks of MBR systems

The MBR system has many advantages over conventional activated sludge process (APS) in that, it has a small footprint, high quality effluent and low sludge production (Deowan *et al.*, 2013). Nonetheless, the technique has faced a major drawback attributed to membrane fouling problem (Gkotsis *et al.*, 2017). Severe membrane fouling leads to a significant decline in membrane performance and durability (Gorzalski & Coronell, 2014). Membranes therefore need to be replaced frequently depending on the strength of the wastewater. Membrane replacement takes about 30 to 50% of the plant's operation cost (Lo *et al.*, 2015). This significantly increases the cost of maintenance and operation and is a limiting factor to the advancement of MBR technology (Mancuso *et al.*, 2017).

Membrane fouling in MBR may occur as cake layer formation and growth of biofilm on the membrane surface (Kochkodan *et al.*, 2014). This can be reversible or irreversible depending on the physical and chemical interactions that occur between the foulants on the surface of the membrane (Iorhemen *et al.*, 2016).

2.3.1.1 Reversible fouling

Reversible membrane fouling occurs as external fouling or cake formation on membrane surface attributed to the particle deposition on the surface and in the pores of a membrane during filtration process (Hao *et al.*, 2016). However, it may also result from accumulation of metal hydroxides, inorganic precipitates such as CaSO₄,

Fe (OH)₂, and other organic materials on the membrane surface (Iorhemen *et al.*, 2016). These constituents form foulants during filtration process thus build up a layer on the membrane surface (Iorhemen *et al.*, 2016). The layer grows with time and creates resistance to permeate flow (Oliver *et al.*, 2016). Reversible fouling is however non-adhesive and does not depend on surface chemistry of the membrane (Gkotsis *et al.*, 2017). It is therefore removable by back flashing with water or physical washing and chemical cleaning (Liu *et al.*, 2018). Flux decline in membrane can also be attributed to concentration polarization apart from membrane fouling. This is the increase in foulant concentration which decreases the driving force of water flow across the membrane. The effect can however be reversed by modifying the flow over the membrane (Gkotsis *et al.*, 2017).

2.3.1.2. Irreversible fouling

The second type of fouling is irreversible or adhesive (Vanysacker *et al.*, 2014). This type of fouling is caused by adsorption of foulants in the membrane pores (Oliver *et al.*, 2016). Residues or particles adsorb to the membrane surface and get strongly attached due to intermolecular interactions attributed to the hydrophobic interactions, extracellular macromolecular interactions, hydrogen bonding and van der Waals attractions among other forces (Miyoshi *et al.*, 2015). An example of irreversible adhesive fouling is the biofouling phenomenon that is caused by multiplication and growth of bacteria to the membrane surface thus forming a biofilm (Vanysacker *et al.*, 2014). Irreversible fouling is highly dependent on the chemistry of the membrane surface as hydrophobic surfaces have more attraction for organic residues and oils (Bokhary *et al.*, 2018).

2.3.2 Theory of membrane fouling

Pore blocking and cake formation are the two main mechanisms involved in membrane fouling (Zhang *et al.*, 2014). Pore blocking occurs as particles seal off pore entrances and prevent flow thus result to complete blocking (Bokhary *et al.*, 2018). In other cases, a portion of particles may seal off the pores while others get deposited on top of other deposited particles thus result to Intermediate blocking (Miyoshi *et al.*, 2015). Internal pore blocking or standard blocking occurs when small size solutes (smaller

than the size of the membrane pores) get adsorbed or deposited in the pores of the membrane (Liu *et al.*, 2018). Consequently, pore blockage increases the membrane's resistance to volume flow (Iorhemen *et al.*, 2016).

Cake layer formation however is caused by accumulation and build-up of colloidal materials, inorganic and organic matter on the membrane surface (Hao *et al.*, 2016). Cake fouling is reversible and, in most cases, it is cleared through back flashing of the membrane with water (Gkotsis *et al.*, 2017).

2.3.3 Factors that determine severity of membrane fouling

The performance of membranes and severity of fouling phenomena is highly dependent on several factors that include; chemistry (hydrophilicity) of the membrane, nature (roughness) of the membrane surface, configuration of the membrane and its module (Nagy *et al.*, 2017). Other factors are the characteristics of the feed, sludge retention time, organic loading rate (OLR) and operating conditions of the MBR (Ma *et al.*, 2015).

2.3.3.1 Surface tension of membranes

The surface characteristic of membrane is determined by its surface tension value. This is an internal attractive force that tends to keep the liquid molecules together when in contact with a solid surface (Zhu *et al.*, 2012). Surface tension value is therefore determined through measurement of the contact angle between a solid surface and a droplet of liquid (Qiang *et al.*, 2013). Polymeric membranes are generally hydrophobic with low surface tension values (Amir *et al.*, 2011). They have low degree of wettability due to their inability to form hydrogen bonding with water molecules (Miyoshi *et al.*, 2015). Table 2.1 presents the various surface tension values for different types of polymeric materials.

Table 2.3: Surface tension values for different polymeric materials (Amir *et al.*, 2011)

Polymeric Material	Surface tension value (dynes/cm)
Polytetrafluoroethylene (Teflone)	18
Polypropylene	25
Polystyrene	33
Polyethylene	31
Polyethylene terephthalate (Polyester)	43
Polysulphone	41

However, polymeric membranes have a strong attraction for organic substances (Miyoshi *et al.*, 2015). This makes their surface highly susceptible to organic fouling as they adsorb oils and protein residues in a wastewater stream more strongly (Kochkodan *et al.*, 2014).

2.3.3.2 Nature of membrane

Nature of the membrane in terms of roughness of the surface, pore type and pore size have a significant influence on the severity of fouling (Galiano *et al.*, 2015). Membranes with rough surface tend to foul more as compared to those with smooth and uniform surface (Wang *et al.*, 2011). This is attributed to the accumulation of suspended matter on rough and uneven surface of the membrane thus resulting to fouling (Bokhary *et al.*, 2018). Membrane fouling is also influenced by the range of pore sizes being used (Gkotsis *et al.*, 2017). Pores that are much larger allow small size solutes to get adsorbed or deposited on to the pore walls in the membrane (Kochkodan *et al.*, 2014). These results to pore blockage and increased resistance to volume flow through the membrane (Miyoshi *et al.*, 2015).

2.3.3.3 Membrane and module configuration

Membrane configurations are of different types that include, flat sheet (FS), multitubular (MT), capillary tube (CT), hollow fiber (HF) and spiral-wound (SW) among others (Nagy, 2019). They are packaged in modules in order to create larger surface area required for good performance (Miyoshi *et al.*, 2015). Severity of membrane

fouling depends on how it's mounted and oriented relative to the flow of water (Norfamilabinti *et al.*, 2014). A good membrane design should be configured to have a high contact for surface area to module bulk volume ratio (Liu *et al.*, 2018). It should facilitate easy physical cleaning through back flash (Shao *et al.*, 2014). Based on this factor, flat sheet (FS) membrane modules are the most suited for use in submerged membrane bioreactors since they have a simple structural design that allows easy cleaning through back flash among other advantages (Deowan *et al.*, 2013).

2.3.3.4 Operating conditions of MBR

The microorganisms in the MBR aeration tank use their enzymes to hydrolyze and degrade organic and inorganic matters into carbon dioxide, water and biomass (Vanyacker *et al.*, 2014). However, enzyme activities are highly dependent on temperature (Saadia *et al.*, 2015). Unfavorable temperatures lead to reduced enzyme activities thus resulting into less biodegradation of organic substances and increased accumulation in the bioreactors (Liu *et al.*, 2018). This may result into membrane fouling potentially induced by microbial deposition and growth (Bing & Anthony, 2012). Saadia, *et al.*, 2015 established optimal conditions for MBR performance as temperature range of 15 to 25°C. At lower temperatures, the treatment efficiency deteriorated due to reduced microbial activity in the reactor (Saadia *et al.*, 2015).

2.3.3.5 Sludge retention time (SRT)

Sludge retention time (SRT) is the frequency at which sludge is taken away from MBR reactor. High sludge age leads to accumulation of inorganic compounds, increased biomass concentration and high viscosity of sludge in the reactor (Bing & Anthony, 2012). Consequently, the system suffers from mass transfer limitations, mainly for oxygen and substrate thus resulting to extensive membrane fouling (Bokhary *et al.*, 2018). In a study conducted using a lab-scale MBR, Tan *et al.*, 2016 confirmed a biomass concentration range of 8-10 g/L as the optimal range at which MBRs operated best (Tan *et al.*, 2016).

2.3.3.6 Organic loading rate (OLR) and Hydraulic residence time (HRT)

Organic loading rate (OLR) is the rate of inflow of organic matter (g) in the reactor while hydraulic residence time (HRT) is the duration of time the feed remains in the reactor before being removed as permeate (Bokhary *et al.*, 2018). High OLR leads to accumulation of extracellular polymeric substances (EPS) in MBRs (Vanysacker *et al.*, 2014). These are foulants excreted from cells and present in the mixed liquor and are responsible for initial rapid irreversible fouling even at zero flux as they interact strongly with membranes to form biological floc (Zhang *et al.*, 2014). On the other hand, high HRT allows the bacteria to acclimate to the reactor conditions more easily thus improves the biodegradation performance of the reactor (Bing & Anthony, 2012).

2.3.3.7 Feed wastewater characteristics

Feed wastewater characteristics are significant factors that influence severity of membrane fouling in MBRs (Thang *et al.*, 2012). Some of these include the feed temperature, pH, dissolved organic matter and suspended solids among other factors (Zhang *et al.*, 2014). Unfavorable feed temperature causes reduced microbial activities thus less biodegradation of organic substances in the reactor (Saadia *et al.*, 2015). As a result, organic substances accumulate in the reactor thus accelerate membrane fouling (Hao *et al.*, 2016). Feed pH affects permeability of the membranes depending on the chemical properties of the membrane polymer matrix (Zhang *et al.*, 2014). At high pH the non-solvent additives entrapped in the membrane polymer matrix swell as a result of strong repulsive forces in them (Zhang *et al.*, 2014). Consequently they cause a reduction in the pore size of the membranes thus lead to increased membrane resistance and increased fouling (Iorhemen *et al.*, 2016). Internal pore blocking may also be caused by particles in the suspended solid with sizes less than that of the membrane pores. This is by continued deposition in the membrane pores (Miyoshi *et al.*, 2015).

2.3.4 Techniques used to control fouling in MBRs

Membranes used for wastewater treatment are highly susceptible to fouling problems (Thang *et al.*, 2012). The techniques used to control membrane fouling are based on

the complexity of fouling mechanisms and severity of fouling (Liu *et al.*, 2018). Some of these include pretreatment of feed, use of physical or chemical cleanings, change of operating conditions (process optimization) and surface membrane modification (Bokhary *et al.*, 2018).

2.3.4.1 Feed Pretreatment

Methods applied for pretreatment of feed solution are dependent on the type of effluent being treated. Some of the approaches used include:

- Pre-filtration of suspended solids: This is a physical pretreatment method that entails removal of large objects and debris from the influent using screens (Liu *et al.*, 2018). This is very effective in prevention of damage to pumps and module clogging (Hongtao *et al.*, 2014). The other physical pretreatment method includes heat treatment followed by settling and removal of settleable impurities through a pre-filtration process (Iffat *et al.*, 2015).
- pH adjustment: The pH is important as it defines electronic polarity of particles in the feed solution (Zhang *et al.*, 2014). Bokhary *et al.*, 2018 reported severe fouling observed under acidic conditions than in alkali conditions. The reason could be, at alkaline conditions particles in the effluent are negatively charged. They therefore have increased electrostatic repulsive force between them and the negatively charged particles in the membrane surface. As a result, alkali effluent does not adsorb strongly on the membrane surface (Qiang *et al.*, 2013).
- Coagulation: The use of coagulants during pretreatment helps to destabilize the surface charges of hydrophilic colloids thus cause them to come into contact and aggregate to form larger particles that can easily be removed (Ramadan & Ponce, 2016). In the process micro-particles are easily removed through filtration (Bokhary *et al.*, 2018). Some of the coagulants commonly used include alum, polyaluminium silicate sulphate (PASS) and lime (Gkotsis *et al.*, 2017).

2.3.4.2 Use of physical or chemical cleanings

Membranes can be cleaned using physical or chemical methods (Thang *et al.*, 2012). Physical cleaning in MBRs is conducted through a back flashing process (Liu *et al.*, 2018). In this process the filtrate is pumped back through the membrane by applying a backwash pressure that is higher than the operating filtration pressure (Deowan *et al.*, 2016). This helps to dislodge and remove surface foulants from the membrane thus prevent formation of biofilm and cake deposit (Vanysacker *et al.*, 2014). The technique is effective in reducing fouling and improving permeate flux over time (Bouhadjar *et al.*, 2016). However, its efficiency is limited to removal of surface deposits for reversible fouling and does not eliminate adhesive irreversible pore fouling (Oliver *et al.*, 2016). When physical cleaning is not effective, chemical cleaning is conducted using cleaning agents such as acids, base, surfactants and disinfectants (Thang *et al.*, 2012). During this process, membranes are soaked for some minutes with a solution of the cleaning agent and back flashed to remove the contaminants. This process helps to recover permeate initial flux (Liu *et al.*, 2013). However, where chemical cleaning does not help to regain the flux membranes have to be replaced (Zhang *et al.*, 2014).

2.3.4.3 Change of operating conditions (process optimization)

Optimization of operating conditions is a process control method used for mitigating membrane fouling in MBRs (Liumo *et al.*, 2019). In a study conducted on treatment of model textile wastewater, Tan *et al.*, (2016) confirmed that MBRs should be operated at modest flux and preferably below the critical flux to avoid clogging of the membrane pores (Tan *et al.*, 2016). As Saadia *et al.*, (2015) reported, acclimation period was important to allow bacteria present in the bioreactor adapt to its environment and therefore obtain a constant flux. Further studies confirmed that by using the right airflow rate, it was possible to reduce rapid accumulation of fouling material on membrane surface (Bouhadjar *et al.*, 2016). According to Gkotsis *et al.*, (2014) there is an optimal aeration rate and sequence at which membrane fouling is significantly suppressed in submerged MBRs. Studies have also shown that MLSS

concentration, particle surface charge and pH have influence on fouling and should therefore be controlled (Liu *et al.*, 2018).

2.3.4.4 Modification of membrane surface

Polymeric membranes are generally hydrophobic in nature (Miyoshi *et al.*, 2015). Surface modification is an effective technique used to improve the surface chemistry of the membrane by making it more hydrophilic (Kochkodan *et al.*, 2014). These can be carried out by introducing charged groups on the membrane surface (Francesco *et al.*, 2018). These have an effect on improving the surface chemistry of the membrane thus preventing adhesive fouling (Qiang *et al.*, 2013). A good membrane material is one that has properties of hydrophobic polymers but with surface chemistry of hydrophilic materials (Galiano *et al.*, 2015).

2.4 Membrane surface modification techniques

2.4.1 Surface grafting and coating

Surface grafting and coating are two main techniques used for membrane surface modification in order to improve their antifouling properties (Moghimifar *et al.*, 2014). Surface grafting entails covalent attachment of monomers (carrying reactive groups) to the membrane surface, or the use of active functional groups existing on the membrane surface to initiate polymerization of monomers from the surface (Ma *et al.*, 2015). However the chemical treatment processes involved may affect the structural properties of the membrane modified (Kochkodan *et al.*, 2014). Furthermore the long processes involved in grafting make the technique expensive for large-scale operation (Moghimifar *et al.*, 2014). Mondal *et al.*, (2014) conducted a study on modification of polymeric membrane surface using photo-induced grafting copolymerization technique. The grafted membrane showed better separation performance with salt rejection rate of 48% in comparison to 7.2% observed with unmodified commercial PES membrane (Mondal *et al.*, 2014). However extensive use of organic solvents and monomers in grafting processes makes the process expensive and not appropriate for commercial use (Hong *et al.*, 2017).

Surface coating on the other hand entails applying a layer of coating material on the membrane surface or dipping the membrane in a solution containing polymers that have antifouling properties (Deowanet *et al.*, 2016). The coating material forms a thin layer that non-covalently adheres to the membrane surface (Galiano *et al.*, 2018). The microemulsion is a coating material commonly used in membrane coating technique. Microemulsions occur in various forms that include: water-in-oil W/O microemulsions, oil-in-water O/W microemulsions and biocontinuous microemulsions (Galiano *et al.*, 2015).

2.4.2 Polymerisable bicontinuous microemulsion technique

Polymerisable bicontinuous microemulsion technique is a process used to improve surface characteristics of organic polymers. In this process a polymerizable bicontinuous microemulsion (PBM) coating material is applied on the membrane to be modified. This may contain functional groups that make the membrane surface more hydrophilic (Galiano *et al.*, 2015). Polymerizable bicontinuous microemulsion (PBM) is prepared from a surfactant-rich hybrid phase constituting poor phases of water and oil (Francesco *et al.*, 2018). This occurs as one of the multi-phase equilibria observed during preparation process of microemulsions. (Galiano *et al.*, 2015).

Microemulsion is a mixture of two immiscible liquids (oil and water) stabilized by a surfactant and a co-surfactant (short chain alcohol) to form a dispersion that is clear, transparent and thermodynamically stable (Malik *et al.*, 2012). During preparation, microemulsions occur in different multi-phase equilibria described as Winsor systems (Francesco *et al.*, 2018). Winsor I (O/W) arises at the point when a surfactant-rich water phase coexists with surfactant poor oil phase (Malik *et al.*, 2012). Winsor II (W/O) arises at the point when a surfactant-rich oil phase coexists with surfactant-poor water phase (Mehta & Kaur, 2011). While Winsor III (bicontinuous) arise as a surfactant-rich hybrid phase coexisting with poor phases of water and oil, respectively (Mehta & Kaur, 2011). Bicontinuous microemulsion is therefore a network of interconnected water and oil channels with the surfactant located at the interface between phases of water and oil (Francesco *et al.*, 2018). When prepared using a

polymerisable surfactant, it is referred to as a polymerisable bicontinuous microemulsion (PBM) (Galiano *et al.*, 2015).

Microemulsion preparation was first discovered in the year 1959 by Schulman *et al.*, 1959 (Malik *et al.*, 2012). In that work, the author reported to have prepared microemulsions by mixing components of water, oil, surfactant and co-surfactant at different ratios (Malik *et al.*, 2012). Stoffer & Bone, 1980 conducted further studies on polymerization of methyl acrylate (MA) in water/oil systems (W/O) where formation of phase regions for thermodynamically stable W/O microemulsion was observed (Deowan *et al.*, 2013). This study opened the field to more investigations on preparation of bicontinuous microemulsions using cationic surfactants, anionic surfactants, polymerisable and non-polymerisable surfactants (Kochkodan *et al.*, 2014).

2.4.2.1 Background of microemulsion polymerization

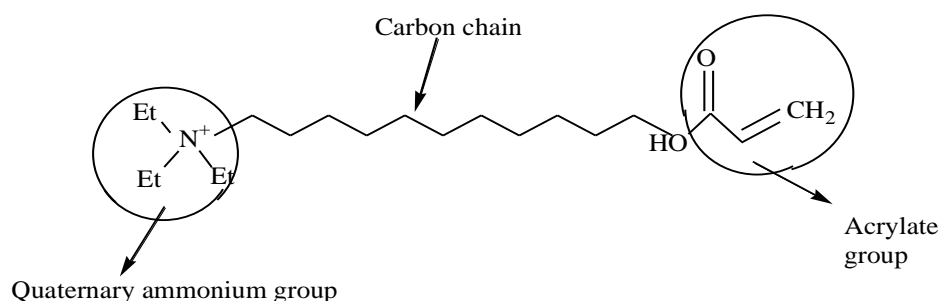
Polymerization mechanisms were first studied in 1930's as reported by (Candau & Ottewill, 2012). The study investigated on preparation of polymer latexes through emulsion polymerization process that involved application of water soluble initiators and micelle forming emulsifiers (Candau & Ottewill, 2012). According to the findings made by the researchers, the particle latexes formed inside the micelle had varying particle sizes in the ranges of 0.05 to 0.5 μm (Candau & Ottewill, 2012). Further research aimed at getting efficiently small droplet size leading to the concept of preparation of polymer latexes through microemulsion polymerization process (Wang *et al.*, 2011). These lead to production of thermodynamically stable micro latexes with small particle size in the range of 2–5 nm (Wang *et al.*, 2011).

Unlike in emulsions, polymerization in microemulsion occurred only in the monomer droplet thus producing latex particles with smaller size than obtained with emulsion polymerization (Yuan *et al.*, 2013). However these findings faced a major challenge as large amount of surfactant was needed to stabilize the system prepared through microemulsions polymerization (Yuan *et al.*, 2013). This lead to further studies on the use of polymerizable surfactant as this would allow mixing of large amounts of water and oil with less mounts of surfactant. In 2015, the author Galiano *et al.*, (2015) carried

out a study on the use of polymerizable surfactant and non-polymerizable surfactant for preparation of transparent, continuous porous polymeric solids by polymerizing the biocontinuous microemulsion thus providing a much more applicable process (Galiano *et al.*, 2015).

2.4.2.2 Preparation of a polymerizable bicontinuous microemulsion (PBM)

Preparation of a polymerizable bicontinuous microemulsion (PBM) has been widely investigated (Galiano *et al.*, 2015; Deowan *et al.*, 2016). According to the method developed by Galiano *et al.*, 2015, the coating material was prepared using a mixture of monomer methyl methacrylate (MMA), a co-surfactant 2-Hydroxyethyl methacrylate (HEMA), a cross-linker Ethylene glycol dimethacrylate (EGDMA) and a synthetically made polymerizable surfactant acryloyloxyundecyltriethylammonium bromide (AUTEAB). The cationic surfactant AUTEAB applied in the study was prepared in Italy as per the method developed by ITM-CNR, Italy (Figoli *et al.*, 2014). The chemical structure of the cationic surfactant had a quaternary ammonium group that was confirmed to have antimicrobial activity against bacteria present in the MBR that cause biofouling (Raffaella *et al.*, 2017). The chemical structure had an alkyl chain group constituting 11 atoms of carbon and was also found to enhance antimicrobial activity but only up to a certain limit (Mancuso *et al.*, 2017). Furthermore, the acrylate group in the structure had double bonds that made the PBM more reactive and polymerizable (Figoli *et al.*, 2014). Scheme 6.1 is a presentation of the structure of the synthetic polymerizable surfactant (AUTEAB).



Scheme 6.1: Acryloyloxyundecyltriethylammonium bromide (AUTEAB)

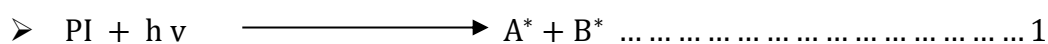
(Mancuso *et al.*, 2017)

Further research is ongoing for application of polymerizable bicontinuous microemulsion (PBM) as coating material for PES commercial membranes used in MBR for wastewater treatment. The PBM is polymerized using various techniques to get stable and clear micro latex that produce transparent porous polymeric solids.

2.4.3 Polymerization and initiation techniques

Polymerization is a process used to form polymer chains by reacting monomer molecules in a chemical reaction (Meléndez-Ortiz *et al.*, 2015). Initiation of polymerization can be carried out through photochemical, thermal and high-energy radiation techniques among others (Francesco *et al.*, 2018). In photochemical polymerization, suitable photoinitiators (molecule that create reactive species) are subjected to UV light of specific wavelength (Galiano *et al.*, 2018). These molecules absorb energy from the UV light and become activated resulting to disintegration into reactive fragments of radicals or ions (Francesco *et al.*, 2018). Consequently the reactive fragments initiate polymerization in subsequent steps as illustrated in Equation 1-3.

Radical formation



Where h is Planck's constant

ν is the frequency

PI is the photo initiator

A^* and B^* are ions or radicals formed

The reactive fragments of radicals or ions initiate polymerization reactions by reacting with molecules having double bond thus form more radicals with unpaired electrons.



Where R represents molecules having double bond

A* and B* are the initial ions or radicals that react with the molecules having double bond

AR* and BR* are resultant radicals with unpaired electrons

In propagation step the free radical species with unpaired electrons further react with a monomer molecule to produce chain initiating species (AR*) (Galiano *et al.*, 2018). The species then react with other molecules to form a polymer chain as shown in Equation 4 – 5.

Chain polymerization reaction process



Where R represents molecules having double bond

AR* represents the resultant radicals with unpaired electrons (chain initiating species)

ARR* represents short polymer chains with unpaired electrons

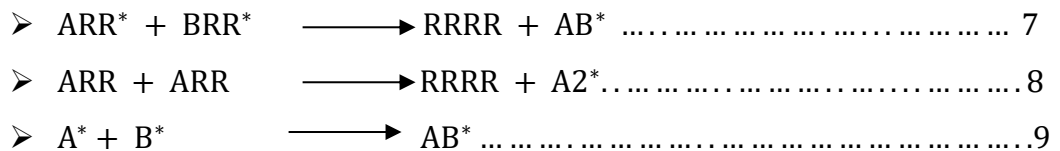
This process continues until it gets to chain transfer and termination step as illustrated in Equation 6-9.

Chain transfer



Where C is the atom or species transferred

Termination step occurs by combination of reacting species



Where ARR* or BRR* are short polymer chains with unpaired electrons

RRRR represents the resultant polymer chain formed

In other cases high-energy radiation technique is used to initiate polymerization (Espinoza *et al.*, 2014). The technique uses a radiation source to produce ionizing radiations such as gamma rays, X-rays, accelerated electron and ion beam (Meléndez-Ortiz *et al.*, 2015). These radiations come in to contact with organic matter and provide activation energy needed to cause degradation of the molecules into energetic radicals that initiate polymerization (Espinoza *et al.*, 2014). On the other hand, thermal polymerization technique is also used to initiate polymerization. In this technique, thermal energy is applied to initiate a reaction between monomer molecules thus cause chain reactions and formation of polymers (Retailleau *et al.*, 2014).

Galiano *et al.*, 2018, conducted a study on polymerization of a polymerizable bicontinuous microemulsion (PBM) using the UV light as a photo initiator (Galiano *et al.*, 2018). The PBM was made up of polymerizable components that could be co-polymerized into a strong network. These were the monomer methyl methacrylate (MMA), co-monomer 2-Hydroxyethyl methacrylate (HEMA), a cross-linker Ethylene glycol dimethacrylate (EGDMA) and a synthetically made polymerizable surfactant acryloyloxyundecyltriethylammonium bromide (AUTEAB). The process was conducted in a series of steps. The first step was to introduce photo initiators (1-Hydroxycyclohexylphenyl ketone) to the PBM to be polymerized (Francesco *et al.*, 2018). The photo initiators were then exposed to ultraviolet light where they absorbed energy at a specific wavelength needed to cause bond cleavage thus form free radical species with unpaired electrons (Galiano *et al.*, 2018). Figure 2.9 illustrates the formation of two radical species from a photo initiator, through bond cleavage at carbonyl group and an adjacent carbon.

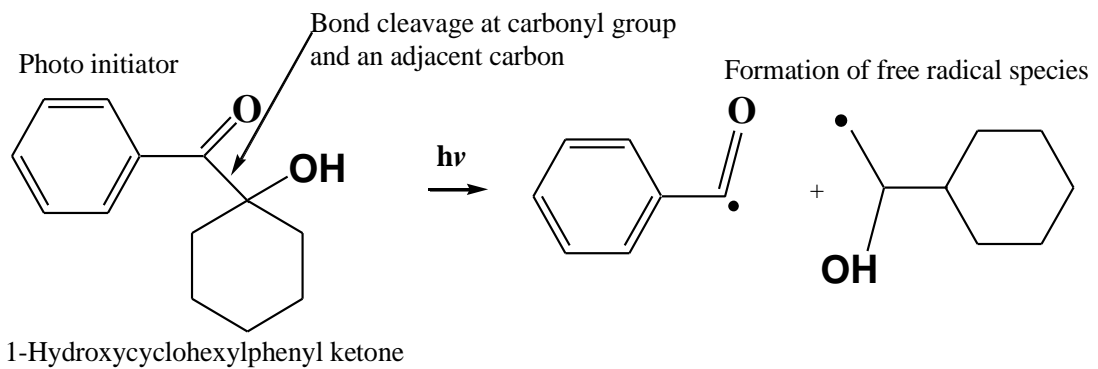


Figure 2.9: Photo initiated reaction

In a subsequent reaction, the reactive species would start reacting with monomer molecules dispersed in the aqueous phase of the PBM thus initiate formation of oligomeric radicals polymer chain (Galiano *et al.*, 2018). The reaction is illustrated in Figure 2.10

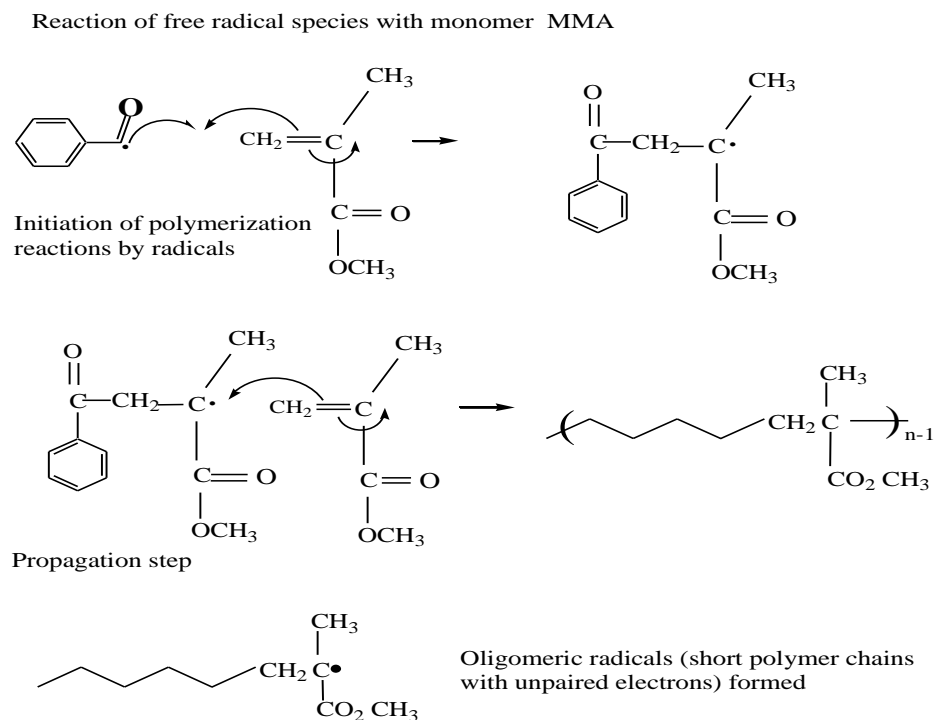


Figure 2.10: Reaction of free radical species with monomer methyl methacrylate

Water and surfactant were the media where the monomer was dispersed. The excess surfactant in the aqueous phase would then create micelles where small amounts of monomer diffuse through to form a monomer-swollen micelle.

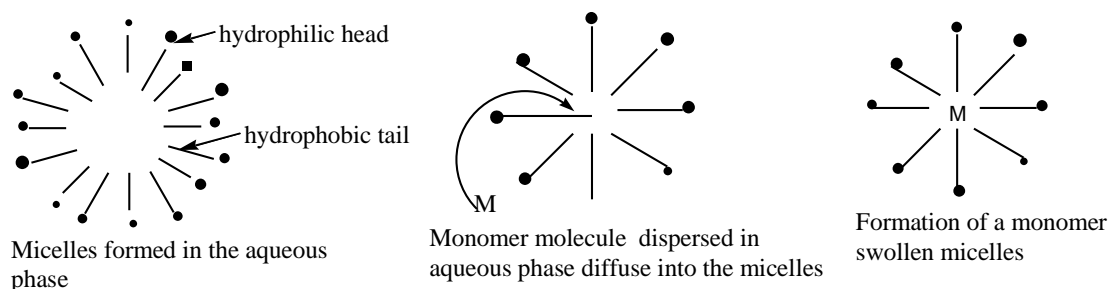


Figure 2.11: Formation of micelles and monomer-swollen micelle

Oligomeric radicals formed were more hydrophobic than the monomer molecules and thus would enter into the monomer swollen micelles (step 2 in Figure 2.12) where polymerization occurred to form latex particles (dispersions of polymer particles in water) (Francesco *et al.*, 2018). The growth of latex particles continued by nucleation or diffusion of monomer molecules through the water to the monomer swollen micelles (polymer particle) and by collision and subsequent coalescence between two latex particles (Figoli *et al.*, 2014). The process continued until all monomer molecules were consumed. Finally surfactant stabilized polymer particles were formed with empty micelles (Galiano *et al.*, 2018). The sequence observed during this process is illustrated in Figure 2.12.

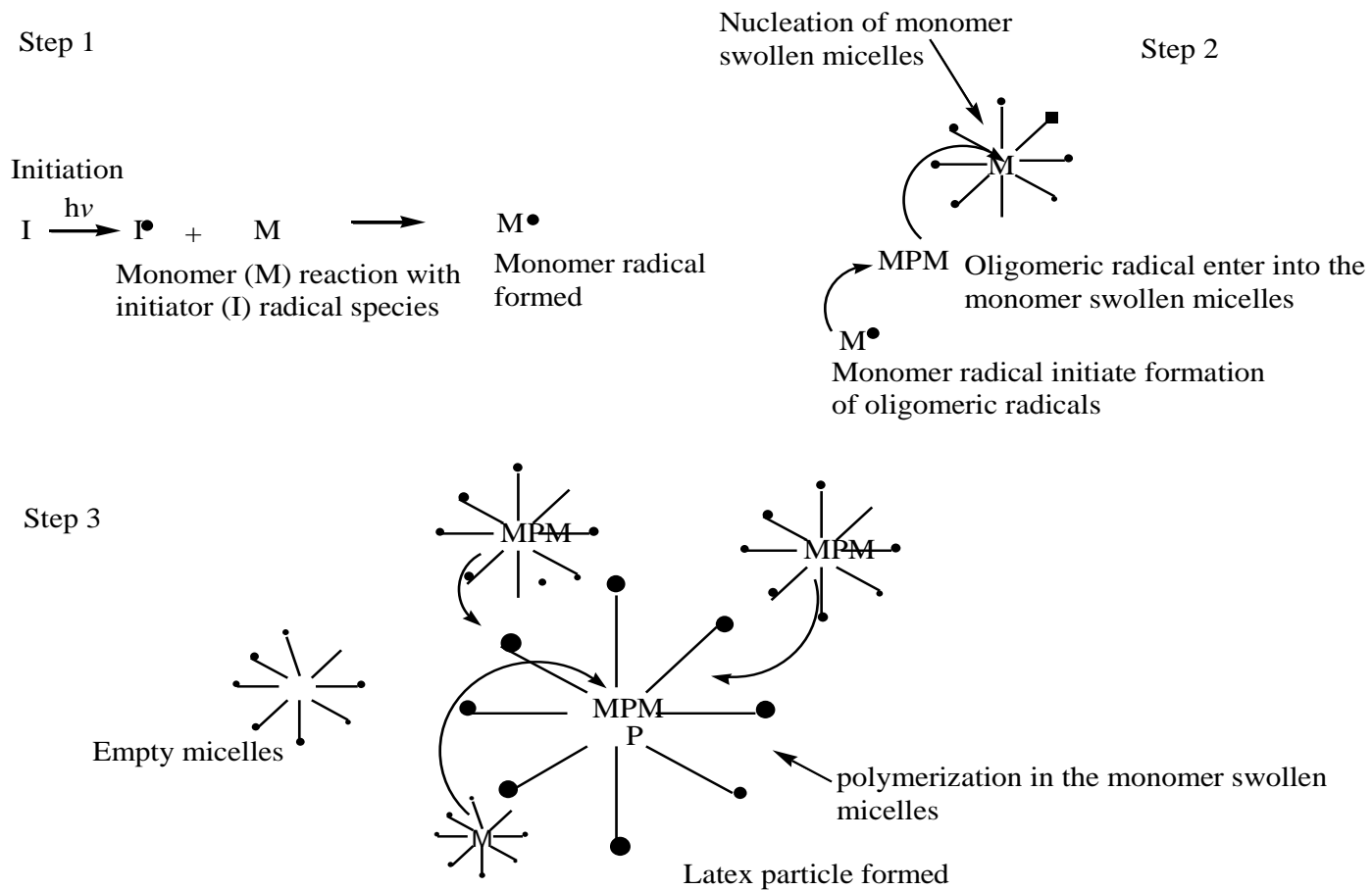


Figure 2.12: UV initiated PBM polymerization process (Galiano *et al.*, 2018)

The current study aimed to optimize the performance of commercial PES membranes, develop low fouling membranes and test for the first time in a pilot-scale membrane bioreactor (MBR) for treatment of fish processing wastewater. The study is a follow-up of the research work carried out by Galiano *et al.*, 2015 and, Deowan *et al.*, 2016. The authors developed the PBM as a coating material for commercial membranes that were tested using modeled textile dye wastewater.

CHAPTER THREE

MATERIALS AND METHODS

3.1 Study Area

This study investigated a potential application of MBR technology for the treatment of fish processing wastewater in industries. The study was conducted within the Victoria Integrated Aquaculture (VicInAqua) project funded by the European Union's Horizon 2020 research and innovation program under grant agreement number 689427. Within this study, lab-scale MBR pilot trials were conducted in JKUAT. The study aimed to optimize the performance of commercial ultrafiltration polyethersulphone (UF/PES) membranes, develop the novel low fouling membranes, and test for the very first time for treatment of fish processing wastewater through membrane bioreactor (MBR) technology. The output of this study would be integrated into the VicInAqua pilot plant set up in Nyalenda stabilization ponds in Kisumu, Kenya (VicInAqua, 2017). The pilot plant uses an MBR as the principal treatment unit for sanitation of wastewater received from households, industries and recirculating aquaculture systems (RAS). Figure 3.1 shows the study site for the VicInAqua pilot plant in Kisumu Nyalenda ground.



Figure 3.1: Map of the Lake Victoria Basin showing (Lake Victoria Basin Commission, 2017)

Nyalenda is one of the largest unplanned peri-urban settlements located in Kisumu, Kenya that is situated in the region of Lake Victoria. The urban settlement mostly lacks coverage of sewerage systems with only 10% of its population having access to services offered by the sewerage system pond in the region. The demand for water and sanitation services is high in the region thus an appropriate site for setting up the wastewater treatment pilot plant. Some experiments were conducted at the Kisumu Nyalenda plant and the process study was done using pilot Lab scale tests conducted in JKUAT using samples from the Makindi fish farm processing unit. The farm is located 20.6 km from Jomo Kenyatta University of Agriculture and Technology (JKUAT) along the old Murang'a road which is within the proximity to the University, thus preferred as an appropriate collection point for fish processing wastewater samples.

3.2 Sampling of raw fish processing wastewater

The raw fish processing wastewater multiple sample units were collected from the processing drainage system in Makindi fish farm and were placed in 100L clean plastic containers. The samples were sealed and transported immediately to the JKUAT laboratory for analysis and for pilot testing in the MBR unit. Plates 3.1 and 3.2 show photos for the processing unit and a wastewater drainage system where representative samples were collected.



Plate 3.1: Sample collection point along the wastewater drainage system



Plate 3.2: Fish processing unit in Makindi fish farm

The individual samples were mixed in a feed tank and the quality of the composite raw fish processing wastewater (feed) samples was determined. This was done by conducting analysis for a variety of physicochemical parameters within 3 hours after sampling and after storing in the feed tank to determine the quality before treatment in the MBR unit.

Other experiments to determine the quality of domestic wastewater at the Nyalenda waste stabilization ponds were done on-site within the VicInAqua pilot trials.

3.3 Research design

Experimental work on application of membrane bioreactor (MBR) technology for the treatment of fish processing wastewater was essentially carried out in 3 experiments at using lab-scale pilot trials. The experiments were done as follows:

1. The MBR start-up (1st) experiment was carried out by testing the performance of two commercial Polyethersulfone (PES) membrane modules immersed in a lab-scale Membrane Bioreactor (MBR) unit for the treatment of fish processing wastewater followed by the optimization process. Further, a comparative study for the performance of two modules (Microdyn-Nadir module and Martin Membrane Systems module) with different construction but made of the same UF/PES material was carried out. Quantitative chemical analysis was conducted to ascertain the effluent quality after treatment during the experimental period.
2. The 2nd experiment entailed the development of a low fouling membrane through surface modification of commercial PES membranes using a bicontinuous microemulsion polymerization technique. Further, a comparative test for fouling propensity and physicochemical characteristics for PES membrane and the modified PBM-coated PES membrane was done using an auto-controlled cross-flow testing cell, Attenuated total reflectance infrared (ATR-FTIR), and a contact angle (CA) meter.
3. In the 3rd experiment, a CUBE Mini 0.45m² flat sheet (FS) membrane module of 5 panels laminated with PES membranes and a CUBE mini of the same dimension laminated with PBM-coated PES membranes was used. The PBM-coated membrane module was for the very first time tested for the treatment of fish processing wastewater. The performance of the two tested modules was compared and recommendations were made based on the results obtained.

4. Further, a cost-benefit analysis, for a containerized MBR system suitable for the treatment of fish processing wastewater for industries was conducted to determine the economic viability of the technology. A correlation of the MBR systems, activated sludge process (ASP) and wastewater stabilization pond (WSP) treatment systems was carried out using basic cost model equations.
5. The data obtained from the process study was subjected to statistical data analysis, Q-test was used to test for accuracy of the results, means, standard deviation, variance (ANOVA) and t- test was used to test the hypothesis. A schematic overview of the study is illustrated in Figure 3.3.

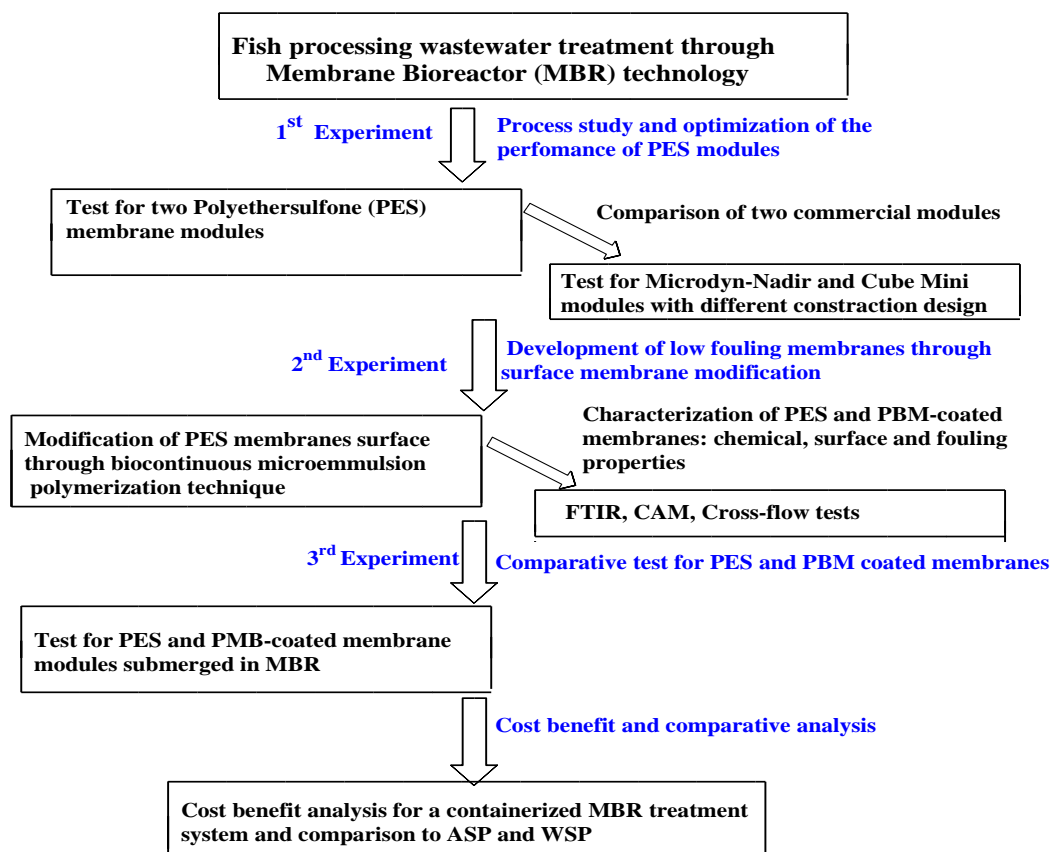


Figure 3.2: A schematic overview of the study

3.4 Experimental design

3.4.1 Membrane Bioreactor specifications and operations

The lab-scale (immersed membrane bioreactor) iMBR unit was set in the JKUAT-IEET laboratory. The unit constituted 97L Polyvinyl chloride (PVC) aeration tank and two immersed PES membrane modules. The iMBR unit had two permeate lines for each module, installed with permeate (suction) pump with a speed control of 0.2 to 2 L/h, a manometer, and an analog rotameter having a volume flow indicator with a range of 0.5 to 5 L/h. The aeration tank was installed with a blower (air pump) having a flow volume of 100 L/min and connected to an aeration system constituting air diffusers located below the membrane modules. Air was injected through the diffusers to create a turbulent cross-flow current across the membrane thus limit fouling phenomena. The operation of the coarse bubble aeration system however requires high energy which drives higher the operational expenditures of MBR. Air was also supplied to the suspended micro-organisms in the aeration tank using the blower connected to the diffusers. The MBR unit permeate lines were installed with a temperature sensor model EGA 142, two electric conductivity cells model LTC 0.35/23VP with a range of 5 μ S/cm to 500 mS/cm, and two pH meters. A level sensor was installed to control water levels and detect foam formation in the tank respectively. The MBR unit was connected to a computer having a Lab program that recorded and stored online data. A denitrification tank of about 70L (fitted with a digital stirrer) was connected to the MBR treatment unit during a follow-up experiment. This would facilitate in the removal of nutrients from the wastewater during a recirculation process between the aeration and the denitrification tank. A schematic diagram of the lab-scale MBR unit and photo (caption) of the pilot plant used in this experiment are shown in Figure 3.3 and Plate 3.3

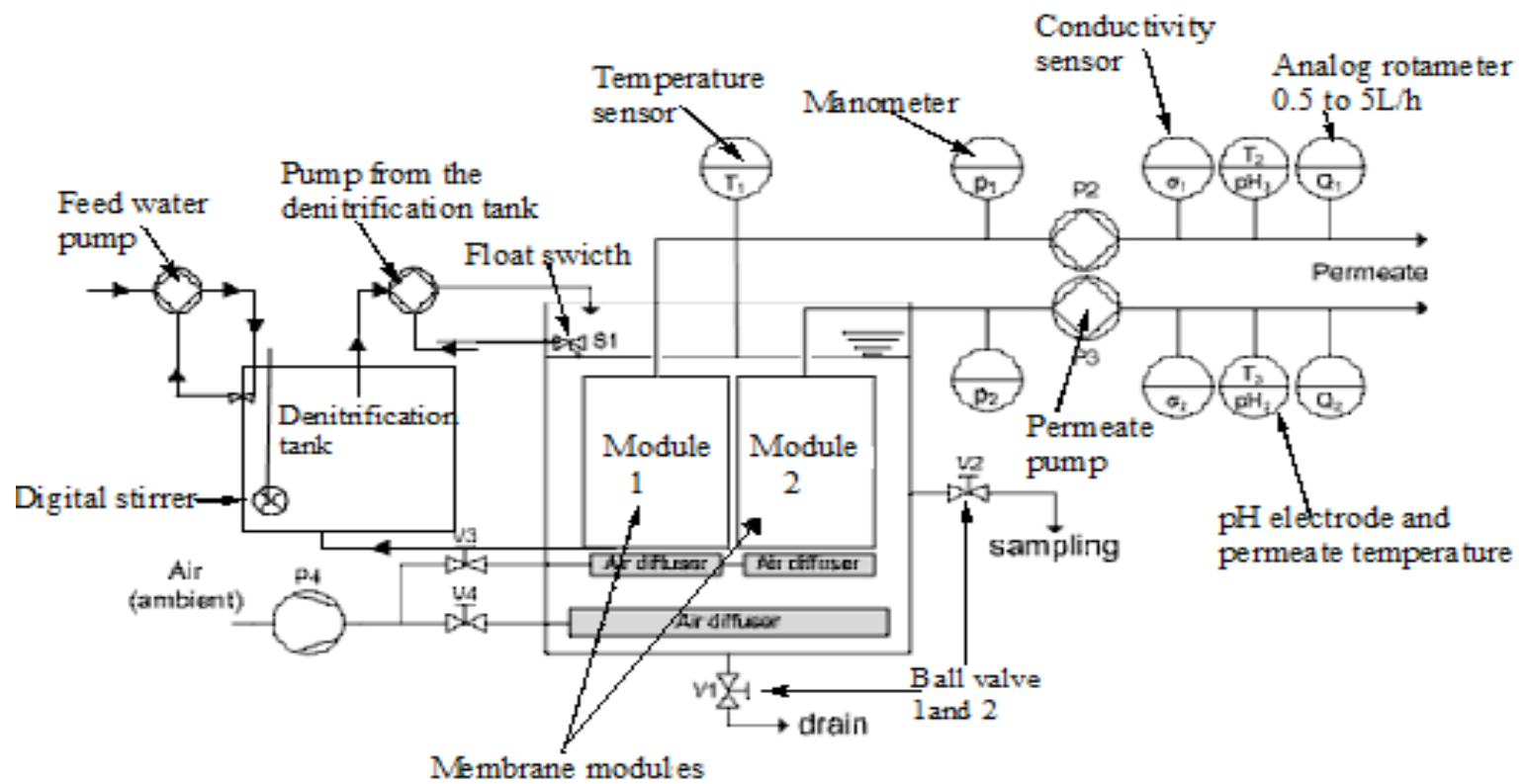


Figure 3.3: Schematic diagram for the immersed membrane bioreactor (Karlsruhe University of Applied Sciences, Germany)

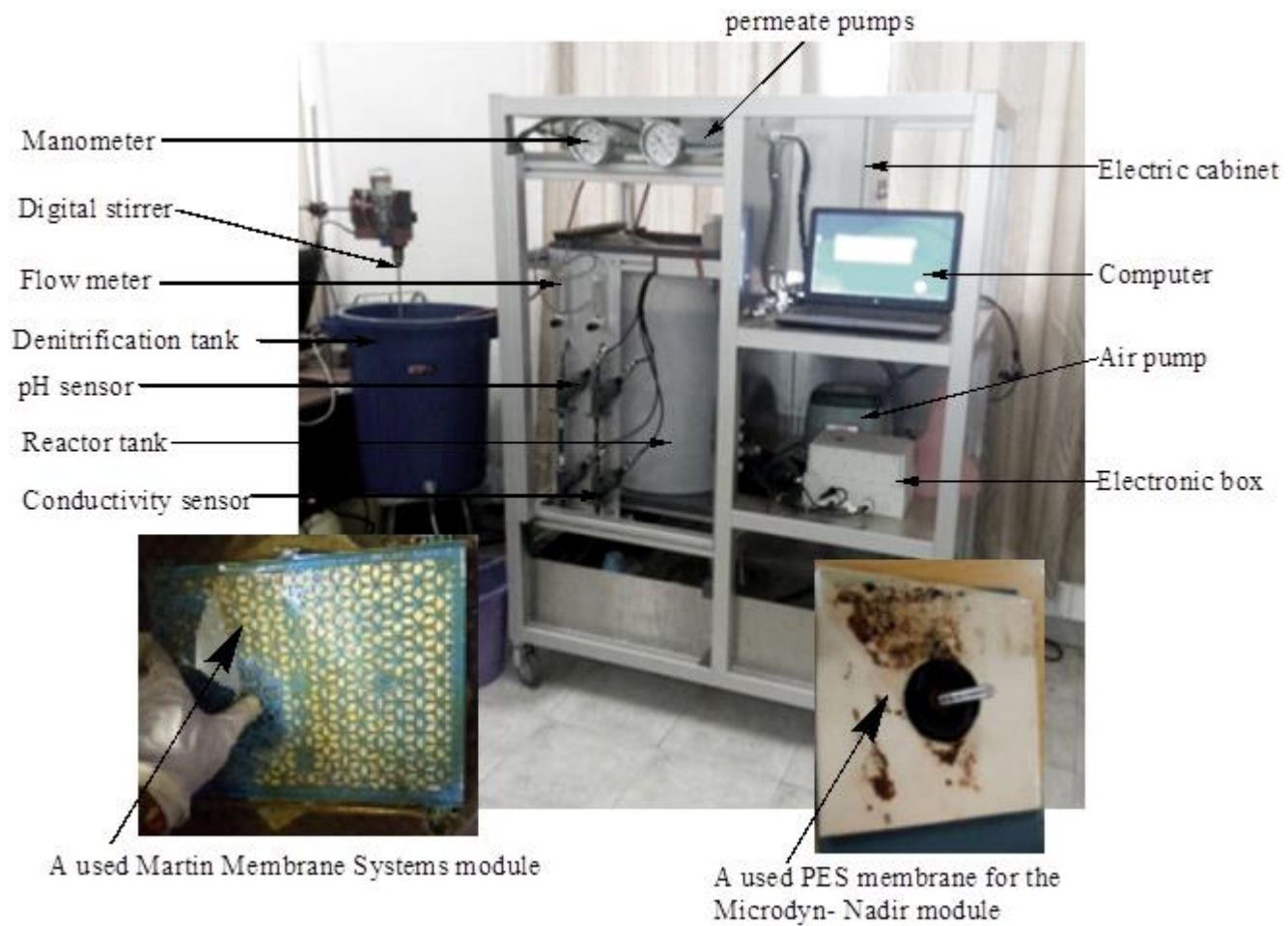


Plate 3.3: Photo of the immersed membrane bioreactor (iMBR) pilot plant

The commercial UF/PES and PBM-coated membranes used for this study were assembled into modules to be tested in lab-scale MBR by Microdyn-Nadir and MARTIN Systems. Table 3.1 presents the technical specifications for the PES membrane modules used.

Table 3.1: Technical specifications for the PES membrane modules

Technical data	Membrane module	
	Microdyn-Nadir UF	Martin CUBE Mini
Active layer	PES	PES
Support layer	PET/PES	PET/PES
MWCO (kDa)	150 kDa	150 kDalton
Pore size (μm) / Pore size (μm) nominal-maximal	0.04	0.035-0.1
Membrane area	2 panels of 0.33m^2 each, total 0.66m^2	5 panels of 0.09m^2 each, total 0.45m^2
Gaps between the membranes	8mm	6mm
Water permeability ($\text{L}/(\text{m}^2\text{ h bar})$)	> 280	> 280

Source: www.microdyn-nadir.com and www.martin-membrane.de

3.4.2 Membrane Bioreactor operation

The experimental work began by verifying the functionality of the laboratory immersed membrane bioreactor (iMBR) unit using tap water. Two commercial PES modules were immersed in the bioreactor filled with tap water. Air volume flow of $1\text{m}^3/\text{h}$ was supplied in the bioreactor tank through the diffusers installed under the membrane modules and the functionality of the aeration system was ensured. The MBR operating conditions were set by adjusting the suction pump speed to 25.3 ml/minute with an operation time interval of 12 min in suction mode, followed by relaxation for 2 minutes then suction again for 12 minutes and so on. The proper performance of the pH meters, temperature sensor, conductivity meters, feed pump, sampling valves and other components of the MBR unit

was ensured. The period for acclimation of the membrane pores (pore swelling) was allowed until a relatively constant water permeability of around $90 \text{ L} / (\text{m}^2 \text{ h bar})$ was attained. Proper performance of the MBR system was ensured and the unit was confirmed to be ready for experimental work using raw fish processing wastewater.

To start off the experiments, the tap water was discharged and bioreactor tank was seeded with 5L of bacteria rich (activated) sludge. This was obtained from a secondary treatment sedimentation tank at the JKUAT water treatment plant. It was then refilled with pre-filtered raw fish processing wastewater, screened through a mesh of 0.8 mm and the volume topped up to 97L. A low water flux rate of up to $1.5 \text{ L}/(\text{m}^2 \text{ h})$ was set for both modules. The dissolved oxygen concentration in the aeration tank was maintained in the range of 2 to 5mg/L. The aerobic microorganisms in the aeration tank metabolized organic carbon and nitrogen pollutants in the wastewater as filtration occurred simultaneously. The resultant clarified effluent (permeate) was drained through the outlet and was collected in clean containers for analysis. Refilling of the reactor tank with pre-filtered fish processing wastewater was carried out after every 24 to 48 hours to maintain the level above 60L mark and ensure the membrane modules remained immersed throughout the experimental period.

In a follow-up experiment a 70L PVC denitrification tank installed with a digital stirrer was introduced to the MBR unit to optimize the reduction of nitrates in the aeration chamber. The wastewater was recirculated between the aeration tank and the denitrification tank at a rate of approximately 7-10L/h, and for a hydraulic residence time (HRT) of approximately 21-64h. In the process, ammonia in the aeration tank was converted to nitrates and subsequently the nitrates were converted to nitrogen gas in the denitrification tank. Other biodegradable contaminants were also simultaneously metabolized as filtration subsequently occurred. The resultant clarified effluent (permeate) was drained through the outlet valve and was collected in clean containers for analysis during the experimental period. Some permeate was returned in the aeration tank to facilitate in diluting the MLSS thus enabling a slow adaption of the activated sludge while the rest was collected in permeate collection containers for other use. The MBR unit

was operated continuously for each experimental period with refilling done after every 24 to 48 hours in the same manner as described earlier. However, breaking intervals were applied to allow cleaning of the modules and removal of excess sludge generated during the process (about 2-3 L). The membrane modules were cleaned in an extra tank after having removed them from MBR. 12% sodium hypochlorite solution was used for removing fouling, the membranes were rinsed with clean water and were soaked in 50% citric acid to remove scaling. After cleaning the membranes, hydrogen peroxide diluted to 100mg/L was used to inactivate residual chlorine. Removal of excess sludge generated in the process was done after every 30 days via an outlet valve fixed at the bottom of the aeration tank. The sludge recovered was used in the surrounding farm as manure. For the MBR experiments, an acclimation period of about 3 weeks after start-up was allowed, before the start of data collection. Thereafter data collection started when the system had attained stable conditions in terms of Water Permeability (WP), flux rate and Transmembrane Pressure (TMP). Other parameters tested from the treatment process were the removal rate for COD, phosphate (P-PO₄³), ammonium-nitrogen (NH₄⁺-N) and nitrate-nitrogen (NO₃⁻-N). The parameters measured during the treatment process are described in the following section;

3.4.2.1 Water permeability (WP)

Water permeability test for the membrane modules was calculated as the flux rate per trans-membrane pressure (TMP) in accordance to Equations 10 to 12. Permeability was thus observed by plotting a curve for flux vs. TMP.

$$\text{➤ Flux} = \frac{\text{Volume Flow(Q)L}}{\text{SurfaceArea (m}^2\text{)} \times \text{hour (h)}} = \frac{\text{L}}{\text{m}^2\text{h}} \dots\dots\dots 10$$

$$\text{➤ Transmembrane Pressure (TMP) = Feed pressure (mbar) - Permeate pressure (mbar) } \dots\dots\dots 11$$

$$\text{➤ Water permeability (P) = } \frac{\text{Flux}}{\text{TMP}} = \frac{\text{L}}{\text{m}^2 \times \text{h} \times \text{mbar}} \dots\dots\dots 12$$

3.4.2.2 Mixed liquor suspended solid (MLSS)

The MLSS was carried out by collecting 40 ml of the reactor and permeate samples separately in clean ceramic crucibles. Each of the samples was dried in the oven for 24 hours and at temperatures of around 103-105 °C. The dried samples were cooled in desiccators to room temperature and weighed. The MLSS was therefore calculated as illustrated in Equation 13.

$$\text{MLSS} = \frac{C_1 - D_1}{40} - \frac{C_2 - D_2}{40} \times 1000 = \frac{g}{l} \dots \dots \dots 13$$

Where:

C₁ weight (g) of ceramic crucible and dried residue of reactor sample

D₁: weight (g) of empty ceramic crucible used for reactor sample

C₂: weight (g) of ceramic crucible and dried residue of permeate sample

D₂: weight (g) of empty ceramic crucible used for permeate sample

3.4.2.3 Hydraulic Residence Time (HRT)

The duration of time taken by the water in the reactor before being removed as effluent was determined by calculating the HRT. This was calculated as the hydraulic volume of the MBR divided by the permeate flow rate. This is illustrated in Equation 14

$$\text{HRT} = \frac{\text{Hydraulic volume of the MBR (97 L)}}{\text{Permeate flow } \left(\frac{L}{h}\right)} = h \dots \dots \dots 14$$

3.4.2.4 Food to microorganism (F/M) ratio

The relationship between food available and micro-organisms present in the reactor was determined by calculating the F/M ratio as illustrated in Equation 15.

$$\text{F/M} = [\text{COD Kg/L} \times \text{Q (L/d)}] / (\text{MLSS (Kg/L)} \times \text{tank volume(L)}) \dots\dots\dots 15$$

Where: COD was the chemical oxygen demand in Kg/L

Q was the volume flow (L/d) per day

3.4.2.5 Organic loading rate (OLR)

The rate of inflow of organic matter (g) in the reactor was determined by calculating the (OLR). This is illustrated in Equation 16

$$\text{OLR} = (\text{COD Kg}) / (\text{L}) \times (\text{Q (L/d)}) / (\text{tank volume}) \dots\dots\dots 16$$

Where:

COD was the chemical oxygen demand in Kg/L

Q was the volume flow (L/d) per day

3.4.3 Critical flux determination

A sequential test for PES and PBM membrane module was conducted in the MBR to determine the critical flux for the tested modules. This was achieved by increasing the speed of the suction pump from 0.5V (25.3 ml/minute) to 1.11 V (55.6 ml/minute) with time intervals of 24 hours (where 5000 ml/minute = 99 Volts). Critical flux was observed by plotting a curve for flux vs. TMP.

Operation conditions for the MBR used for experimental study during initial tests with tap water and for subsequent tests with raw fish processing wastewater are presented in Table 3.2.

Table 3.2: Operating conditions of the MBR

Process parameters	Test with tap water, PES-membrane	Exp.1 (start-up exp.) PES membrane	Follow-up exp. PES membrane	Exp.2- Microdyn-Nadir module and	Exp.3, PES and PBM-coated membrane
Air flow (m ³ /h)	1±0.1	1±0.1	1±0.1	1±0.1	1±0.1
Temperature (°C)	25±1	25±1	25±1	25±1	25±1
TMP (mbar)	45-55	45-55	45-55	120-180	200-230
pH	7.0±0.5	7.0±0.5	7.5±0.5	7.0±0.5	7.0±0.5
Permeate flux (L/m ² ×h)	2.3-6.9	3.8-7.6	6.8-7.6	5.3-7.6	4.4- 4.9
Water permeability (L/m ² hbar)	90.9-153.1	82.9-165.8	68.2-151.5	56.4-61.1	22.2-24.4
HRT (h)	21.6-64.7	21-64	18-64	27.7-45.0	38.4 - 45.7
F/M ratio Kg COD/ (Kg MLSS.d)	< LOD	0.05-0.26	0.03-0.21	0.05-0.27	0.09-0.38
Organic Loading Rate (OLR)(Kg COD/m ³ .d)	< LOD	0.3-1.6	0.6-1.4	0.8-2.6	0.8-2.3
Mixed Liquor Suspended Solid (MLSS) (g/L)	< LOD	5.8-6.3	6.0-8.0	6.3-8.2	6.0-8.0

Where (< LOD) means below the limit of detection.

The various analytical methods used to characterize the effluent (permeate) obtained from the treatment process are described as follows;

3.4.4 Analytical methods

3.4.4.1 Dissolved oxygen (DO) determination

The wastewater was analyzed for dissolved oxygen concentration (amount of oxygen present in water) using the HQ30d Portable multi-parameter meter from Hach (Germany) with a measurement range of 0.01 to 20mg/L and a resolution of 0.01mg/L.

3.4.4.2 Biological Oxygen Demand (BOD)

The wastewater was analyzed for 5-day Biological Oxygen Demand (BOD₅) in accordance to the standard methods for the examination of water and wastewater (APHA, 2017).

3.4.4.3 Chemical Oxygen Demand (COD)

The concentration of COD in feed and permeate was determined using COD cell tests (Method 1.14541) and spectrophotometer Spectroquant® NOVA 60 from Merck KGaA (Germany). The method had a measurement range of 25–1,500 mg/L (COD) and standard deviation of ±0.65%. COD removal rate was determined as illustrated in Equation 17.

$$\text{➤ } \% \text{COD (removal rate)} = 1 - \left(\frac{\text{COD}_P}{\text{COD}_F} \right) \times 100 \dots \dots \dots 17$$

Where COD_P is the COD of permeate and COD_F is the COD of the feed.

3.4.4.4 Nitrogenous compounds measurement

For the raw wastewater (feed) and permeate, the (nitrogenous) N-compounds were analyzed as nitrate-nitrogen (NO₃⁻-N) and ammonium-nitrogen (NH₄⁺-N). All NH₄⁺-N and NO₃⁻-N were analyzed with the spectrophotometer Spectroquant® NOVA 60 using ammonium cell test (method: 1.14752.0001) and nitrate cell test (method: 1.14542.0001) from Merck KGaA (Germany) respectively. The range of measurement was 0.2–8 mg/L (NH₄⁺-N) with a standard deviation of ±1.0%. The method for NO₃⁻-N analysis had analytical measuring range of 0.5–18 mg/L, with a standard deviation of ±1.5%. Percentage removal rate was determined as illustrated in Equation 18.

$$\text{➤ } \text{Nitrogenous compounds (removal rate)} = 1 - \left(\frac{N_P}{N_F} \right) \times 100 \dots \dots \dots 18$$

Where N_P is the N- Nitrogenous compounds of permeate and N_F is the N- Nitrogenous compounds of the feed

3.4.4.5 Phosphates measurement

The phosphate in the raw wastewater (feed) and permeate was determined as orthophosphate with a spectrophotometer Spectroquant® NOVA 60 and cell test (method: 1.14729.0001) from Merck KGaA (Germany). The analytical measuring range for the method was 0.5-30mg/L (P-PO₄³⁻ mg/l), with a standard deviation of ±0.55%. Percentage removal rate in permeate was calculated as illustrated in Equation 19.

$$\text{➤ Phosphates (removal rate)} = 1 - \left(\frac{P_P}{P_F} \right) \times 100 \dots \dots \dots 19$$

Where P_P is the P- Phosphates of permeate and P_F is the P- Phosphates of the feed.

3.5. Optimization of commercial PES membrane modules

Process optimization was conducted using two commercial flat Polyethersulfone (PES) membrane modules (from Microdyn-Nadir). The two modules were immersed in the MBR unit aeration tank that was filled with raw fish processing wastewater (screened through a mesh of 0.8mm). The initial operating conditions were set as described in Table 3.2. The operation of the MBR unit was then started with a low water flux rate of up to 1.5 L/(m² h) for both modules to allow acclimation of the membrane pores as they get used to the new feed. The dissolved oxygen concentration was maintained in the range of 2 to 5mg/L. After acclimation, the flux rate was gradually increased from 1.5 to 6.0L/(m² h), while maintaining a constant transmembrane pressure (TMP), until a stable water permeability (WP) rate was achieved. The hydraulic residence time (HRT) in the bioreactor was varied in the range between 21-25h to optimize biodegradation performance. The modules were tested in parallel as per the procedure described in details in Section 3.4.2. The MBR was operated continuously for 120 days during the start-up experiment with refilling done to maintain the modules immersed as described in Section 3.4.2. The process parameters for the WP, flux and TMP were determined as described in Section 3.4.2.1. The removal rate for COD, NO₃⁻-N, NH₄⁺-N and PO₄³⁻-P in the treatment system was determined as described in Sections 3.4.4.1-3.4.4.5

In a follow-up experiment removal of NO_3^- -N and NH_4^+ -N was optimized by recirculating the wastewater between the denitrification tank and the aeration tank at a rate of approximately 7-10L/h, and for a hydraulic residence time (HRT) of approximately 22-25h. The recirculation process was carried out continually throughout the experimental period with constant stirring of the wastewater in the denitrification tank at a rate of 300 revolutions per minute and with refilling of the reactor tank after 24-48h as described in section 3.4.1. Reduction of PO_4^{3-} -P was improved by adding 55.2mg/L of Alum as Aluminum sulphate $\text{Al}_2(\text{SO}_4)_3 \cdot 18\text{H}_2\text{O}$ continually into the denitrification tank for a period of 30 minutes whenever the MBR was refilled with new feed (Gkotsis *et al.*, 2017). The pH of wastewater varied between 6.9 and 7.0. The optimal operating parameters for treatment of fish processing wastewater in an immersed membrane bioreactor (iMBR) unit were determined and established.

3.6. Performance of Microdyn-Nadir and CUBE Mini Martin module

The MBR unit was further operated with two modules of different construction but made of the same UF/PES material. One commercial UF/PES MBR 0.33m² flat sheet membrane module of 2 panels from Microdyn-Nadir and one UF/PES MBR CUBE Mini 0.45m² flat sheet membrane module of 5 panels from MARTIN Systems were immersed in the MBR aeration tank. The optimized operating conditions of the MBR unit were set and the process was conducted as described in Section 3.5. A sequential test for the two modules was conducted for a period of 80 days to compare their performance with respect to improved resistance to fouling. In this experiment, the fish processing wastewater was recirculated between the denitrification tank and the aeration tank at a rate of approximately 10L/h, and for a hydraulic residence time (HRT) of approximately 22.4-29.0h with Microdyn-Nadir module and 27.2-35.0h with Martin Systems module. Refilling of the reactor tank was ensured after 24 - 48h as described in Section 3.4.2 to keep the modules submerged during the experimental period. The ability of the two modules to resist fouling was determined by evaluating the change in the rate of WP, flux and TMP (Section 3.4.2.1) with operation time. Further, the removal efficiency for COD,

NO_3^- -N, NH_4^+ -N and PO_4^{3-} -P in the treatment system was determined as described in section 3.4.4.1-3.4.4.5.

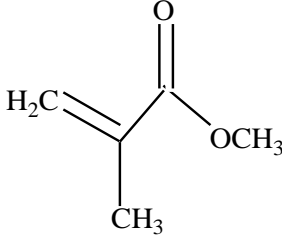
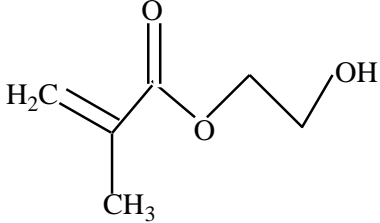
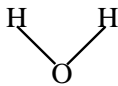
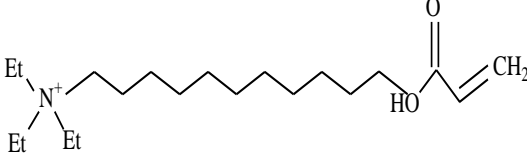
3.7 Development of low fouling PBM-coated membrane

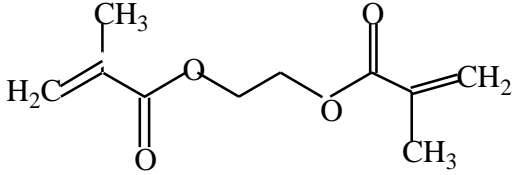
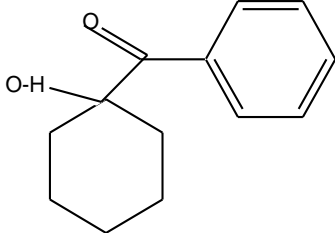
3.7.1 Materials and methods

3.7.1.1 Chemical reagents and composition

The 2nd experimental stage of this study was carried out by developing a low fouling membrane through surface modification of commercial PES membrane using a polymerizable bicontinuous microemulsion (PBM) technique by use of ultraviolet (UV) light. The chemical reagents used in this work were of high purity (>98%), purchased from Sigma-Aldrich. A laboratory made Acryloyloxyundecyltriethylammonium bromide (AUTEAB) polymerizable surfactant was used (Mancuso *et al.*, 2017). A list of the chemical reagents used for preparation of the coating material (polymerisable bicontinuous microemulsion-PBM) is presented in Table 3.3. The coating was developed within a collaborative co-operation between the University of Calabria, the Institute of Membrane Technology and the Karlsruhe University of Applied Sciences (Galiano *et al.*, 2015).

Table 3.3: Chemicals used for photo initiated PBM preparation

Name	Molecular formula (MF), Chemical structure and Molecular weight (MW)	Function
Methyl methacrylate (MMA)	 <p data-bbox="613 709 1243 779">MF: C₅H₈O₂ g/mol MW: 100.12</p>	Monomer constituting the oil phase
2-Hydroxyethyl methacrylate (HEMA)	 <p data-bbox="613 1050 1243 1121">MF: C₆H₁₀O₃ g/mol MW: 130.14</p>	Co-surfactant
Water	 <p data-bbox="613 1318 1243 1388">MF: H₂O g/mol MW: 18</p>	Aqueous phase
Acryloyloxyundecyl triethyl ammonium bromide (AUTEAB)	 <p data-bbox="613 1669 1243 1732">MF: C₁₇H₃₅O₂ 271g/mol MW:</p>	Cationic surfactant

Ethylene glycol dimethacrylate (EGDMA)		Cross-linker
	MF: C ₁₀ H ₁₄ O ₄ g/mol	MW: 198.22
1-Hydroxycyclohexyl phenyl ketone		Photo initiator
	MF: C ₁₃ H ₁₆ O ₂	MW: 204.27g/mol

The chemical composition used for preparation of UV-LED PBM microemulsion is shown in Table 3.4

Table 3.4: Chemical composition of PBM coating solution

Chemical	Viscosity (mm ² /s)	Percentage weight (w%)	Amount of chemical added	Total amount of PBM (g)	Unit
DI- water	1	41	4100 μl	10	μl
MMA	0.569	21	2240 μl	10	μl
HEMA	6.36	10	932.5 μl	10	μl
EGDMA	3.038	3	280 μl	10	μl
AUTEAB	Powder	25	2517.5mg	10	M
Photo Initiator (Irgacure 184)	Powder	1.8	63mg	3.5	Mg

Source: (Galiano, *et al.* 2018).

3.7.1.2 Preparation of the PBM coating solution

The polymerizable biocontinuous microemulsion (PBM) coating solution was prepared by placing 41% of deionized water (DI) to a 25ml reagent bottle. The DI water had a conductivity of 5μS/cm. A portion of 21% monomer MMA was added to the deionized

water thus forming a mixture of oil and water. The mixture was stirred for about 2 minutes using a magnetic stirrer and to this, 10% of co-surfactant HEMA was added. A portion of 3% of EGDMA (a cross-linker) was slowly added to the mixture with continued stirring and 25% of AUTEAB surfactant was then added to make a clear and transparent PBM solution. After preparation, the PBM solution was kept at a temperature between 20°C and 25°C ready for the polymerization process.

Polymerization of the PBM solution was carried out using UV based initiators. To initiate the process, a portion of 63mg photoinitiator (Irgacure 184) was added to 3.5g PBM solution. The mixture was mechanically stirred to dissolve the photo-initiator and the resulting solution was finally ready for membrane coating. The PBM preparation process is illustrated schematically in Plate 3.4.

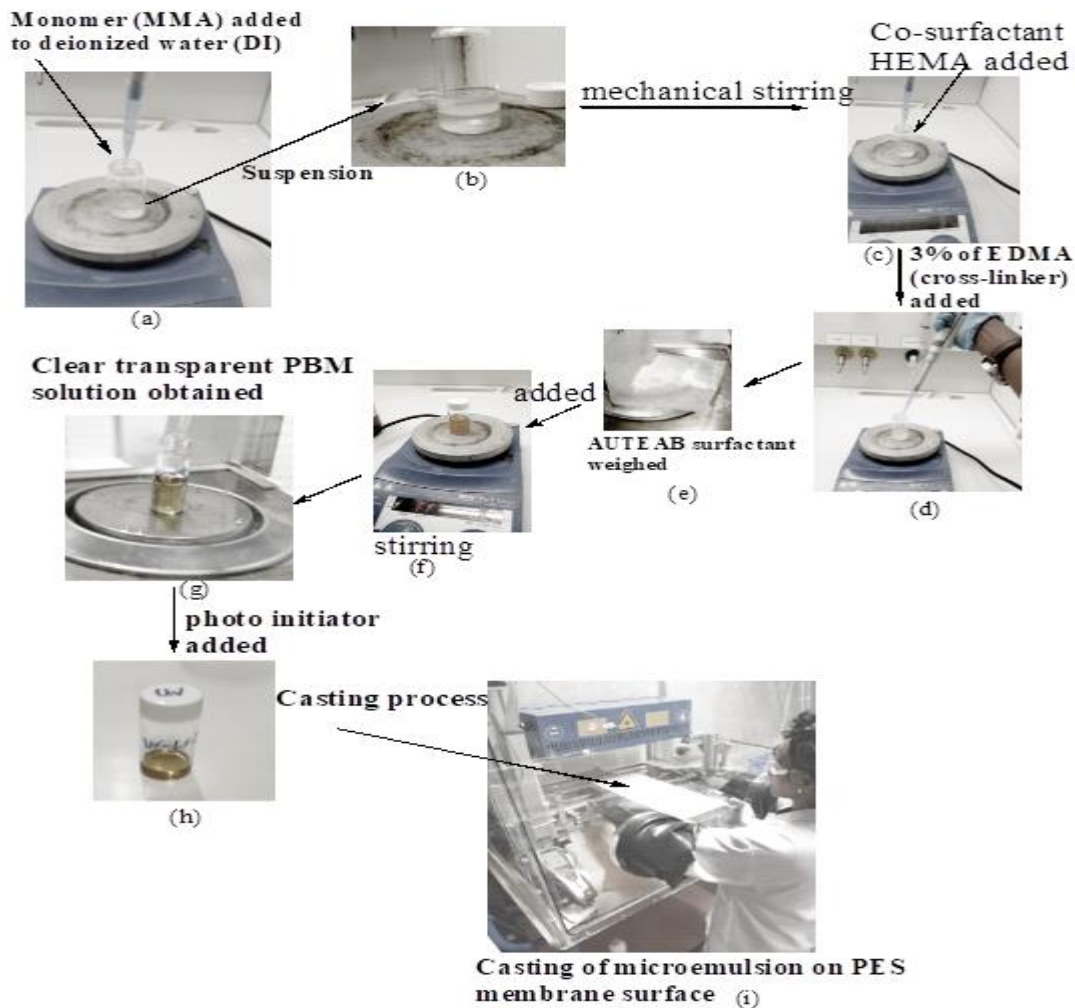


Plate 3.4: Preparation process for PBM microemulsion (Karlsruhe University of Applied Sciences, Germany)

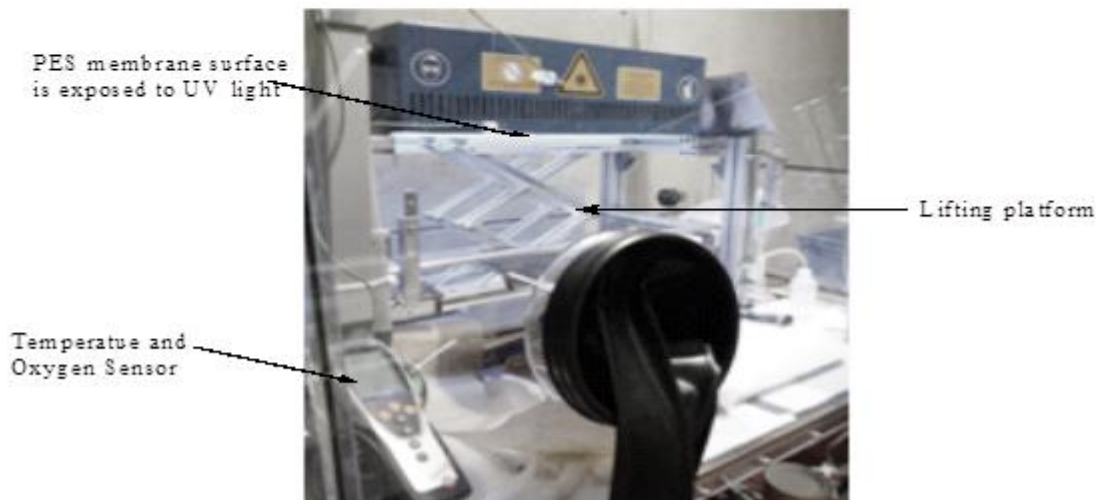
3.7.1.3 Membrane casting chamber

Coating process for the PES membranes was conducted in a membrane casting chamber purged with gaseous nitrogen (N_2). The chamber was installed with a thermostat to facilitate control of temperature and a cooling fan. A UV-LED lamp was installed in the upper part of the chamber. Other components placed in the chamber included a temperature sensor, an oxygen sensor, and a casting knife with $4\mu\text{m}$ wet coating layer thickness. A photo of the membrane casting chamber is shown in Plate 3.5 and the coating process is presented in plate 3.6 respectively.

Plate 3.5: Photo of membrane casting chamber (Karlsruhe University of Applied Sciences, Germany)



(a) PBM coating process conducted in a casting chamber



(b) Photo initiated polymerization

Plate 3.6: Coating of membrane and irradiated with UV light

3.7.1.4 Membrane coating process

A low fouling membrane was developed by casting the PBM coating solution on a commercial PES membrane sheet. The process was initialized by attaching the membrane

sheet to a glass plate that was placed inside the casting chamber. The chamber was continually purged with nitrogen to ensure oxygen level remained below 1% and with temperature maintained at $24\pm 1^\circ\text{C}$. The PBM solution with photo initiators added was cast on the surface of PES membrane sheet using a casting knife of $4\mu\text{m}$ (Plate 3.6a). The membrane was then lifted to the desired height and was irradiated with **ultraviolet** (UV) light of wavelength 365nm (Plate 3.6b). The irradiation time was set for 60 seconds to ensure a complete curing of the layer. The procedure was in agreement with that of Galiano *et al.*, 2018. In their study, the authors confirmed that UV photoinitiated polymerization process took a shorter curing time and was thus more viable for commercial scale-up in comparison to REDOX-based process that required a longer time. The UV photo-initiated polymerization process was therefore adopted for the current study. During the casting process, small membranes of size 0.0085m^2 for testing in a cross-flow testing cell were prepared. Subsequently, bigger membranes of size 0.06m^2 were prepared and sent to MARTIN Systems for lamination, and assembling to a 0.33m^2 membrane module for testing in the lab-scale MBR unit.

3.7.2 Characterization of PES and PBM- coated membranes

3.7.2.1 Chemical characterization

The chemical composition analysis for the PES membrane and PBM-coated membrane was conducted using the attenuated total reflectance infrared (ATR-FTIR) spectrophotometer (Bruker TENSOR II, Germany). This helped in identifying the presence of a variety of peaks being characteristic for the PBM coating on the modified membrane. The instrument was initialized by acquiring a background spectrum (without any sample in the optical path) as part of setting up measurement parameters. The resulting background spectrum was compared to a reference spectrum provided in the manufactures manual. The instrument was calibrated by placing a polystyrene standard in the optical path. A scan was conducted and the resulting spectrum compared against a reference spectrum. In the same manner, samples were analyzed in triplicates and spectrums of absorbance against wave number obtained in the range 400 cm^{-1} to 7500cm^{-1} . For this

work, 32 number of scans were conducted with a resolution of 4cm^{-1} to ensure good peak resolution. Correlation of the absorbance bands obtained from the two tested PES and PBM- coated membranes was used for data interpretation.

3.7.2.2 Surface characterization

Surface characterization was done by measuring the contact angle using a contact angle measurement (CAM) instrument (Data Physics SCA 20, Germany), by evaluating the water contact angle for the active side of PES membranes and the modified PBM-coated membranes. The instrument was initialized and calibrated by leveling the sample stage and by viewing the lens angle in order to obtain an acceptable value. Measurement of surface tension was carried out using the sessile drop method. A portion of $5\mu\text{L}$ deionized water was dropped on to the active side of PES membranes using a microliter syringe. A drop profile fitting method was used to analyze the captured drop image within a span of 0-8 seconds. At least 3 measurements for contact angle were taken for each sample. The mean value and standard deviation for the measurements were calculated to determine their significant difference. Figure 3.4 and Plate 3.7 illustrate a schematic diagram of the CAM apparatus and, the measurement activity conducted on PES and PBM membrane active surface respectively.

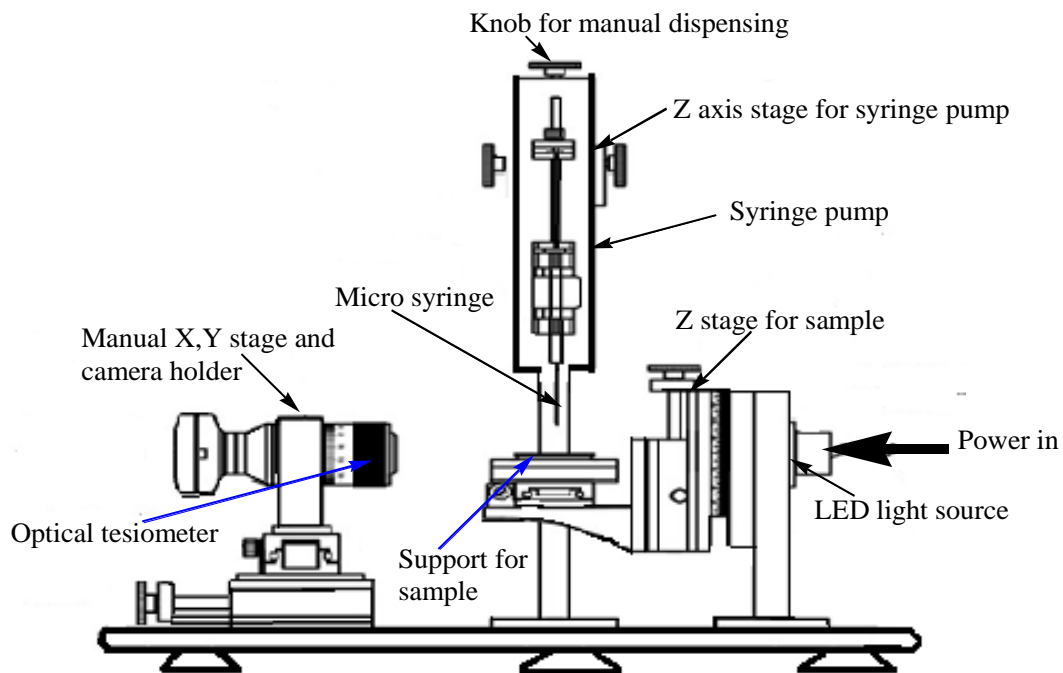


Figure 3.4: Schematic diagram for contact angle measurement (Data Physics SCA 20, Germany)

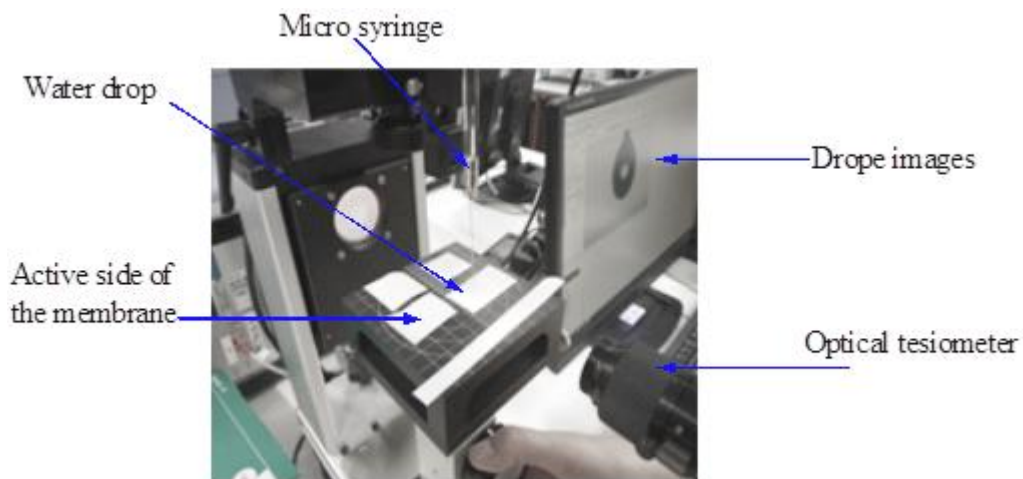


Plate 3.7: Measurement of contact angel for PES and PBM membrane surface (Data Physics SCA 20, Germany)

3.7.2.3 Preliminary fouling test for PES and PBM-coated membrane

An automated cross-flow testing cell (SIMAtec GmbH, Germany), was used for testing the fouling propensity of the PES and PBM-coated membranes using humic acid as the fouling agent. Humic acid constitutes a brown color and was therefore used to treat the membranes by inducing fouling. The fouling characteristic of the membranes was evaluated by comparing the intensity of color deposited on membrane surface after treatment. The test was initiated by placing two membranes (commercial and PBM coated) with an active membrane area of 0.0085m^2 each, in series in the flat membrane test cell of the automated cross-flow testing cell. The experiment was conducted using humic acid with a concentration of 100mg/L . In this process, 2L humic acid solution was added into the feed tank and the operation start switch put on to pump the feed solution into the membrane module and through the membrane at the set pressure of 500 mbar . The experiment was conducted continuously for 24h by recirculating permeate and concentrate coming out of the membrane module back to the feed tank. The permeate water flux and the visual appearance of the membranes after testing with humic acid was compared. The intensity of their color was noted as an indication of the membrane's fouling propensity. A schematic illustration and a photo of the auto-controlled cross-flow testing cell used are shown in Figures 3.5 and Plate 3.8.

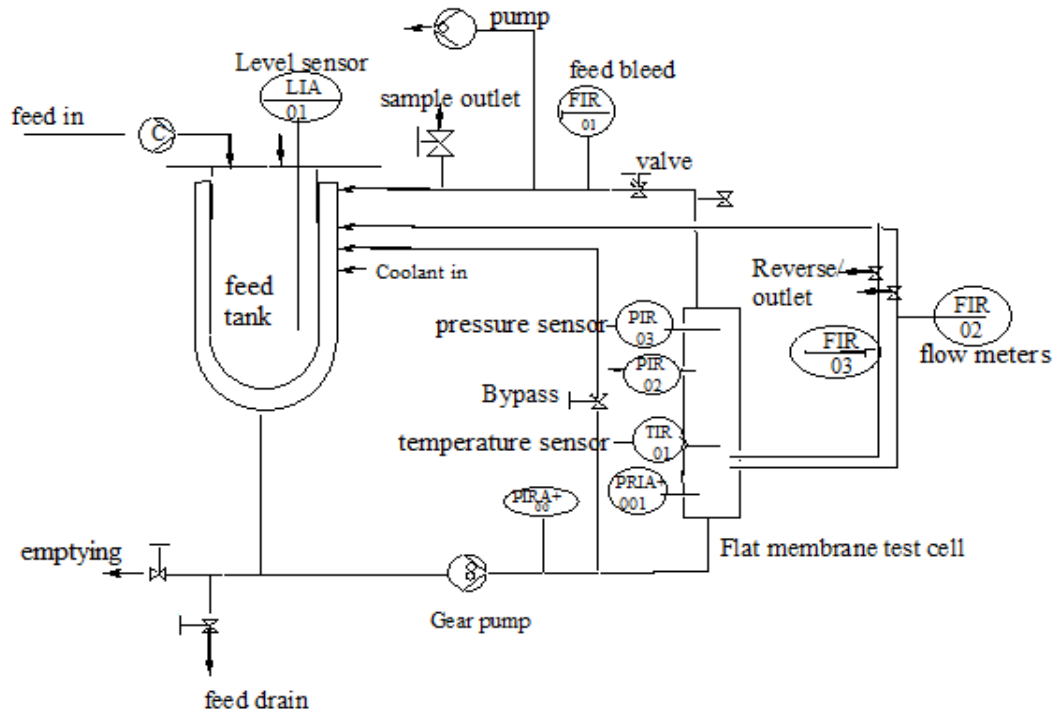


Figure 3.5: Schematic diagram of an auto-controlled cross-flow testing cell (SIMAtec GmbH, Germany)

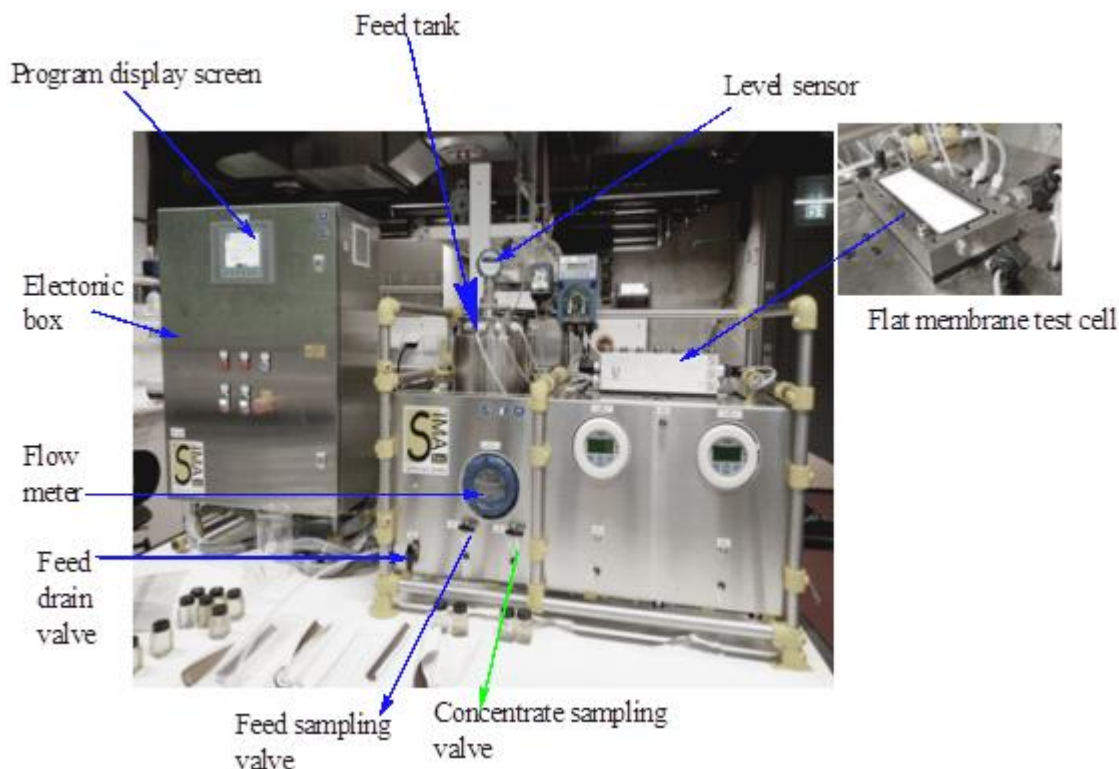


Plate 3.8: Schematic diagram of the cross-flow testing cell (SIMAtec GmbH, Germany).

3.7.3 Comparative study of PBM-coated and commercial PES membrane modules

A comparative study was conducted to determine the significant differences between the performance of PBM coated PES membrane module and commercial PES membrane module with respect to improved resistance to fouling, removal of COD, NO_3^- -N, NH_4^+ -N and PO_4^{3-} -P among other parameters. CUBE Mini 0.45m² flat sheets (FS) membrane modules of 5 panels laminated with PES membranes and a CUBE mini of same dimension laminated with PBM-coated PES membranes were immersed in Membrane Bioreactor (iMBR) unit. The process was initiated by pumping the fish processing wastewater into the denitrification tank, and by recirculating the feed between the denitrification tank and the aerobic tank at a rate of approximately 10L/h, and for a hydraulic residence time (HRT) of approximately 27.4 h -31.7h for PES module and 38.4 – 46.0 h for the PBM coated module. The MBR operating conditions optimized during the start-up experiment

were used for testing the modules as described in Section 3.4.2. A sequential test for the two membrane modules was conducted continuously in the iMBR for 80 days. The ability of the two modules to resist fouling was determined by evaluating the rate of WP, flux and TMP (Section 3.4.2.1) among other parameters and through critical flux measurement described in Section 3.4.3. The removal of COD, NO_3^- -N, NH_4^+ -N and PO_4^{3-} -P in the treatment system was determined as described in Section 3.4.4.1-3.4.4.5. The PBM-coated membrane module was tested for the first time for treatment of fish processing wastewater in a lab-scale immersed membrane bioreactor (iMBR) unit in the JKUAT-IEET laboratory. The lab-scale iMBR used is illustrated in Figure 3.6.

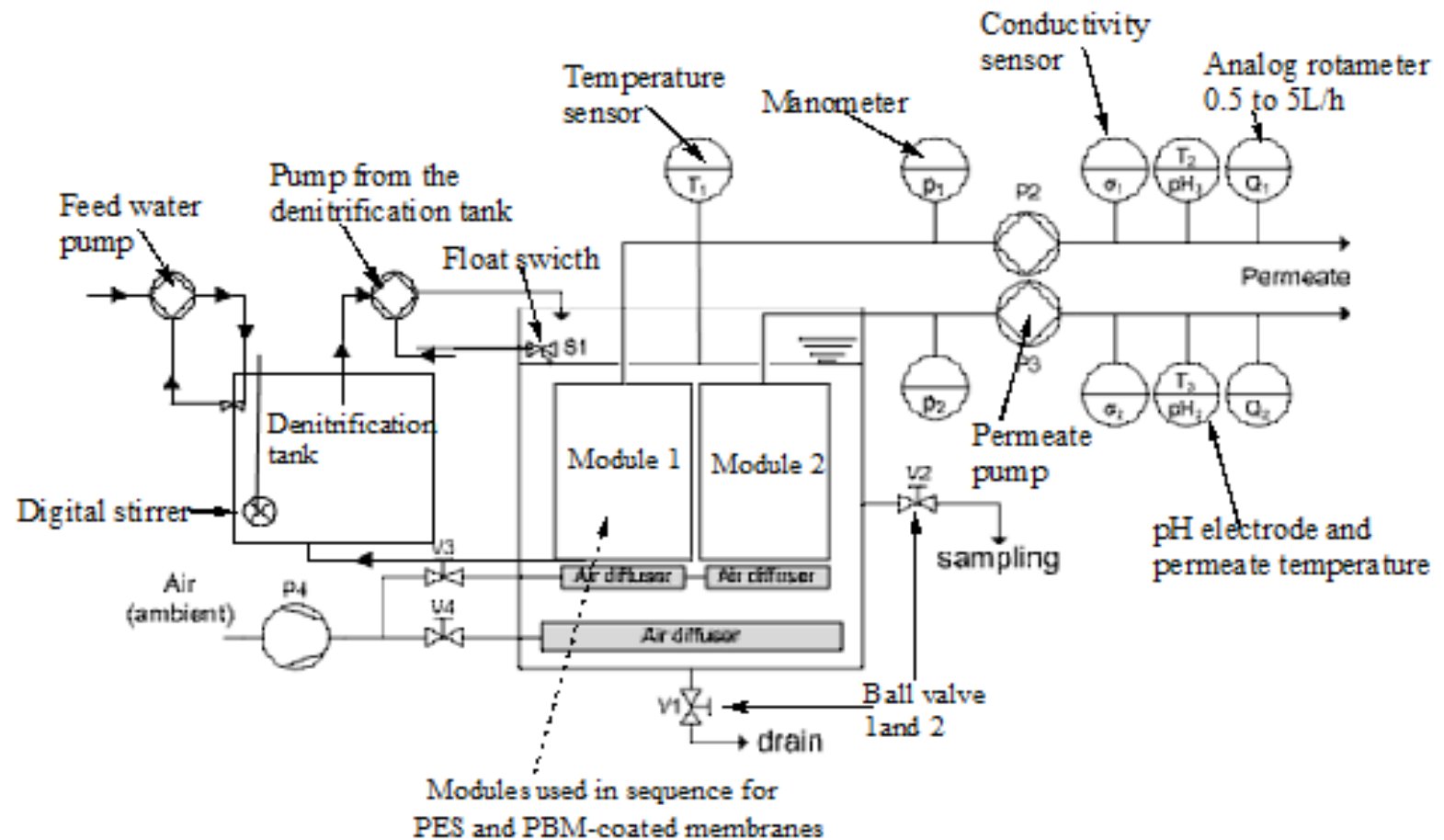


Figure 3.6: Schematic diagram for the immersed membrane bioreactor (Karlsruhe University of Applied Sciences, Germany)

3.8 Cost analysis methodology

3.8.1 The cost-benefit analysis for a containerized MBR system

The cost analysis for a containerized MBR with a volume flow capacity of 10m³ per day was calculated as the difference between the Total input and Total output. The total input was the sum of capital expenditure (CAPEX) and operational expenditure (OPEX). The total output was obtained as the cost per m³ of treated water generated and the benefit of reuse over the course of the plant life (Young *et al*, 2013). All equipment and components were priced as per the information provided by suppliers from the various companies. The unit currency used for this work was in Kenya shillings (Ksh). The specification for MBR components put into consideration in calculating capital expenditure are presented in Table 3.5.

Table 3.5: MBR components and equipment specification

Components and equipment			Description/ Quantity
Energy consuming components		permeate pump	1
		MBR feed pump	1
		recirculation pump	1
		blower for aeration	1
		Blower for membrane module	1
Tanks		stirrer	1
		denitrification tank	1000 L
		nitrification/ filtration tank	3000 L
		permeate collection tank	3000 L
Sensors		feed tank	3000 L
		dissolved oxygen sensor	1
		pressure sensor permeate line	1
		float switch intake tank/nitrification tank /permeate tank	3
		volume flow sensor permeate line	1
Infrastructure and other components		tubes and pipes	50m
		connectors	20
		drain valves	4
		sampling valve for nitrification tank, and permeate tank	2
		pre-filter (1mm mesh size)	1
		electronic installation (fuses, residual current dive (RCD), cables)	1
	Membrane module	membrane module	1 with membrane module area of 20 m ²

3.8.2 Calculation of CAPEX

The capital cost (expenditure) was calculated as indicated in equation 20.

$$\text{CAPEX} = \left\{ \frac{E + \left(\frac{L_m \text{ ksh}}{20 \text{ m}^2} \right)}{8 \text{ years (} t_{\text{mem}} \text{)}} \right\} = \text{ksh} \dots \dots \dots 20$$

Where: E= cost of equipment

L_m = membrane cost per m^2 membrane area (ksh/ m^2)

t_{mem} = membrane life in years

Equation 21 illustrates the calculation of capital expenditure per unit volume per day for a period of 25 years.

$$\text{CAPEX} = \frac{\left\{ \frac{E + \left(\frac{L_m \text{ ksh}}{20 \text{ m}^2} \right)}{8 \text{ years (} t_{\text{mem}} \text{)}} \right\}}{25 \text{ years} \times 364 \text{ days}} = \text{x} \frac{\text{ksh}}{\text{m}^3 \text{d}} \dots \dots \dots 21$$

3.8.3 Operation expenditure

The operational expenditure was determined as a summation of the cost for energy input, chemicals, waste management, labor and miscellaneous site services. The MBR had a total membrane area of 20 m^2 (one module) and flux set to $25 \text{ L/m}^2 \cdot \text{h}$ with a net production volume flow of 417 L/h ($10 \text{ m}^3 \text{d}^{-1}$), for a permeate pump working in intermitting mode (12

min suction mode, and relaxation for 2 minutes). The MBR had a daily volume flow capacity of 10m³ and expected energy expenditure of 800W was considered (Vicinaqua, 2017). The expected energy cost was 27-34% of the total operational cost (Young *et al.*, 2013). Labor cost was estimated in terms of contact hours depending on cleaning cycles conducted per year. Removal of sludge was estimated at 5 times per year (Vicinaqua, 2017). The maintenance cost was estimated at 30-50% of the cost of membrane replacement, blower and pump repairs and for other miscellaneous site services.

Determination of the total specific energy demand was done as illustrated in Equation 22.

$$\text{➤ } E_{\text{tot}} = \sum 24Wt / Q_p \dots\dots\dots .22$$

Where: W= rating for sum of the power consumption for each component (in kW)

E_{tot} = total specific energy demand (kWh/m³)

t = hours per day of operation divided by 24

Q_p = permeate flow in m³/d

Determination of specific energy cost was done as illustrated in Equation 23.

$$\text{➤ } \text{Specific energy cost} = (E_{\text{tot}} \times \text{ksh18}) = \text{ksh} \dots\dots\dots .23$$

Where: 1 kWh = 18ksh.

Table 3.6 presents the expected operational costs (expenditure) (OPEX) for the MBR.

Table 3.6: MBR operational expenditure (OPEX)

Operation costs / required items per year	Description	Estimate costs per year in Ksh
Chemical cost	Citric acid, Sodium Hypochloride (NaOCl), Sodium hydroxide Pellets (NaOH)	327
Waste management	Sludge removal	600
Labor cost	Technical support	12,000
Maintenance	Repairs	5,081

Operational expenditure (OPEX) was determined as shown in Equation 24 (Judd *et al*, 2015).

$$\text{OPEX} = L_E E_{\text{tot}} + \frac{364 L_M}{(J t_{\text{mem}})} + L_C + L_W + L_L + M = \text{ksh.} \dots \dots \dots 24$$

Where: L_E = cost of electrical energy in ksh /kWh

E_{tot} = total specific energy demand (kWh/m³)

L_M = membrane cost per m² membrane area (ksh/m²)

J = flux in L/m²h

t_{mem} = membrane life in years, t- (8 years)

L_C = chemical cost (3 times per year)

L_W = waste management (5times per year)

L_L = labor cost (12 times per year)

M= maintenance cost

The determination of operational expenditure (OPEX) per unit volume per day for a period of 25 years was done as shown in equation 25.

$$\text{OPEX} = \frac{(x \text{ ksh}/10^3)}{(364 \text{ days} \times 25 \text{ years})} = \frac{x \text{ ksh}}{\text{m}^3\text{d}} \dots \dots \dots 25$$

Where: the plant life is estimated as 25 years.

The total expenditure (TOTEX) or total input was determined by adding CAPEX and OPEX as indicated in equation 26.

$$\text{TOTEX} = \text{CAPEX} \times \text{m}^3 \left(\frac{x\text{ksh}}{\text{m}^3\text{d}} \right) + \text{OPEX} \times \text{m}^3 \left(\frac{x\text{ksh}}{\text{m}^3\text{d}} \right) = x\text{ksh}/\text{d} \dots \dots \dots 26$$

Where $x\text{m}^3$ = volume of treated water

3.8.4 Calculation of the total output

Total output was determined as the cost per meters cubed of treated water, rated according to the approved water tariff per month as stipulated by the water Act (No. 8 of 2002), for institutions using over 600m³ of water per month.

The total output was calculated as illustrated in Equation 27.

$$\begin{aligned} \text{Total output} &= \text{Treated water (x ksh/m}^3) \times \text{Total volume (x m}^3/\text{d)} \\ &= x \text{ ksh}/\text{d} \dots \dots \dots 27 \end{aligned}$$

Where 1m³ of treated water cost 48ksh as per the price offered by water service provider

The Total cost benefit was determined as the difference between total input and total output as shown in equation 31.

$$\begin{aligned} \text{➤ Total Output (x ksh/d) - Total Input (x ksh/d) =} \\ \text{x ksh/d Total cost benefit29} \end{aligned}$$

Where labor cost for operating a small containerized MBR system is assumed to be minimal

3.8.5 Comparative analysis of ASP, WSP and MBR treatment systems

A comparative analysis was conducted to evaluate the cost of a small containerized MBR plant relative to wastewater stabilization pond (WSP) and activated sludge process (ASP) all with a volume flow capacity of 10m³/d to 100m³/d (Judd *et al.*, 2015; Nobuyuki *et al.*, 2007). Table 3.7 presents the basic cost model equations used for comparing the 3 treatment systems (Young *et al.*, 2015; Judd *et al.*, 2015; Nobuyuki *et al.*, 2007).

Table 3.7: A cost model of MBR, ASP, and WSP treatment systems

Process	Design capacity (m ³ /day)	Capital expenditure (CAPEX) ksh m ³ /day	Land requirement (m ² m ³ /d)	Operating expenditure (OPEX) ksh m ³ /day	Reference
MBR	10-100	$y = 1060 x^{0.872}$	Small scale MBR containerized system minimal land requirement	$y = -0.0509 \ln x + 0.664$	Judd <i>et al.</i> , 2015
ASP	10-100	$y = 49,630 x^{0.277}$	$y = 212 x^{-0.514}$	$y = 578 x^{-0.190}$	Nobuyuki <i>et al.</i> , 2007
Waste stabilization ponds	10-100	$y = 474 x^{-0.32}$	$y = 326 x^{-0.37}$	$y = 995 x^{-0.71}$	Nobuyuki <i>et al.</i> , 2007

CAPEX, OPEX and land requirements were expressed as presented in equation 30.

➤ $Cost\ per\ unit\ volume\ (y) = (x)^b \dots\dots\dots 30$

Where: where x, and b are the variable constants

y = capital cost, annual operation and maintenance cost per unit volume, ksh/m³d

x = treatment volume in m³/d.

b = variation of cost per unit volume relative to size of a process

The costs may vary according to the capacity of the treatment plant, site design requirements and installation costs (where small-scale MBRs are available as containerized decentralized systems with minimal costs for installations, site redesign requirements and construction) (Judd et al., 2015). The capital expenditure (CAPEX) equation included the costs for acquiring and installation of screens, grit chamber, equalization tank, sedimentation tanks, and clarification ponds, sludge treatment facility, and construction of administrative offices among other necessary facilities. The cost of

power, maintenance, chemicals and labor was included in the equation used for determination of operational expenditure (Nobuyuki *et al.*, 2007). Graphs were used to determine the relationship between CAPEX and OPEX relative to the treatment volume for the 3 types of treatment systems.

CHAPTER FOUR
RESULTS AND DISCUSSIONS

4.1 Fish processing wastewater quality parameters

The quality of the fish processing wastewater used for Lab-scale MBR experiments was determined in JKUAT-labs. Tables 4.1-4.3 present the mean values for all measurements taken during the period of the study.

Table 4.1: Fish processing wastewater quality for lab scale MBR tests for PES membrane modules

Parameter	Mean values for wastewater quality in 2017				
Measured values	April	May	June	July	August
NH ₄ ⁺ -N (mg/l)	11.2±0.1	9.1±0.3	12.1±0.3	11.1±0.1	9.7±0.2
NO ₃ ⁻ -N (mg/l)	35.1±0.4	13.70±0.6	21.3±0.3	34.93±0.6	21.31±0.5
P-PO ₄ ⁻³ (mg/l)	10.3±0.5	8.3±0.3	18.7±0.7	10.1±0.3	6.8±0.5
COD (mg/L)	2349±113	1380±102	2100±124	960±102	509±105
BOD ₅ (mg/L)	320±0.5	260.87±0.2	300.60±0.5	204.91±0.5	300.10±0.3
pH	7.0±0.5	6.9±0.5	7.0±0.5	7.2±0.5	7.0±0.5
Conductivity (µS/cm)	376±0.5	317±0.5	369±0.5	391±0.6	356±0.5

Mean ± std. deviation, where n=17

Table 4.2: Fish processing wastewater quality for MBR lab scale test for PES Microdyn-Nadir, and CUBE Mini modules

Parameter	Mean values for wastewater quality in 2017-2018				
	December	January	February	March	April
COD (mg/L)	2042±121	1398±101	1593±137	1118±115	1716±151
BOD ₅ (mg/L)	526±0.5	336±0.5	363±0.9	278±0.6	345±0.9
NH ₄ ⁺ -N (mg/l)	32.1±0.1	30.7±0.5	32.1±0.3	28.2±0.2	31.7±0.2
NO ₃ ⁻ -N (mg/l)	1.9±0.5	2.9±0.1	3.8±0.5	3.9±0.5	1.6±0.2
P-PO ₄ ⁻³ (mg/l)	11.02±0.5	8.6±0.5	10.1±0.2	8.2±0.3	7.3±0.1
pH	7.0±0.5	7.0±0.5	7.0±0.5	7.4±0.5	6.8±0.5
Conductivity (µS/cm)	380±0.2	321±0.2	390±0.5	413±0.3	370±0.5

Mean ± std. deviation, where n=17

Table 4.3: Fish processing wastewater quality for MBR lab scale test for PES and PBM-coated CUBE Mini modules

Measured parameters	Mean values for wastewater quality in 2018-2019				
	December	January	February	March	April
COD (mg/L)	2067±131	1603±110	2123±217	1003±107	2123±121
BOD ₅ (mg/L)	362±0.4	289±0.4	324±0.3	289±0.4	324±0.3
NH ₄ ⁺ -N (mg/l)	21.8±0.3	24.2±0.3	21.4±0.3	9.2±0.5	10.2±0.1
NO ₃ ⁻ -N (mg/l)	6.7±0.4	5.5±0.7	9.7±0.3	20.8±0.2	22.7±0.3
P-PO ₄ ⁻³ (mg/l)	15.7±0.5	16.1±0.2	12.5±0.7	16.5±0.3	12.3±0.1
pH	7.0±0.5	7.2±0.5	7.6±0.5	7.0±0.5	7.2±0.5
Conductivity (µS/cm)	569±0.2	537±0.5	632±0.1	557±0.6	628±0.5

Mean ± std. deviation, where n=17

The Tables 4.1-4.3 presents wastewater parameters for the fish processing wastewater used for MBR tests at lab-scale. The wastewater was of high strength with 5-day biological oxygen demand (BOD₅) and chemical oxygen demand (COD) concentration varying between 289-516mg/l and 509-2349 mg/l respectively. This concentration was above <30mg/L and <100mg/L recommended by WHO guidelines for wastewater reuse for irrigation (WHO, 2006). The concentration of nitrogenous compounds was determined

as nitrate-nitrogen (NO_3^- -N) and ammonium-nitrogen (NH_4^+ -N) and varied between 12.1-37.2mg/L and 17.7-40.8mg/L respectively. Orthophosphate (PO_4^{3-} -P) concentration in feed varied between 7.7-20.1mg/L. The NH_4^+ -N, NO_3^- -N and PO_4^{3-} -P concentrations in the wastewater (feed) were all above the maximum allowable concentration of <5mg/L, 5-30mg/L and ≤ 5 respectively as per the WHO guidelines for wastewater reuse for irrigation (WHO, 2006). Discharge of effluent with high nutrient content in water bodies may cause pollution and eutrophication problems. The wastewater therefore requires biological treatment before releasing to natural water bodies.

It should be noted that the fish processing wastewater used for the lab-scale MBR experiments was of higher strength with respect to COD of 509-2349mg/l in comparison to 239-532mg/l for the wastewater at VicInAqua pilot site. These findings are based on the experimental results obtained on-site during pilot testing at the Nyalenda VicInAqua pilot plant. These results are presented in Table 1-3 in the Appendix 1.

4.2 Process performance of PES membranes and optimization results

Process study and optimization results were obtained and recorded as presented in the following section.

4.2.1 Rate of water permeability (WP), flux and transmembrane Pressure (TMP)

Performance of two commercial PES UF membrane modules was obtained by monitoring the rates of WP, flux and TMP with operation time in the MBR. The results for the Experiment 1 showed a successful optimization process as illustrated in Figure 4.1 and Figure 4.2 in the following section.

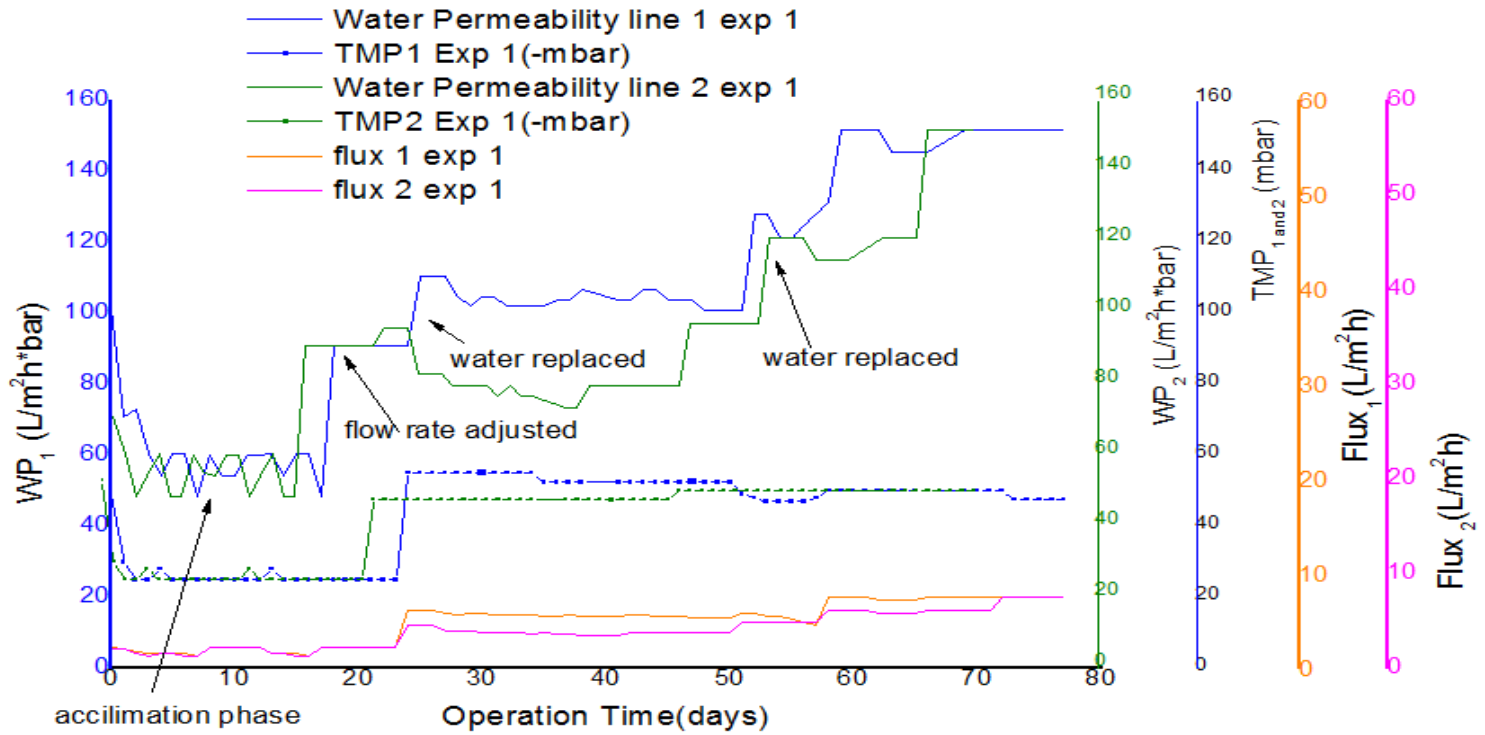


Figure 4.1: Water permeability (WP), flux and transmembrane pressure (TMP) with operation time (days) for Experiment 1

As observed in Figure 4.1 the MBR was operated with an initial low water flux of $1.5\text{L}/\text{m}^2\text{h}$ for both modules 1 and 2 at the start in order to allow the membrane pores adapt to the system during acclimation period. The start-up experiment was characterized by high fluctuations of TMP and was in range of 20 ± 1 to $36\pm 4\text{mbar}$. Low WP was also observed for both permeate lines varying between $56.8\pm 8\text{L}/\text{m}^2\text{hbar}$ and $54.1\pm 6\text{L}/\text{m}^2\text{hbar}$ for both modules 1 and 2 respectively with rather a longer residence time (HRT) in the range of 48h -62h. This was attributed to the instability of the system during acclimation phase as the membranes start getting used to the environment. On day 21, the water flux for both modules were gradually increased to $5.0\text{L}/\text{m}^2\text{h}$ to stabilize the system. Subsequently the HRT in the reactor decreased with the increase of flux to the range of 22 to 25h. Between day 25 and 56, a stable TMP was obtained between 40-50mbar and from 45-50mbar for both modules 1 and 2. High fluctuation on WP was however noted within this period thus the need to readjust the water flux further. From day 58 water flux was readjusted to $6.0\text{L}/\text{m}^2\text{h}$ the time when a slight increase in TMP between 45-55mbar and 46-55mbar was obtained for both modules 1 and 2 respectively. An increase in WP was also noted from 50.5 to $134.6\text{L}/\text{m}^2\text{ h*bar}$) and from 54.1 to $110.2\text{L}/\text{m}^2\text{ h*bar}$ for module 1 and 2 respectively. Notably for this system, WP was increasing when flux was readjusted and gradually increased, while TMP remained relatively constant for the period after acclimation. The membranes showed good performance during the start-up experiment with no fouling was noted. Further, the water permeability of both membranes achieved similar values between $101.8\text{-}115.1\text{L}/\text{m}^2\text{ h*bar}$ and with no significant difference ($t_{\text{calculated}} < t_{\text{critical}}$) for paired T-test (at 95 % confidence level) as illustrated in Table 4.4.

Table 4.4: Comparison of water permeability for the two tested PES UF membrane modules (One-way, paired t-test, n=0.05)

PES membrane modules	Water permeability (WP) Mean and STDEV	t-test	
		t calculated	t critical
Module 1	115.1±34.4	0.68	4.30
Module 2	101.8±33.9		

After achieving stable conditions in the MBR system, further experimental work was conducted in a follow-up experiment to optimize the performance of commercial PES modules. Figure 4.3. illustrates the rates of WP, flux and TMP with operation time in the MBR during a follow-up experiment (Experiment 2).

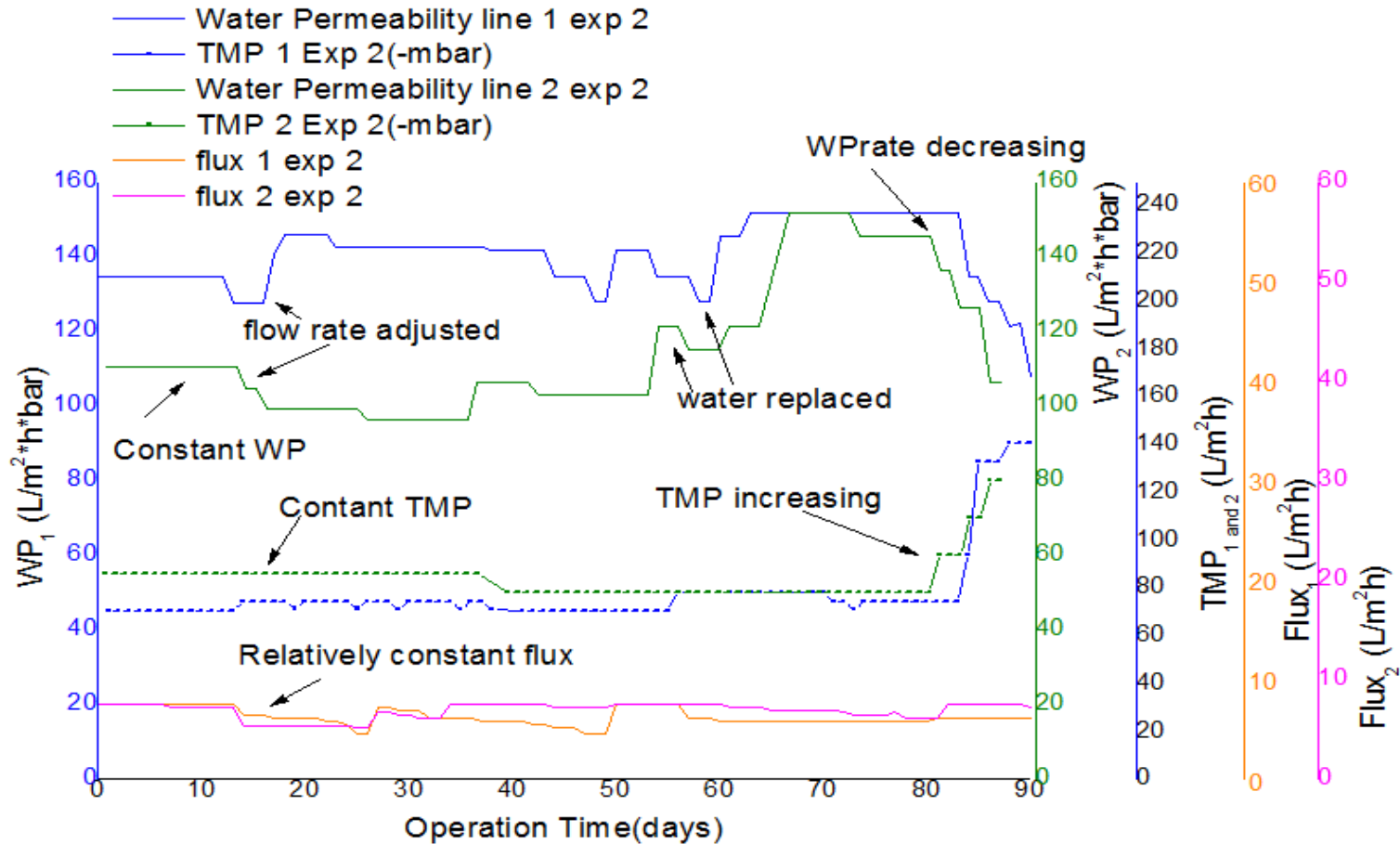


Figure 4.2: WP, flux and TMP with operation time (days) in a follow-up experiment

As observed in Figure 4.2 a constant TMP varying between 45-50mbar was observed for both modules right from the start of the experiment. Water permeability (WP) varying from 110.2 to 121.2L/m² h*bar and 127.6 to 151.5L/m² h*bar was obtained for both permeate lines 1 and 2 respectively with small fluctuations observed during the times when wastewater was refilled. The WP achieved was however high relative to 50.5L/m² h*bar and 54.1L/m² h*bar observed during the onset of Experiment 1 (Finger 4.1). The hydraulic residence time (HRT) was in the range of 22 to 25h. The stable conditions and high WP obtained in the follow-up experiment was an indication that the system had attained optimal operating conditions.

A gradual rise in TMP was however noted in both modules 1 and 2 in the range of 85-250mbar and 60-200mbar between day 80 to day 90 when the experiment ended. Also to be noted, a large difference in water permeability of module 1 and module 2 occurred what might be caused by increased fouling of module 2. A significant drop in WP for both modules was also noted in the same period. This was attributed to the onset of fouling to the membranes.

Membrane fouling is mainly attributed to particle deposition on the surface and in the pores of a membrane during filtration process. This increases mass resistance to influent flow, what might cause the TMP of the system to rise as the WP decreases due to loss of performance of the membranes (Tan *et al.*, 2016). Plate 4.1 illustrates fouling on PES membranes used in the submerged MBR unit during the experimental periods.



Plate 4.1: Membrane fouling

At this point, chemical cleaning of the membranes was conducted to recover the initial TMP. The process was conducted in an extra tank after having removed the modules from MBR. 12% sodium hypochlorite solution and 50% citric acid were used for removing fouling and scaling, respectively. After cleaning the membranes, hydrogen peroxide was used to inactivate residual chlorine (Saadia, *et al.*, 2015).

The optimal operating conditions for the MBR unit installed with PES membrane modules were obtained as presented in Table 4.5.

Table 4.5: Optimal operating parameters for MBR unit installed with PES/UF membrane modules

Process parameter	Unit	Range
Permeate flux	L/m ² *h	4.5-5.8
TMP	mbar	45-50
WP	L/m ² h*bar	110.2 - 151.5
pH	pH scale	6.9-7.1
Temperature	°C	25-26
HRT	h	22-25
Recirculation rate	L/h	10

4.2.2 COD removal efficiency for commercial PES membrane modules

Experimental results for the removal efficiency of COD for the two commercial PES modules showed good biodegradation performance with the mean COD in permeate varying between 85-89.3mg/L and within the maximum allowable concentration of < 100mg/L as per the WHO guidelines for wastewater reuse for irrigation. These results are presented in Figure 4.3 and 4.4 in the following section.

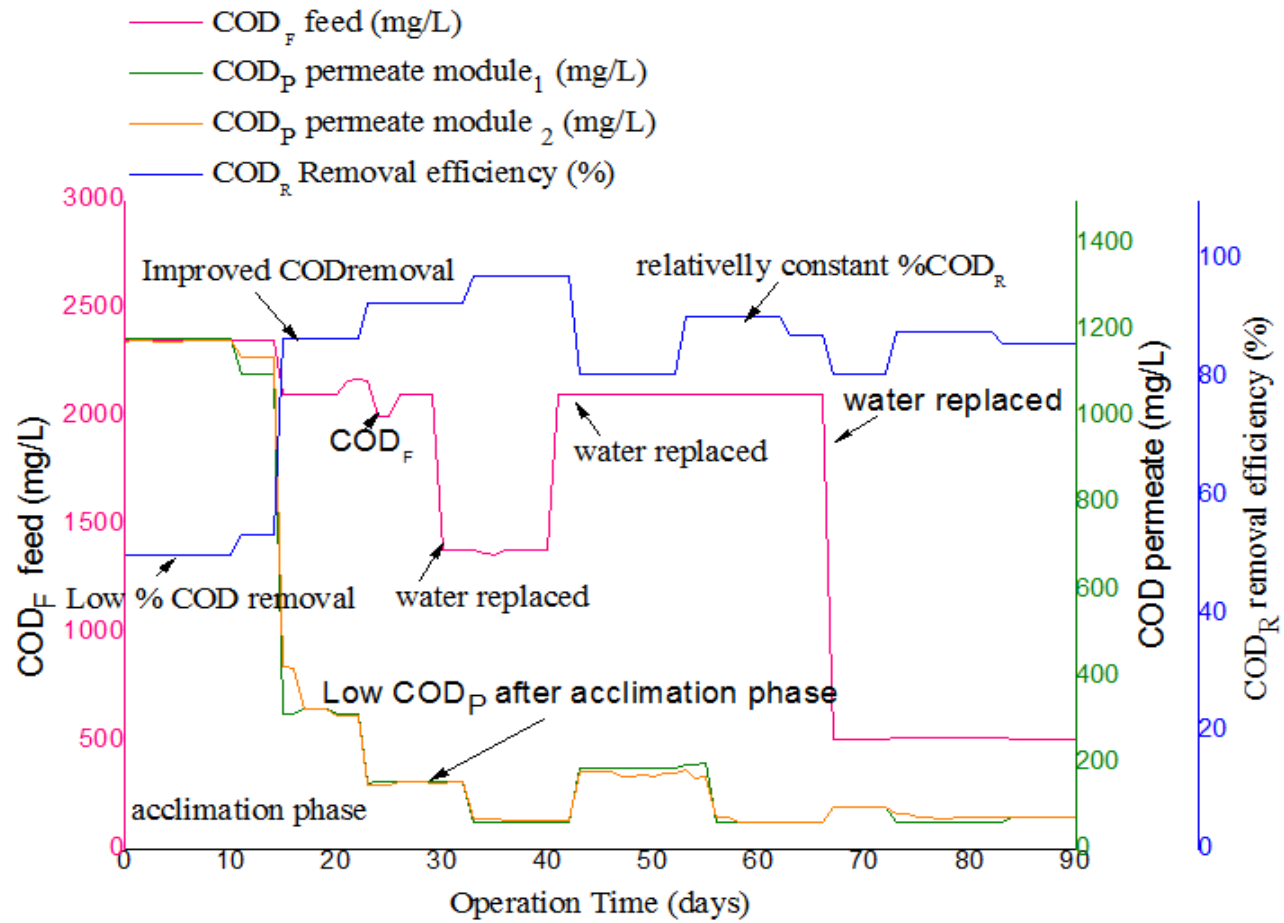


Figure 4.3: COD removal rate during Experiment 1(start-up experiment)

As illustrated in Figure 4.3, the start-phase of the experiment was characterized by low COD removal efficiency (COD_R) in the range of 45-48%, (blue line) from day 1 to day 14. This was attributed to the period required for acclimation, replication and growth of the aerobic bacteria culture inside the MBR reactor. Stable values of COD removal efficiency were however observed in the following period. COD concentration in feed fluctuated between $509.0 \pm 0.5 \text{ mg/L}$ and $2349.0 \pm 0.5 \text{ mg/L}$ while in permeate it varied after acclimation from $63.0 \pm 0.1 \text{ mg/L}$ to $187 \pm 0.3 \text{ mg/L}$ for both membranes. From day 60 the levels of COD in permeate were below the maximum allowable concentration of $< 100 \text{ mg/L}$ as per the WHO guidelines for wastewater reuse for irrigation (WHO, 2006). The COD removal efficiency in permeate varied between 85.0% and 95.9% for module 1 and 2 and was not significantly different ($t_{\text{calculated}} < t_{\text{critical}}$) for paired T-test (at 95 % confidence level) as illustrated in Table 4.6.

Tables 4.6: Comparison of COD removal efficiency in permeate for two commercial PES membranes (One-way, paired t-test, $n=0.05$).

Membrane module	Mean and STDEV COD % removal rate	t-test	
		t calculated	t critical (n = 0.05)
Module 1	85.0 ± 1.1	1.2	4.30
Module 2	89.1 ± 5.7		

Figure 4.4 shows the COD removal efficiency for the two commercial PES membranes during a follow-up experiment conducted after achieving stable conditions in the MBR system.

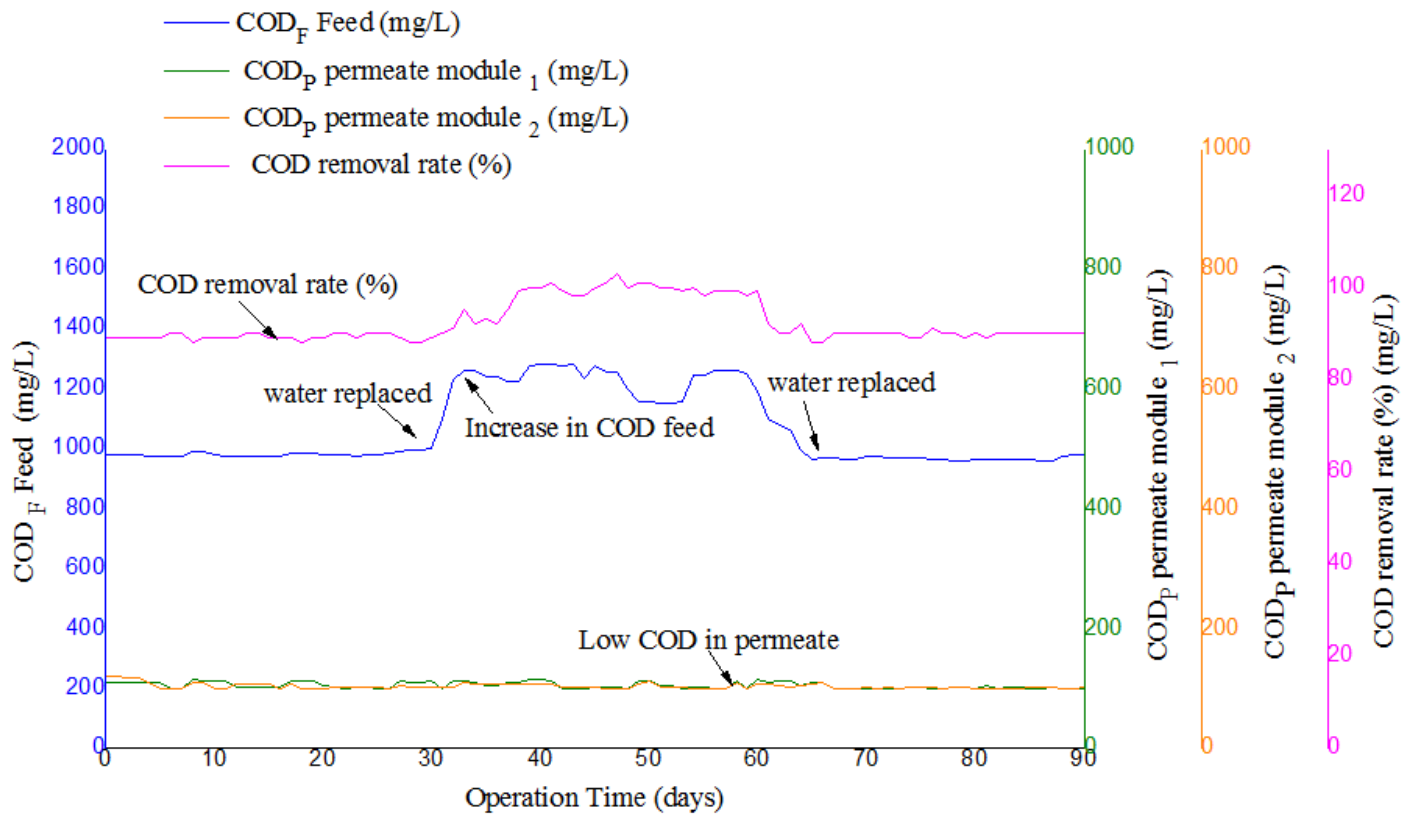


Figure 4.4: COD in feed, in permeate and COD removal efficiency in Experiment 1(in a follow-up experiment)

During the follow-up experiment, stable values for percentage COD removal rate were observed varying between 87.4 ± 7.8 and $89.3 \pm 6.9\%$ respectively for both modules 1 and 2 right from the start and for the entire duration of experimental period. COD concentration for feed was in the range of $960.0 \pm 0.1 \text{mg/L}$ to $1268 \pm 0.5 \text{mg/L}$ while in permeate it varied from $90.0 \pm 0.3 \text{mg/L}$ to $118.2 \pm 0.5 \text{mg/L}$ for both line 1 and 2. The levels were slightly above the maximum allowable concentration of $< 100 \text{mg/L}$ mainly in the period when COD in feed went up from 1000 to 1200mg/L. From day 70, COD in permeate fluctuated around 90mg/L and 100mg/L and was within the maximum allowable concentration of $< 100 \text{mg/L}$ as per the WHO guidelines for wastewater reuse for irrigation (WHO, 2006). The performance of the two modules did not differ significantly ($t_{\text{calculated}} < t_{\text{critical}}$) for paired T-test (at 95 % confidence level) as illustrated in Table 4.7.

Table 4.7: Comparison of COD removal efficiency in permeate for commercial PES membrane modules in a follow-up experiment (One-way, paired t-test, n=0.05)

Membrane module	Mean and STDEV COD % removal rate	t-test	
		$t_{\text{calculated}}$	$t_{\text{critical}} (n = 0.05)$
Module 1	85.0 ± 1.1	1.2	4.30
Module 2	89.1 ± 5.7		

The correlation between COD, HRT and F/M ratio for the two PES modules was carried out to obtain the optimal condition that gave the highest COD removal efficiency. These results are presented in Figure 4.5.

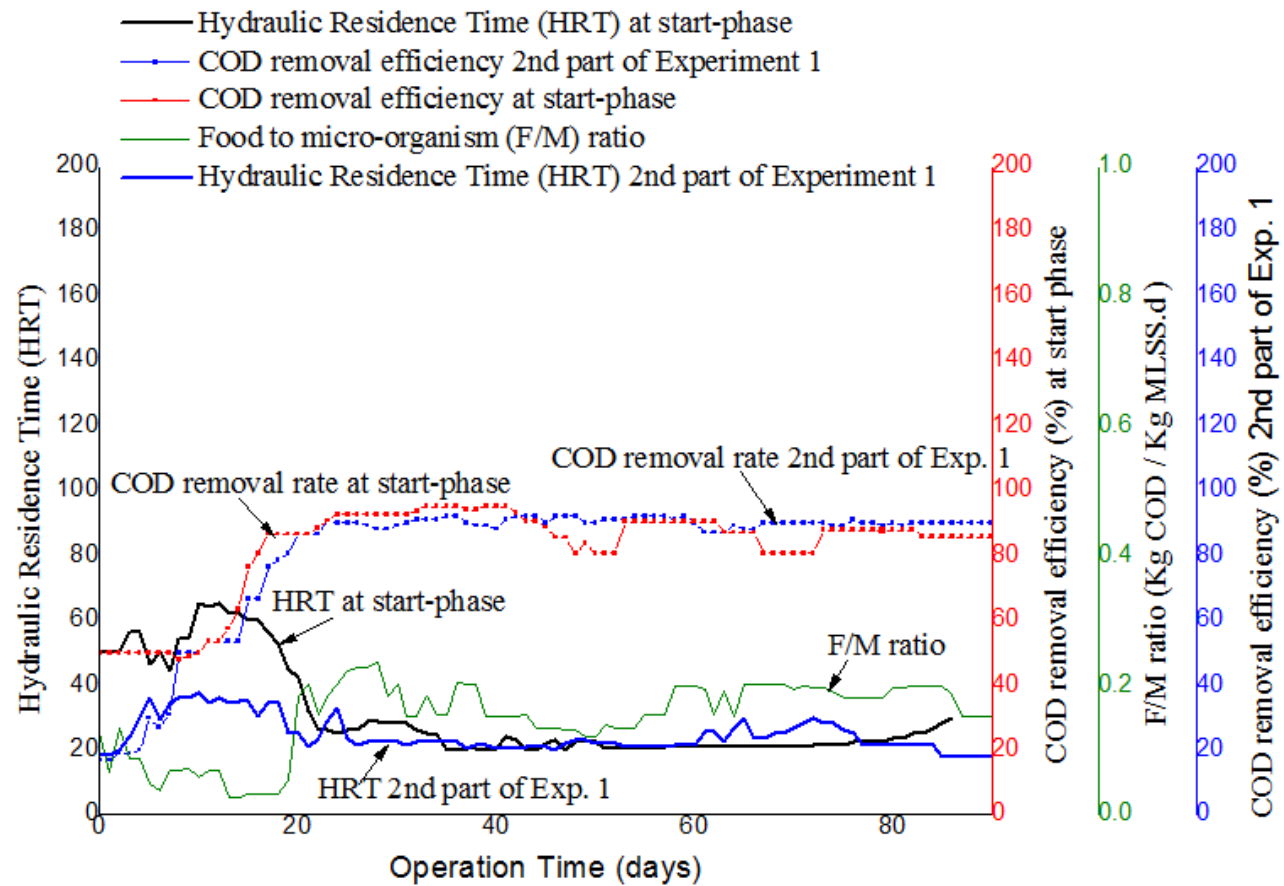


Figure 4.5: Comparison of HRT, F/M ratio and COD removal rate for commercial PES membrane modules

As can be seen in Figure 4.5, the start phase was characterized by rather low COD removal efficiency, low F/M ratio in the range of 0.03-0.05(Kg COD/ Kg MLSS.d) and high HRT varying between 48h -62h. During day 18 to 20, the HRT in the reactor decreased with the increase of flux for both modules. There after a good biodegradation performance was obtained for the two commercial modules as from day 18 in the start-up experiment (illustrated by red line), and day 20 in the follow-up experiment (blue line) respectively. This was mainly in the period when the average F/M ratio in the reactor was varying at 0.16 ± 0.03 (Kg COD/ Kg MSL.d) (dark green line) and with HRT of 22h -25h as illustrated in Figure 4.5. The optimum COD removal rate was achieved between the ranges of 92%-95.9% for the tested PES membrane modules. The results demonstrated that MBR systems can produce higher quality effluent at a shorter residence time (22h - 25h) in comparison to ASP and WSP wastewater treatment systems that have an estimated COD removal efficiency within the ranges of 60-85% and 26-82% with longer HRT of approximately 15-48h and 5-30 days respectively (Vinay *et al.*, 2010; Dipu *et al.*, 2018; Mburu *et al.*, 2019).

4.2.3 Nitrogenous compounds removal efficiency for commercial PES membrane modules

The reduction of nitrogenous compounds (nitrate-nitrogen (NO_3^- -N) and ammonium-nitrogen (NH_4^+ -N) in the treated effluent during the start-up experiment was obtained by comparing the concentration in feed and permeates. The system showed good performance with mean concentration for NO_3^- -N and NH_4^+ -N in permeate varying between 2.3 ± 0.5 and 0.9 ± 0.3 mg/L relative to 5 to 30mg/L and <5mg/L concentrations recommended as per the WHO guidelines for wastewater reuse for irrigation (WHO., 2006). These results are presented the following section in Figure 4.6- 4.7 respectively.

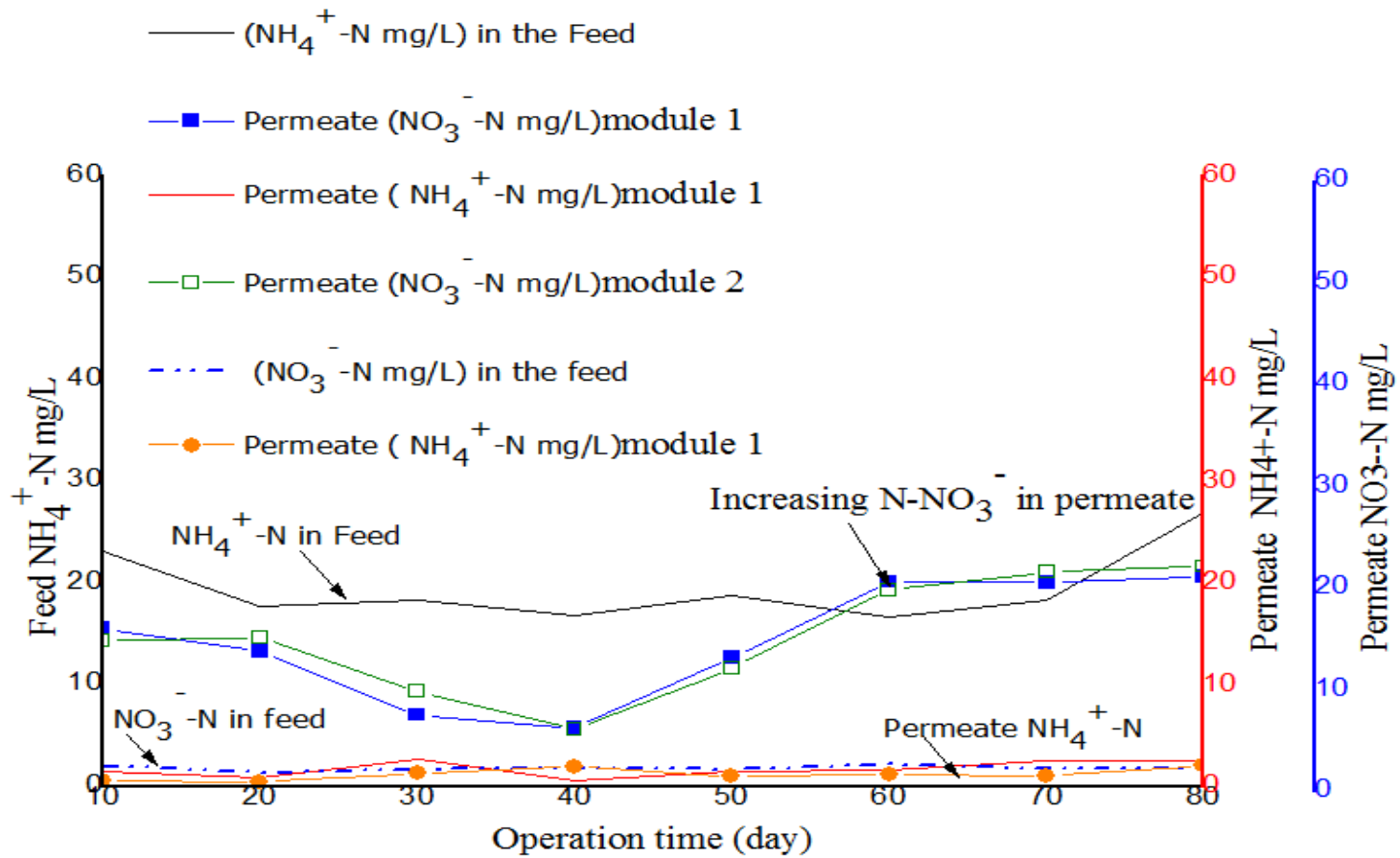


Figure 4.6: Comparison of concentration of NO₃⁻-N and NH₄⁺-N in feed and in permeate during Experiment 1

As seen in Figure 4.6 in the start-experiment, the feed wastewater had high concentration for $\text{NH}_4^+\text{-N}$ in the range of 17.7 to 27.6mg/L illustrated by (black line) while feed $\text{NO}_3^-\text{-N}$ varied between 1.3 to 5.7mg/L (blue dotted line). During this experiment, the two tested commercial UF PES membranes showed relatively improved removal efficiency for nitrogenous compounds after day 20 to day 40 with an average percentage removal efficiency of 78% to 80% respectively. In the same period, the level of $\text{NO}_3^-\text{-N}$ in permeate was varying between 5.7–12.6mg/L and 6.1-14.3mg/L for PES module 1 and 2 respectively and was mainly within an acceptable range of 5 to 30mg/L as per the WHO guidelines for $\text{NO}_3^-\text{-N}$ in wastewater for reuse for irrigation purpose. The concentration for $\text{NH}_4^+\text{-N}$ in permeate remained low for the two tested PES modules and was varying between 0.5mg/L to 2.7mg/L and 0.8 to 2.3mg/L respectively. However, after day 40 and towards the end of the experiment, an increasing amount of $\text{NO}_3^-\text{-N}$ was noted in permeate varying between 20.1 – 20.6mg/L. This was attributed to incomplete nitrification process in the bioreactor that caused continued accumulation.

Excess amounts of $\text{NO}_3^-\text{-N}$ do not have direct effect on fish; it however, supports the growth of aquatic weeds in the ponds that cause extreme fluctuation of dissolved oxygen that result to fish kills (Gidudu *et al.*, 2018). A need for introducing a denitrification tank in the MBR treatment unit was therefore realized as a corrective measure to facilitate in the removal of $\text{NO}_3^-\text{-N}$ through denitrification process. Based on the findings, a denitrification tank (fitted with a digital stirrer) was introduced to the MBR treatment unit in a follow-up step. Figure 4.7 presents the results observed.

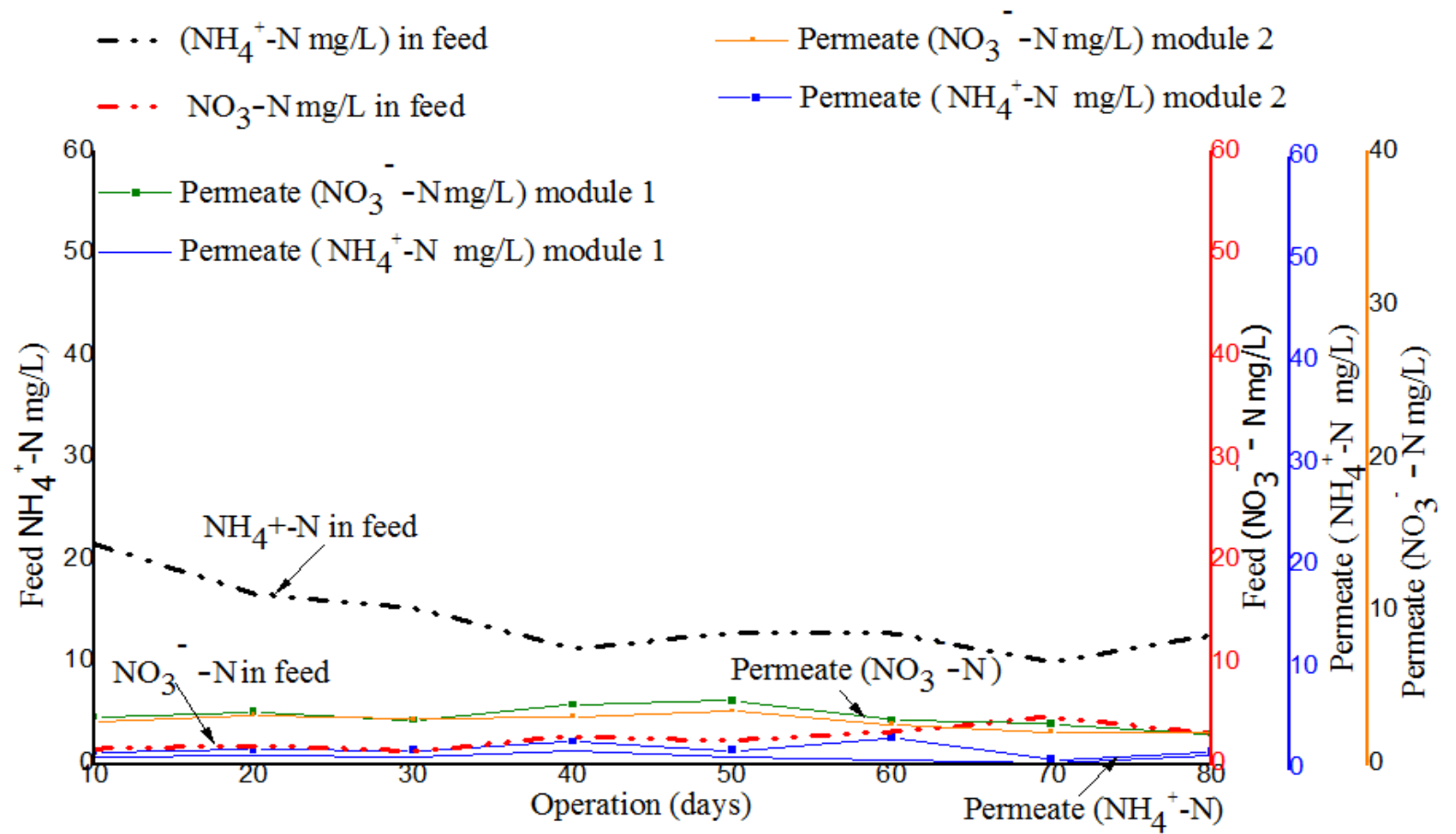


Figure 4.7: Comparison of concentration of NO₃⁻-N and NH₄⁺-N in the feed and in permeate in a follow-up experiment

In the follow-up experiment, the concentration of $\text{NH}_4^+\text{-N}$ and $\text{NO}_3^-\text{-N}$ in the feed wastewater was varying between 12.3 to 21.5mg/L illustrated by (black line) and from 1.2 to 6.3mg/L (red line) respectively. As presented in Figure 4.7, the two tested UF PES modules had good performance after introduction of the denitrification tank with the level of $\text{NO}_3^-\text{-N}$ in permeate varying between 3.6 to 6.1mg/L and 3.2 to 5.7mg/L for PES module 1 and 2 respectively. The level of $\text{NH}_4^+\text{-N}$ in permeate was lowered to the range of 0.4 to 2.8mg/L and 0.6 to 2.5mg/L illustrated (blue line in Figure 4.7) for PES module 1 and 2 respectively. An average nitrogenous compound removal efficiency of $81\pm 3\%$ and $82\pm 2\%$ was achieved for the two tested PES modules 1 and 2 respectively. The optimal removal efficiency between 82.0-82.6% was achieved from day 58 to the end of the experiment at a recycled flow rate of 10L/h between the aeration tank and anoxic tank. The two tested PES modules had nitrate-nitrogen $\text{NO}_3^-\text{-N}$ in permeate within an acceptable range of 5 to 30mg/L as per the WHO guidelines for wastewater reuse for irrigation (WHO., 2006). This was an indication that a successful process for nitrification and denitrification was archived in the treatment process, during the recycled flow of the wastewater between the aeration tank and denitrification (anoxic tank).

During treatment process, nitrification occurs in the aeration tank where aerobic nitrifying bacteria metabolize ammonium in the wastewater into nitrate via two progressive steps. In the first step, nitrosomonas bacteria oxidized ammonium to nitrite and subsequently nitrobacter bacteria to nitrate (Chowdhury *et al.*, 2010). During the second step denitrification was carried out by heterotrophic bacteria that metabolize biodegradable substrate under anoxic conditions using nitrate as the electron acceptor (Chowdhury *et al.*, 2010). Subsequently the nitrate is reduced to gaseous dinitrogen (N_2) which then escape to the atmosphere as an inert gas. $\text{NO}_3^-\text{-N}$ and $\text{NH}_4^+\text{-N}$ removal efficiency obtained in this experiment is in line with the results obtained by the other author (Luong, *et al.*, 2016).

4.2.4 Phosphates compounds removal efficiency for commercial PES membrane modules

The reduction of phosphate ($\text{PO}_4^{3-}\text{-P}$) in the treated effluent was determined and the result analyzed by comparing the concentrations in feed and permeates. According to the findings in this study, reduction of orthophosphates concentration from 21.8 ± 0.5 mg/L to 3.2 ± 0.1 mg/L was achieved by adding Aluminum sulphate ($\text{Al}_2(\text{SO}_4)_3 \cdot 18\text{H}_2\text{O}$) into the denitrification tank as a chemical coagulant. These results are presented in Figure 4.8-4.9 in the following section.

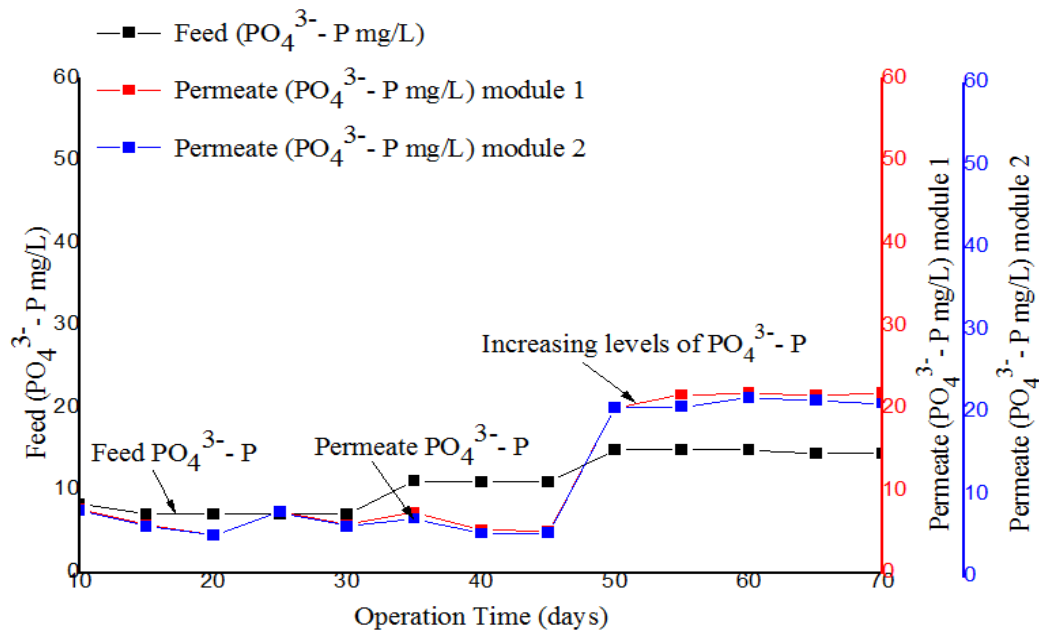


Figure 4.8: Comparison of phosphate ($\text{PO}_4^{3-}\text{-P}$) concentration in feed and permeate during Experiment 1

From Figure 4.8, feed wastewater had $\text{PO}_4^{3-}\text{-P}$ concentration in the range of 7.1 to 14.9 mg/L during the start-up experiment. The level of $\text{PO}_4^{3-}\text{-P}$ in permeate was varying from 4.5 to 21.8mg/L for module 1 and 5.0 to 21mg/L for module 2 respectively. The reduction rate for $\text{PO}_4^{3-}\text{-P}$ in the treatment system was in the range of 34.2- 54.2% from day 15 to day 44. However high $\text{PO}_4^{3-}\text{-P}$ concentration was noted in permeate illustrated (blue line)

from day 49 and towards the end of the experiment. This was signifying a possibility of low removal efficiency and accumulation in the treatment system (Tan *et al.*, 2016). For this experiment $\text{PO}_4^{3-}\text{-P}$ level in permeate was above the acceptable range of ≤ 5 mg/L as per the WHO guidelines for wastewater reuse for irrigation (WHO, 2006).

Extreme amounts of $\text{PO}_4^{3-}\text{-P}$ in water bodies support the growth of aquatic weeds that cause extreme fluctuation of dissolved oxygen. This may result in eutrophication that affects the environment and also cause death of aquatic life (Kevin, *et al.*, 2015). A coagulation agent (hydrated aluminum sulfate/Alum) was therefore used in a follow-up experiment, as a corrective measure to facilitate in lowering of phosphates in the wastewater. Figure 4.9 shows the results obtained after using alum in the treatment system.

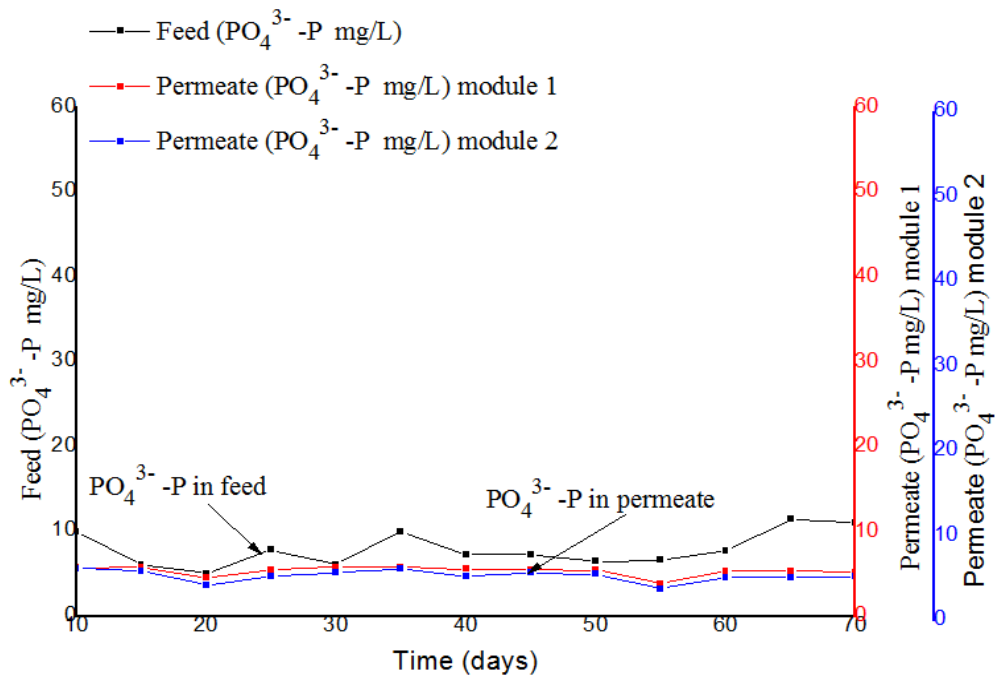


Figure 4.9: Comparison of phosphate ($\text{PO}_4^{3-}\text{-P}$) concentration in feed and permeate during a follow-up experiment

In the follow-up experiment, the level of $\text{PO}_4^{3-}\text{-P}$ in feed was in the range of 6.1 to 10.0mg/L. In permeate, $\text{PO}_4^{3-}\text{-P}$ concentration was varying between 3.8 to 5.2mg/L for module 1 and from 3.7 to 5.1mg/L for module 2 respectively. The level of $\text{PO}_4^{3-}\text{-P}$ in permeate was lowered to an acceptable range of ≤ 5 mg/L as per the WHO guidelines for wastewater reuse for irrigation (WHO., 2006) from day 22 to the end of the experimental period. Reduced $\text{PO}_4^{3-}\text{-P}$ concentration in permeate was attributed to the addition of chemical coagulant ($\text{Al}_2(\text{SO}_4)_3 \cdot 18\text{H}_2\text{O}$) to the wastewater (Bouhadjar, *et al.*, 2016) . The metal ions hydrolyzed to form metal hydrolysis species with positive charge upon being added to the wastewater. These species facilitated in neutralizing the negative charge of $\text{PO}_4^{3-}\text{-P}$ thus causing them to get attracted to each other and therefore stick together to form large particles (insoluble phosphoric complexes). This would remain in the activated sludge and were removed with surplus sludge. The results showed a successful reduction of $\text{PO}_4^{3-}\text{-P}$ levels with a removal efficiency of $63 \pm 5\%$ to $65 \pm 2\%$ after application of coagulants as was also confirmed by (Bouhadjar, *et al.*, 2016).

4.3 Performance of Microdyn-Nadir module and CUBE Mini module of Martin systems

4.3.1 Rate of water permeability (WP), flux and transmembrane pressure (TMP)

The performance of the two tested modules with different construction but made of the same UF/PES material was obtained and the rates of WP, flux and TMP with operation time compared. The analysis of the results demonstrated that both modules were susceptible to fouling as presented in Figure 4.10.

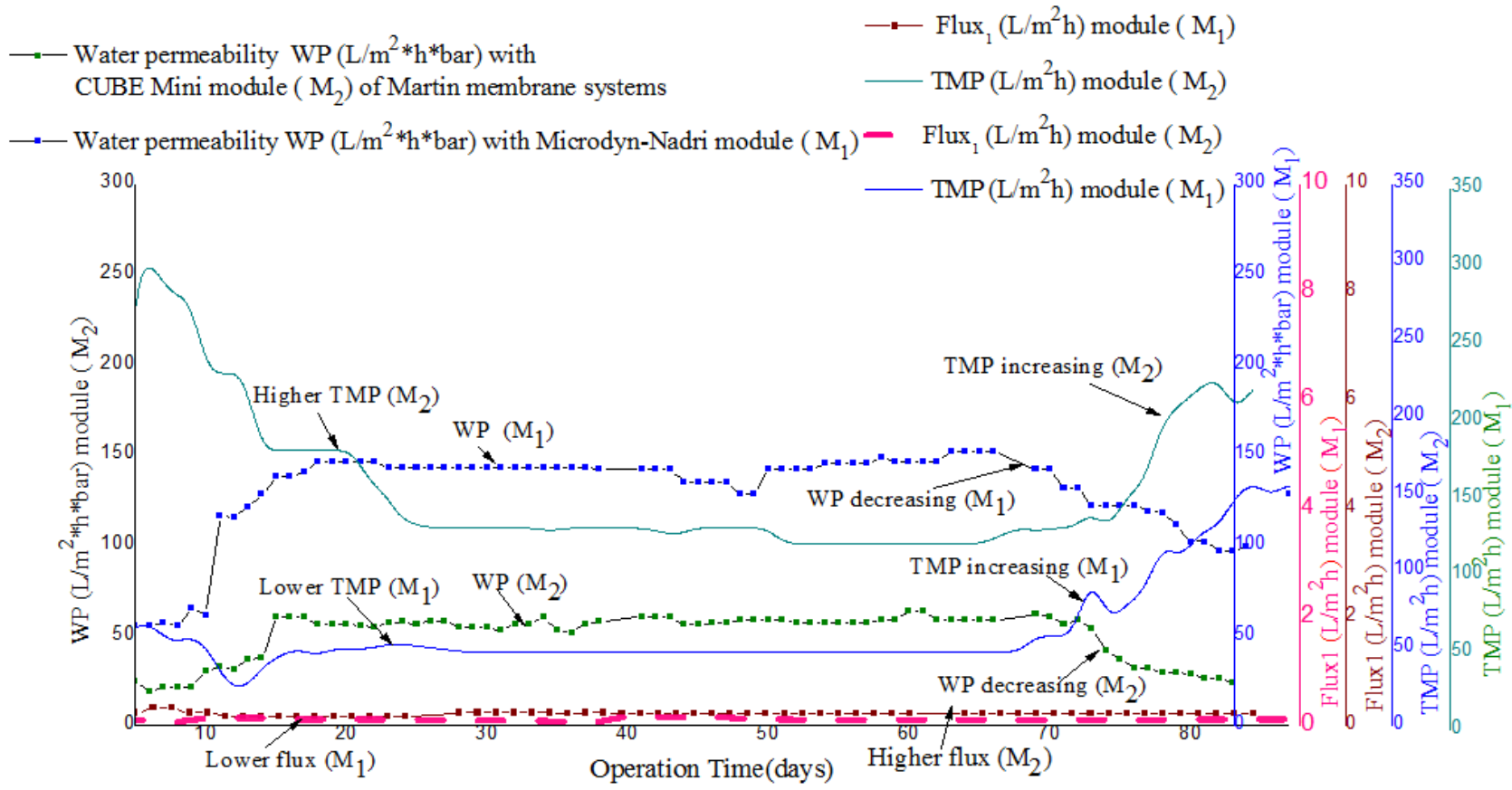


Figure 4.10: WP, flux and TMP for Microdyn-Nadir and CUBE Mini module

From Figure 4.10, the system was operated in sequence at a relatively constant low flux for both modules, and was varying between $5.1\text{L}/\text{m}^2\cdot\text{h}$ - $6.9\text{L}/\text{m}^2\cdot\text{h}$ for Microdyn-Nadir module (M_1) (illustrated by pink line) and from $5.6\text{L}/\text{m}^2\cdot\text{h}$ - $7.8\text{L}/\text{m}^2\cdot\text{h}$ for CUBE Mini module (M_2) (dark red line). The two studied commercial modules had initial low WP during the acclimation phase. However, from day 18 and day 21, both modules had an increase in water permeability (WP) and were fluctuating between $95.7\text{L}/(\text{m}^2\text{ h}\cdot\text{bar})$ and $110.2\text{L}/(\text{m}^2\text{ h}\cdot\text{bar})$ for M_1 and between $56.4\text{L}/(\text{m}^2\text{ h}\cdot\text{bar})$ and $61.1\text{L}/(\text{m}^2\text{ h}\cdot\text{bar})$ for M_2 respectively, for the period when the two experiments were separately conducted. The initial low WP observed during the acclimation phase was attributed to pore-swelling of UF membranes and thereafter, the increase noted was attributed to the system stabilizing achieved after the acclimation phase. However, a significant difference in TMP was observed for the two modules which varied between 45-50mbar for M_1 and 120 ± 1 - 130 ± 1 mbar for M_2 respectively. This could have resulted from several factors that include, the difference in membrane area which was 0.33m^2 for M_1 and 0.45m^2 for M_2 , difference in distance between the envelopes which was 8mm for M_1 and 6mm for M_2 and different module construction since both modules were made of same UF/PES material (same pore size). It might be that M_2 with a bigger surface area required higher force (TMP) to drive the influent through the membrane in comparison to M_1 . As a result, (seen Figure 4.10) a large difference in water permeability was noted with M_1 having higher WP in comparison to that of M_2 .

Further as was noted towards the end of each of the experiments, a significant decrease in WP was observed for both modules varying from 106.1 to $27.5\text{L}/(\text{m}^2\text{ h}\text{ bar})$ for M_1 and from 61.11 to $24.4\text{L}/(\text{m}^2\text{ h}\text{ bar})$ for M_2 respectively. In that same period, a significant rise in TMP was noted for both modules and was varying from 60mbar to 165mbar for M_1 and from 160mbar to 230mbar for M_2 . This resulted from the sudden fouling of the membranes. At this point, chemical cleaning of the membranes was carried out in the same manner as was done during the start phase to recover the TMP. The results demonstrated that a change of membrane module design did not result in improved resistance to fouling.

4.3.2 Results for comparison of COD removal efficiency for Microdyn-Nadir module and CUBE Mini module of Martin systems

The COD removal efficiency for the Microdyn-Nadir module (M_1) and CUBE Mini module of Martin Membrane Systems (M_2) was obtained. The results demonstrated good performance with CUBE Mini module showing higher COD percentage removal rate of 95% COD relative to 92% observed with Microdyn-Nadir module. This was mainly due to longer HRT observed for CUBE Mini module varying between 27-35h relative to 22.4-29h observed for the Microdyn-Nadir module. These results are presented in Figure 4.11.

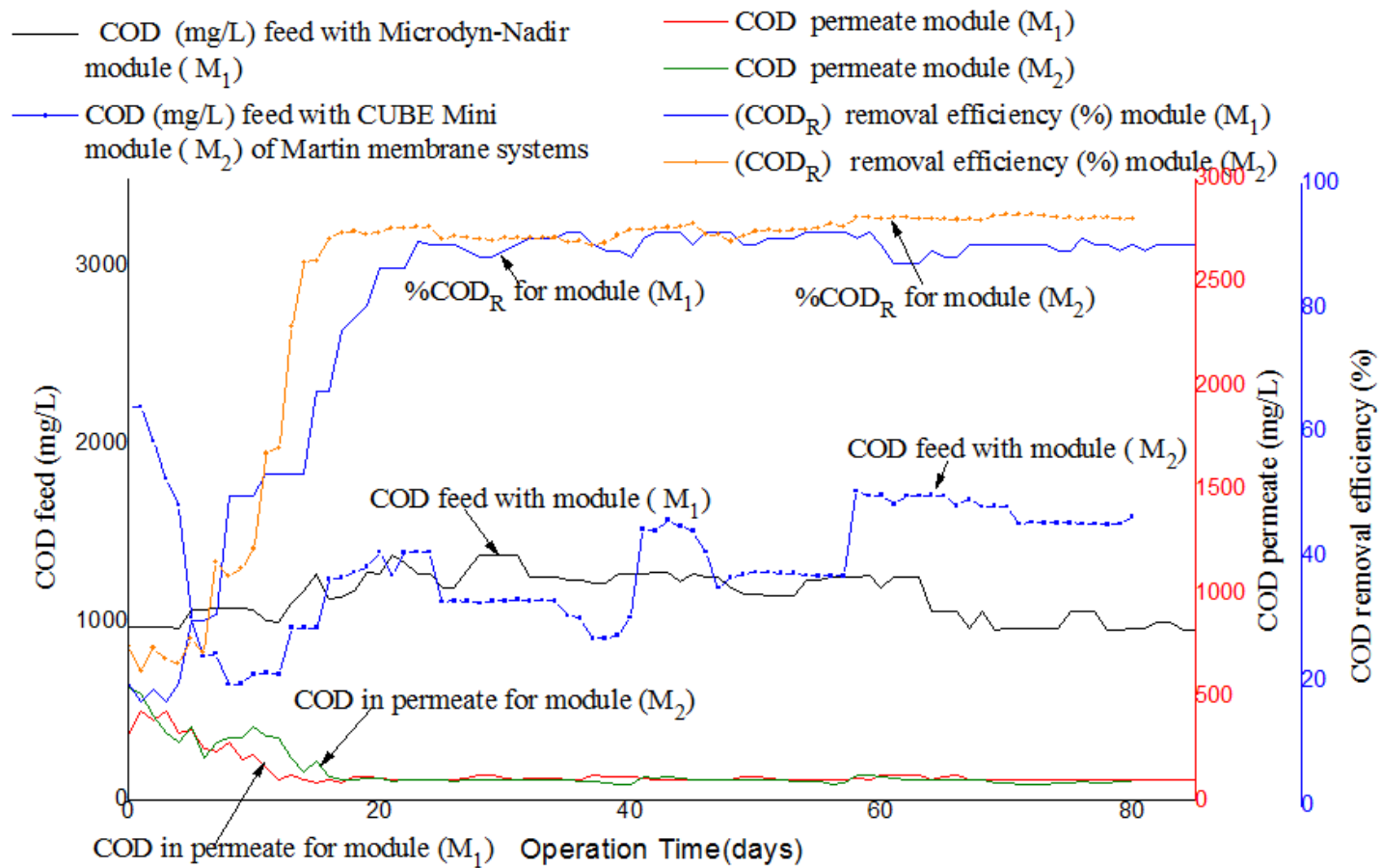


Figure 4.11: Comparison of COD removal efficiency for Microdyn-Nadir and CUBE Mini module

As illustrated in Figure 4.11, the system had unstable conditions for both modules with low biodegradation as COD_R (removal efficiency) was varying between 15-28% (illustrated by the blue line) for the Microdyn-Nadir module (M₁) and from 26-37% for CUBE Mini module of Martin Membrane Systems (M₂) (illustrated by the orange line) from start phase to day 20. This was attributed to the acclimation period, the time required for replication, and growth of the aerobic bacteria culture inside the MBR reactor. However, in the following period both modules showed good biodegradation performance with the average COD_R for M₁ and M₂ varying between 87%-92% and 92%- 95% respectively. The average COD concentration in permeate varied after acclimation from 100.0 ± 0.4mg/L to 121.2 ± 0.5mg/L and from 78.0 ± 0.3mg/L to 123 ± 0.5mg/L for M₁ and M₂ respectively. Mean values for % COD removal for the two tested modules did not differ significantly ($t_{\text{calculated}} < t_{\text{critical}}$) for paired T-test (at 95 % confidence level) as illustrated in Table 4.8.

Table 4.8: Comparison of COD removal efficiency in permeate for Microdyn-Nadir and CUBE Mini module (One-way, paired t-test, n=0.05)

Membrane module	Mean and STDEV COD % removal	t-test	
		$t_{\text{calculated}}$	$t_{\text{critical}} (n = 0.05)$
Microdyn-Nadir	89.2±4.2	0.5	4.3
CUBE Mini	93.3±2.1		

The levels of COD in permeate for the two studied commercial modules were mainly within the maximum allowed concentration of <100mg/L as per the WHO guidelines for wastewater reuse for irrigation (WHO., 2006), except for the time when the MBR was refilled with new feed. A comparison of COD removal efficiency, F/M ratio and HRT for the two tested modules was conducted and the results presented in Figure 4.12.

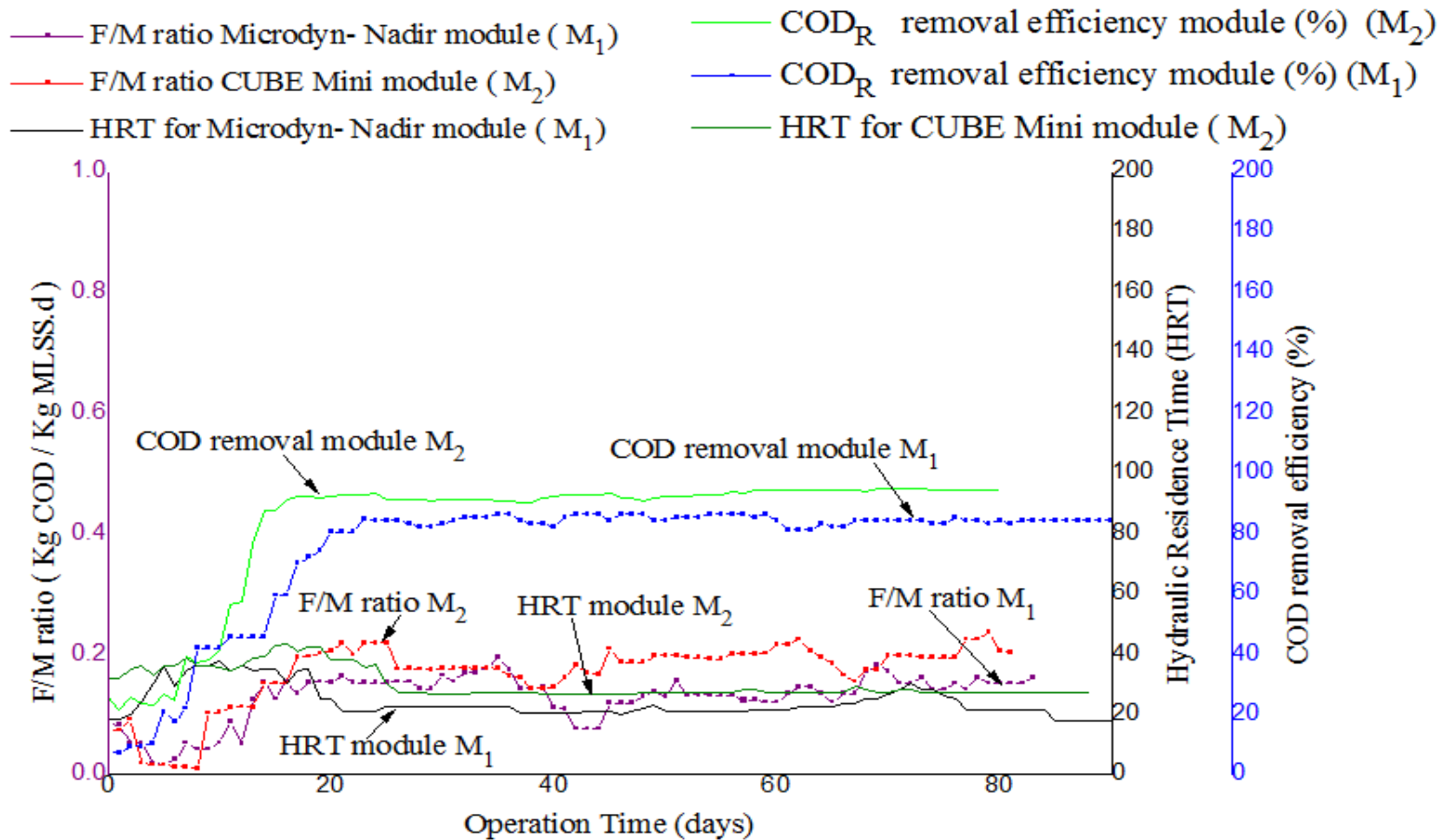


Figure 4.12: Comparison of HRT, F/M ratio and COD removal efficiency for Microdyn-Nadir and CUBE Mini module

As can be seen in Figure 4.12, CUBE Mini modules of Martin Membrane Systems (M_2) showed better performance in terms of biodegradation after day 18. This was attributed to the long hours for HRT exhibited for M_2 in the range of (27.2-35.0h) together with higher F/M ratio of 0.17 ± 0.03 (Kg COD/ Kg MLSS.d) in comparison to HRT of (22.4-29.0h) and F/M ratio of 0.15 ± 0.02 (Kg COD / Kg MLSS.d) for Microdyn-Nadir module (M_1). Based on these findings, it was evident that COD removal was dependent on both HRT and on F/M ratio despite the change of module design. According to the findings of this study, CUBE Mini module (M_2) with longer residence time (HRT) and increased food to microorganism (F/M) ratio had higher biodegradation and improved COD removal efficiency.

4.3.3 Comparison of nitrogenous compounds removal in permeate for Microdyn-Nadir and CUBE Mini module

The removal of ammonium-nitrogen (NH_4^+ -N) and nitrate-nitrogen (NO_3^- -N) from the treated effluent was obtained by comparing the concentration in feed and permeate for each of the two tested modules. The results showed good performance with the mean concentration of NO_3^- -N and NH_4^+ -N varying between 4.9 ± 2.6 and 3.1 ± 0.4 for Microdyn-Nadir module (M_1) and 2.5 ± 0.1 and 3.9 ± 0.5 CUBE Mini module respectively. The concentrations were within the acceptable range of 5 to 30mg/L and < 5 mg/L for NO_3^- -N and NH_4^+ -N as per the WHO guidelines for wastewater reuse for irrigation (WHO., 2006). These results are presented in Figures 4.13 and 4.14 respectively.

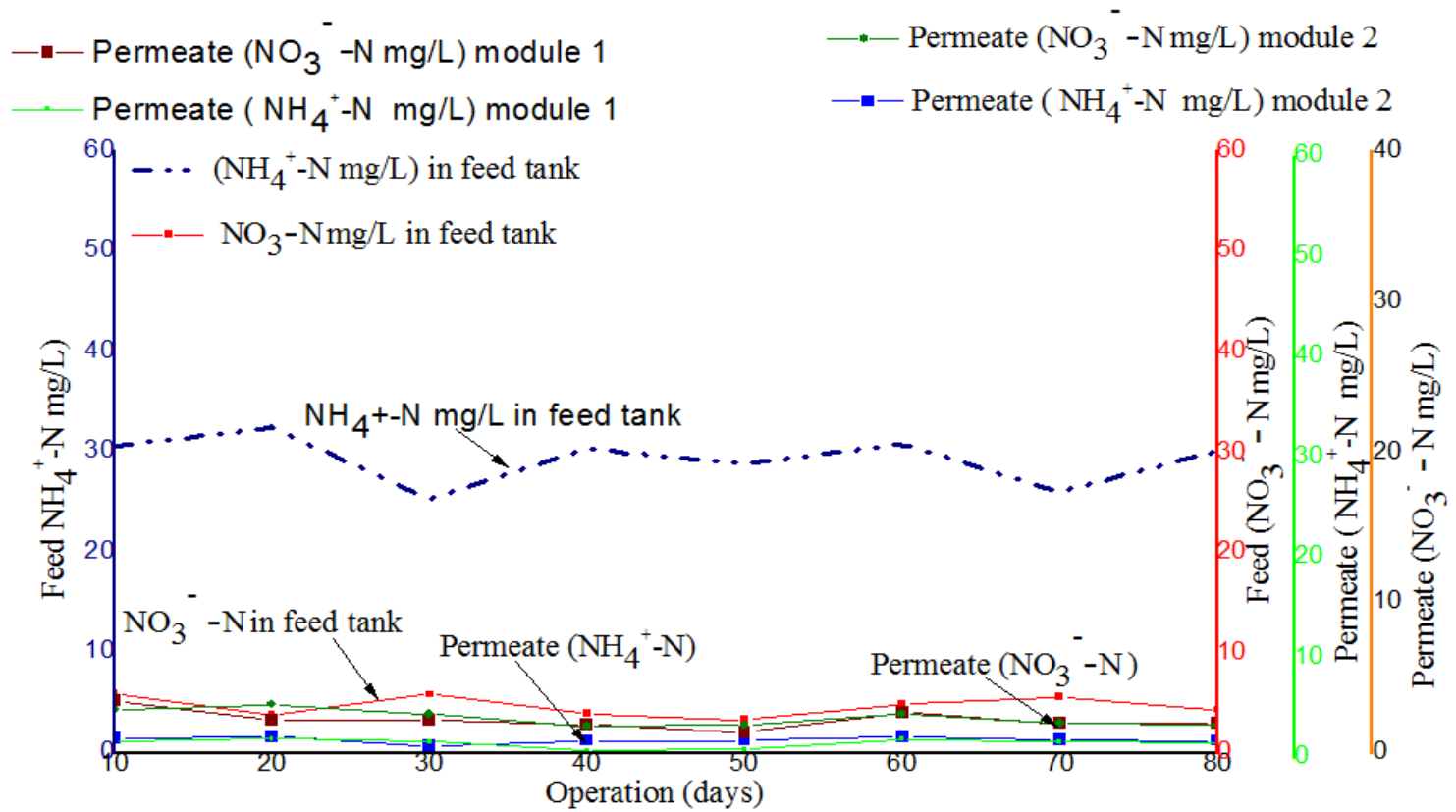


Figure 4.13: Comparison of $\text{NH}_4^+\text{-N}$ and $\text{NO}_3^-\text{-N}$ concentration in the feed and in permeate for Microdyn-Nadir module

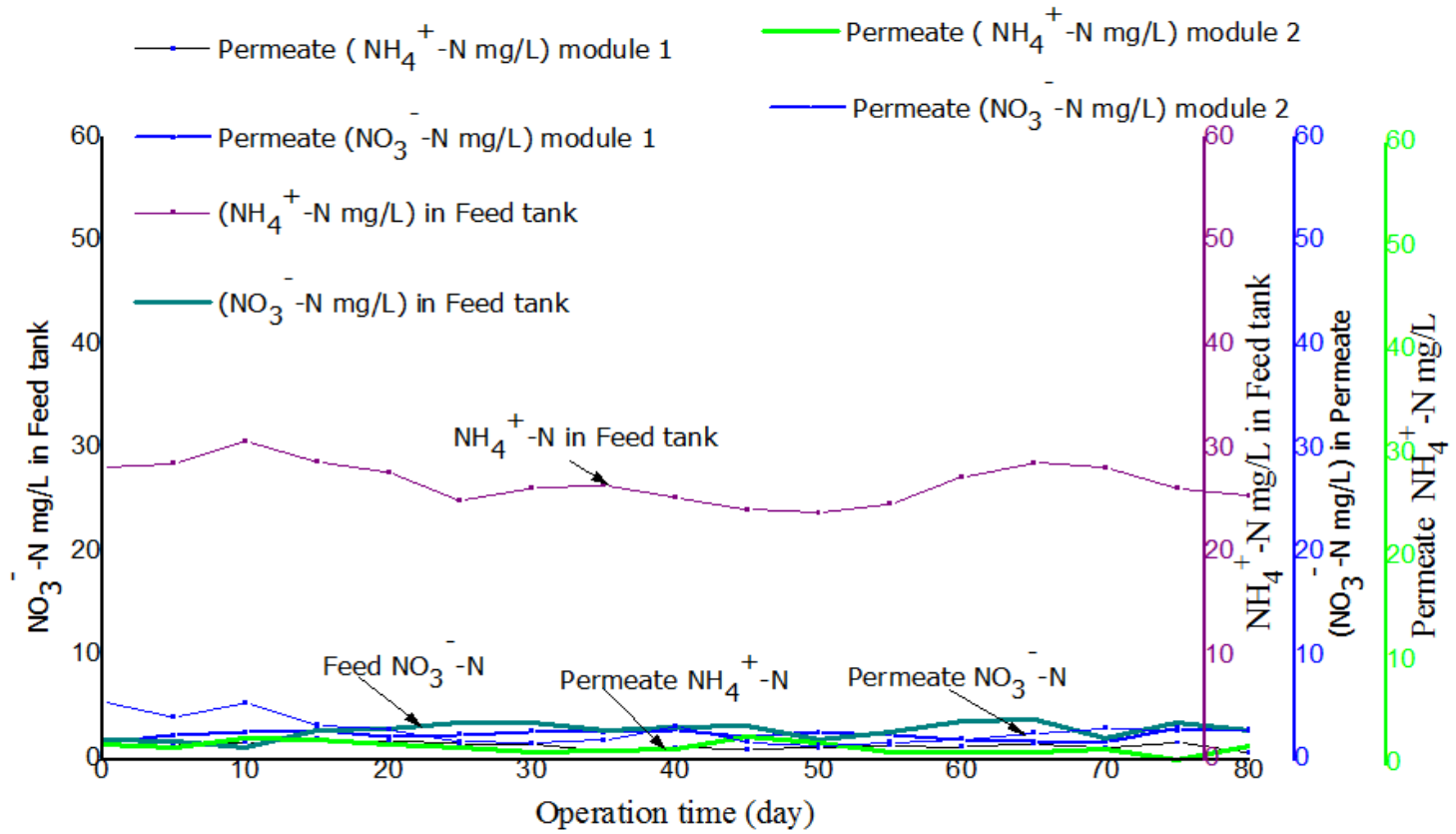


Figure 4.14: Comparison of NH_4^+ -N and NO_3^- -N concentration in the feed and in permeate for Cube Mini module

The results for the sequential tests conducted on the two modules show that the concentration of $\text{NH}_4^+\text{-N}$ and $\text{NO}_3^-\text{-N}$ in the feed wastewater was varying between 23.8mg/L to 30.7mg/L and from 1.9mg/L to 5.8mg/L during the experimental period. The concentration of $\text{NH}_4^+\text{-N}$ in permeate was lowered to the range of 0.4mg/L to 2.7mg/L and 0.2mg/L to 2.3mg/L, while $\text{NO}_3^-\text{-N}$ was lowered to the range of 3.8mg/L –5.3mg/L and 2.4mg/L - 5.6mg/L for the Microdyn-Nadir module (M1) and Cube Mini module of Martin Membrane Systems (M2) respectively. Results from the two modules indicate good removal efficiency for nitrogenous compounds, varying between $79\pm 2\%$ and $82\pm 1\%$, for both commercial modules M_1 and M_2 respectively. The higher removal efficiency observed with the module M_2 might be due to longer HRT as was illustrated in Figure 4.12. The concentration of $\text{NO}_3^-\text{-N}$ in permeate for both modules was mainly within an acceptable range of 5 to 30mg/L as per the WHO guidelines for wastewater reuse for irrigation (WHO, 2006). For this study, the removal efficiency of ammonium-nitrogen $\text{NH}_4^+\text{-N}$ in permeate for both modules did not differ significantly ($t_{\text{calculated}} < t_{\text{critical}}$) for paired T-test (at 95 % confidence level) as illustrated in Table 4.9.

Table 4.9: Comparison of $\text{NH}_4^+\text{-N}$ concentration in permeate for Microdyn-Nadir and Cube Mini module (One-way, paired t-test, $n=0.05$)

Membrane module	Mean and STDEV permeate $\text{NH}_4^+\text{-N}$ (mg/L)	t-test	
		$t_{\text{calculated}}$	t_{critical}
Microdyn-Nadir	4.9±2.6	0.63	12.7
Cube Mini	3.9±1.8		

4.3.4 Comparison of phosphate ($\text{PO}_4^{3-}\text{-P}$) removal in permeate for Microdyn-Nadir and Cube Mini module

Reduction of phosphate ($\text{PO}_4^{3-}\text{-P}$) in the treated effluent using the Microdyn-Nadir module (M_1) and Cube Mini module of Martin Membrane Systems (M_2) showed good performance with the mean concentration of $\text{PO}_4^{3-}\text{-P}$ varying between $4.4\pm 0.6\text{mg/L}$ for Microdyn-Nadir module and $3.5\pm 0.8\text{mg/L}$ for CUBE Mini module respectively. The concentrations were within the acceptable range of $<5\text{mg/L}$ as recommended by WHO

guidelines for wastewater reuse for irrigation (WHO., 2006). These results are presented in Figure 4.15.

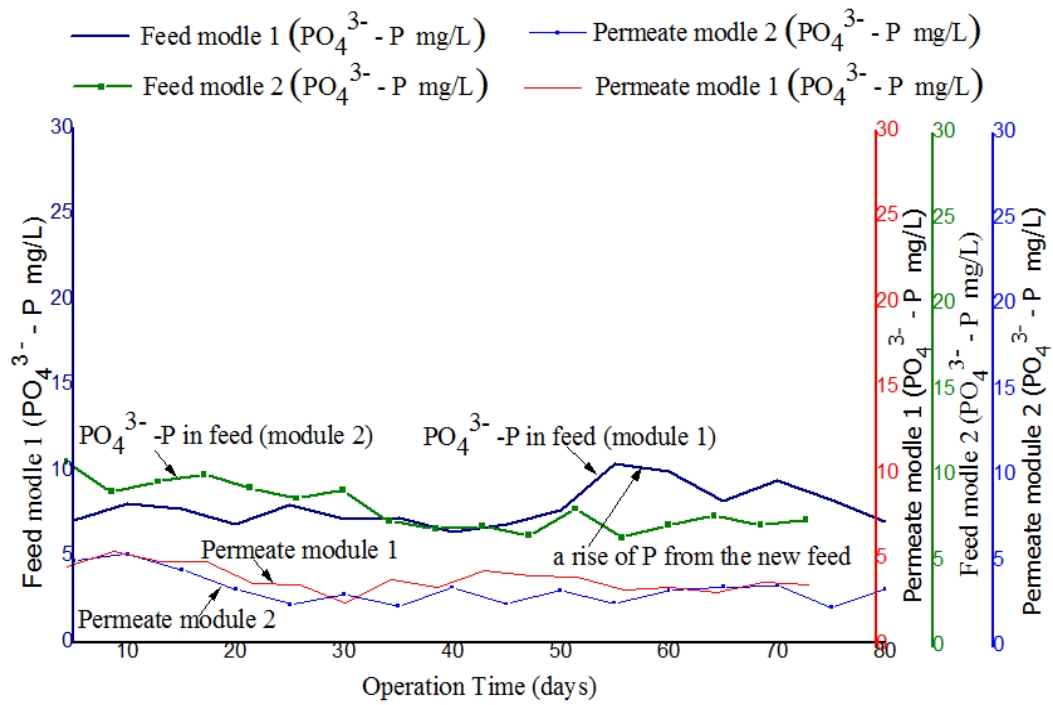


Figure 4.15: Comparison of PO_4^{3-} -P) concentration in feed and permeate for Microdyn-Nadir module and Cube Mini module

As illustrated in Figure 4.15, the system had PO_4^{3-} -P concentration in feed varying between 7.1 to 11.9mg/L illustrated by the (blue line) and between 6.3 to 10.2mg/L (green line), for module 1 and 2 respectively. The two tested membranes had PO_4^{3-} -P in permeate in the range of 3.6 to 5.2mg/L and 1.7 to 5.2mg/L for both modules 1 and 2 respectively. The modules had PO_4^{3-} -P in permeate lowered to an acceptable range of ≤ 5 mg/L as per the WHO guidelines for wastewater reuse for irrigation (WHO, 2006) except for the fluctuations observed mainly at start phase between day 1 to 14 when phosphate levels were slightly higher. An average percentage removal efficiency of $65\pm 3\%$ and $67\pm 1\%$ was achieved for the Microdyn-Nadir module and Cube Mini module of Martin Membrane Systems respectively.

Table 4.10: Comparison of PO_4^{3-} -P concentration in permeate for Microdyn-Nadir and Martin Membrane module (One-way, paired t-test, $n=0.05$)

Membrane module	Mean and STDEV permeate	t-test	
	PO_4^{3-} -P (mg/L)	$t_{\text{calculated}}$	t_{critical}
Microdyn-Nadir	4.5 ± 0.9	0.8	12.7
Cube Mini	3.4 ± 2.3		

As presented in Table 4.10, there was no significant difference for PO_4^{3-} -P in permeate for both modules module 1 and 2 ($t_{\text{calculated}} < t_{\text{critical}}$) for paired T-test at 95 % confidence level (Table 4.9). This was attributed to the similar conditions used to lower PO_4^{3-} -P in permeate, as Aluminum sulphate ($\text{Al}_2(\text{SO}_4)_3 \cdot 18\text{H}_2\text{O}$) was added into the denitrification tank in the same manner as was done during the optimization process in the start-up experiment in Section 4.2.4.

4.4 Characterization of PES and low fouling PBM- coated membranes

Development of a low fouling membrane was carried out through surface modification of commercial PES membranes. The characterization results for PES membrane and the

modified PBM-coated membrane confirmed a successful process as discussed in the following Sections 4.4.1 to 4.4.4.

4.4.1 Chemical characterization

Chemical compositions for the PES membrane and PBM-coated membrane were obtained without IR spectrums for PES and PBM-coated membranes were compared using an overlay in order to recognize characteristic peaks. These results are presented in Figure 4.16

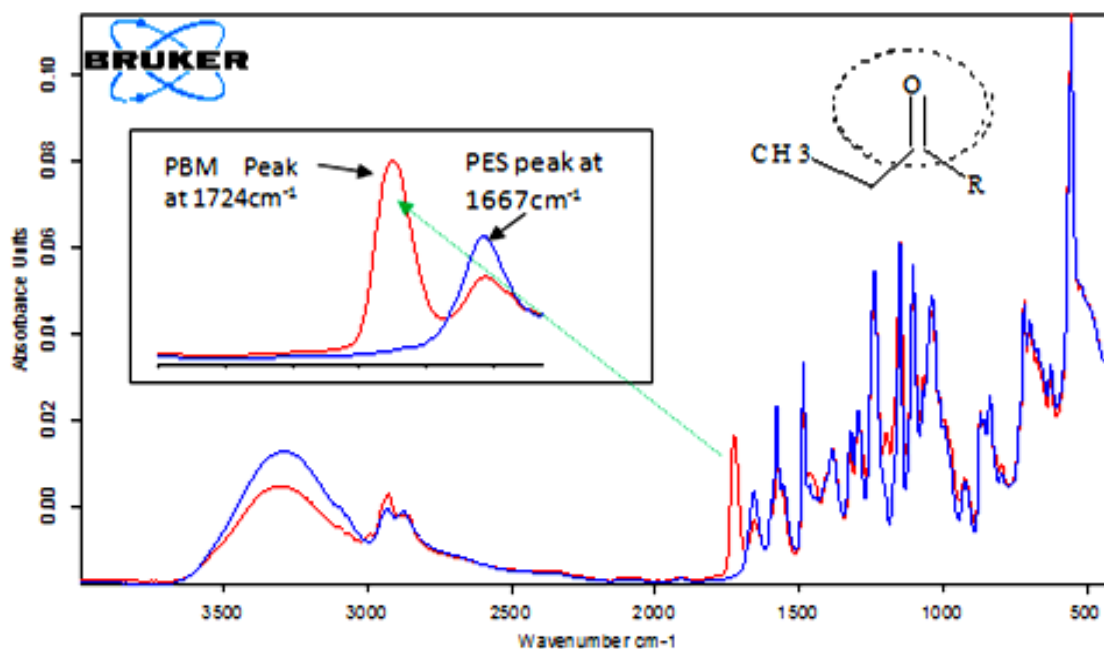


Figure 4.16: IR spectra of PES commercial and PBM-coated membrane

The IR spectrum for the PBM-coated membrane showed a strong peak absorbing at 1724cm⁻¹ (illustrated by the red line) characteristic of the carbonyl functional group (C=O) found in the chemical structure of acrylate groups present in PBM coating. The PBM mixture constitutes the monomer MMA, the co-surfactant HEMA, the polymerizable surfactant AUTEAB and a cross-linker (EGDMA) all bearing an acrylate functional group that is not present in PES commercial membrane (Galiano *et al.*, 2018). Notable for this

experiment, the carbonyl peak was absent in the spectra of unmodified PES commercial membrane illustrated (blue line) in Figure 4.16.

The peak at 1667 cm^{-1} (illustrated by the blue line) characteristic of stretching vibrations of -C=C- of benzene ring had a strong absorbance for PES membrane in comparison to PBM-coated membrane. This phenomenon could be attributed to the transformation of double bonds to single bonds during polymerization of the PBM thus resulting to a lower concentration of -C=C- in the PBM-coated membrane. This is in agreement with the Beer Lambert's law where absorbance is directly proportional to concentration (Mayerhöfer *et al.*, 2016). These results have also been confirmed by others (Francesco *et al.*, 2018;Galiano *et al.*, 2018).

4.4.2 Contact angle measurement for PES and PBM membranes

Results for the sessile drop contact angle measurement (CAM) for PES commercial membrane and PBM-coated membranes were obtained and analyzed. The results showed higher hydrophilic moiety for the PBM membrane in comparison to the PES unmodified membrane. These results are presented in Table 4.10.

Table 4.11: Comparison of contact angle measurement (CAM) for the PES and PBM coated membrane surface at t =0-8 seconds (One-way, paired t-test, n=0.05)

Contact angle (CA) Mean and STDEV				t-test	
Membrane PES commercial	PBM membrane	4µm coated	t _{calculated}	t _{critical}	
60.2±2.1	33.7±3.3		13.8	3.18	
58.7±2.5	32.4±3.3		13.2	3.18	
56.4±2.1	31.6±2.2		14.1	3.18	
55.8±1.2	34.1±2.8		13.3	3.18	

As can be seen in Table 4.11, PBM membrane had an average contact angle (CA) in the range of 31.6° - 34.1° in comparison to 56.4°- 60.2° observed with PES membranes. The reduction in CA for PBM in comparison to PES commercial membrane was between 60.2° and 31.6° which was a change of about 48%. The mean values for the CA observed from the two tested PES and PBM-coated membranes were significantly different ($t_{\text{calculated}} > t_{\text{critical}}$) for paired T-test (at 95 % confidence level) as illustrated in Table 4.10. The low contact angle (CA) observed in PBM coated membranes was attributed to the presence of hydroxyl (^-OH) and ammonium (NH_3^+) groups in the membrane surface (Francesco *et al.*, 2018). The groups were introduced by the application of PBM coating prepared using co-surfactant (HEMA) and surfactant (AUTEAB) that comprised ^-OH and NH_3^+ functional groups in their chemical structure respectively. These affect by decreasing the contact angle and improve the hydrophilic nature of the membrane surface. These findings have also been confirmed by other authors (Qiang *et al.*, 2013) while working on the dependence of contact angles to surface features of membranes.

4.4.3 Comparison of fouling for PES and PBM-coated membrane

Fouling on PES and PBM-coated membranes was induced using humic acid. The intensity of the brown color deposited on the surface after treatment was noted as an indication of the membrane's fouling propensity. The intensity of the brown color was evaluated through visual observation. These results are illustrated in Figure 4.17.

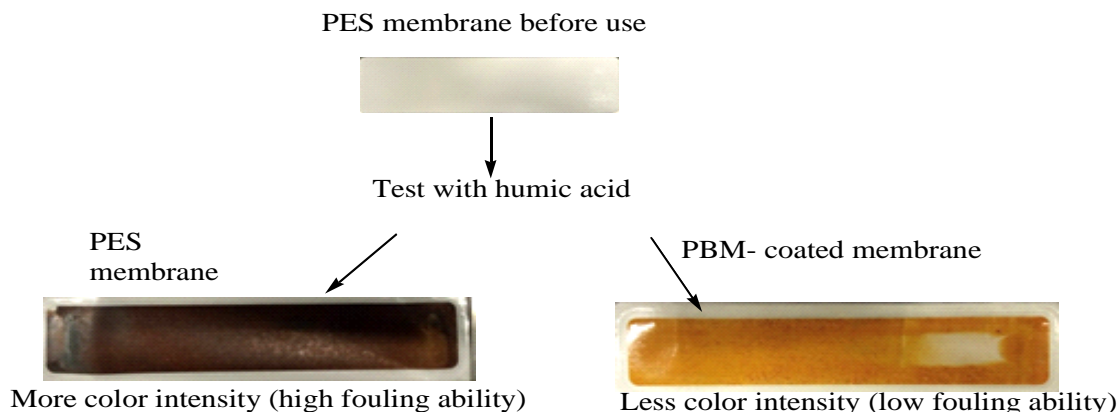


Figure 4.17: Color intensity deposited on PES and PBM-coated membrane after treatment with humic acid

As presented in Figure 4.17, the color intensity deposited on the PES membrane surface was high in comparison to that of the PBM coated membrane, signifying the humic acid layer deposited. Humic acid constitutes aromatic compounds that make it hydrophobic and thus showed a lower binding affinity for the PBM module attributed to improved hydrophilicity of its surface as was demonstrated with contact angle measurements (CAM) in Table 4.10. The PBM-coated membrane surface, therefore, demonstrated improved ability for foulant rejection and was less pronounced to fouling in comparison to the commercial PES membrane. This may also be attributed to the low flow rate for the PBM membrane as was demonstrated in cross-flow water permeability results in Section 4.4.4. The PBM membrane with a lower flow rate had lower fouling due to lower deposits in comparison to PES with higher flow rate thus higher deposits. These findings have also been confirmed by (Galiano *et al.*, 2015). The author worked on membrane surface modification via PBM for the treatment of textile dye wastewater.

4.4.4 Cross-flow water permeability for PES and PBM coated membranes

The preliminary test for water permeability was conducted for PES and PBM coated membranes using automated cross-flow testing cell (SIMAtec GmbH, Germany). The results obtained are presented in Figure 4.18.

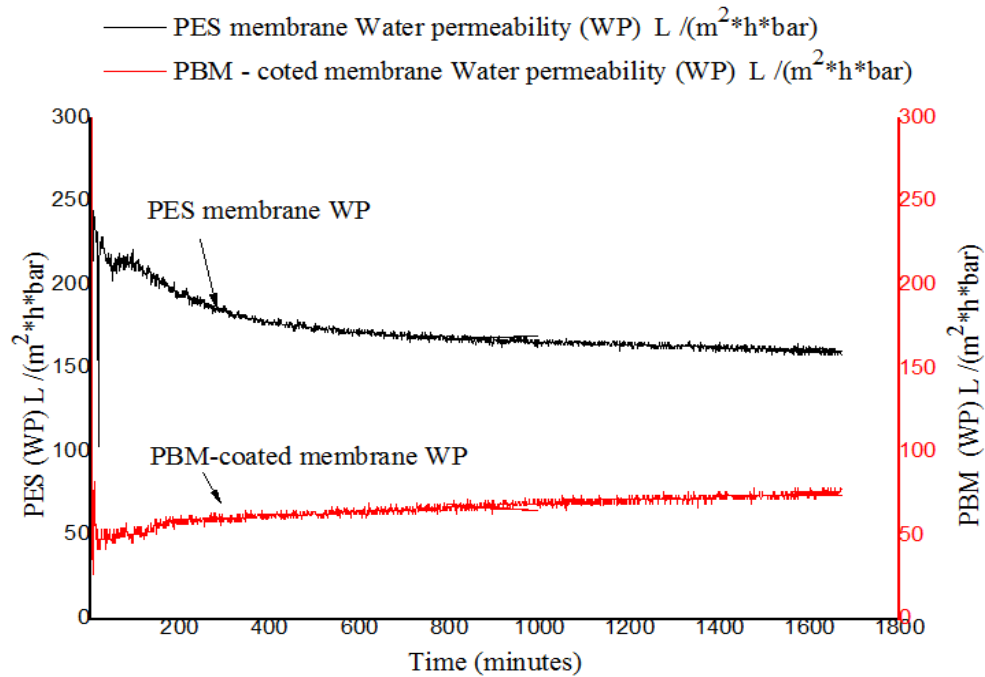


Figure 4.18: Cross-flow water permeability for PES and PBM membranes

As can be seen in Figure 4.18, the start of the experiment was characterized by high water permeability (WP) for the PES membrane ranging between 180 - 244 $L/(m^2 h bar)$ (black line). However, towards the end of the experiment, a gradual decrease in WP was observed for the PES membrane and was in the range of 126 -144 $L/(m^2 h bar)$ (black line). The PBM-coated membrane exhibited relatively constant WP varying between 56-79 $L/(m^2 h \cdot bar)$ (red line) for the period the experiment was conducted and was notably lower in comparison to that of the PES membrane and it showed a slight increase. This was attributed to the increased thickness of PBM coating thus resulting in an increased mass resistance to influent flow through the membrane.

4.5 Performance of commercial PES and PBM coated membrane modules

The performance of PES commercial membrane module and PBM coated membrane module was studied for treatment of fish processing wastewater in the Lab-scale iMBR unit. The results showed better performance for PBM module with the mean concentration

of COD, $\text{NH}_4^+\text{-N}$, $\text{NO}_3^-\text{-N}$, and $\text{PO}_4^{3-}\text{-P}$ in permeate varying between 71.3 ± 12 , 0.6 ± 0.2 , 0.9 ± 0.5 and 1.9 ± 0.1 relative to 99.3 ± 9.8 , 03.9 ± 1.8 , 3.3 ± 1.2 and 3.5 ± 0.4 for PES module. The concentrations were within the acceptable range of $<100\text{mg/L}$, $<5\text{mg/L}$, 5 to 30mg/L , and $<5\text{mg/L}$ as recommended by WHO guidelines for wastewater reuse for irrigation (WHO., 2006). These results are discussed in the following Secession.

4.5.1. Comparison of water permeability (WP), flux and transmembrane pressure (TMP) for PES commercial and PBM coated membrane modules

The performance of PES commercial membrane module and PBM coated membrane module was studied by comparing the rate of WP, flux and TMP when used for treatment of fish processing wastewater in the Lab-scale iMBR unit. The results showed better resistance for fouling for the PBM module while the PES commercial membrane was found to be susceptible to fouling. These results are presented in Figure 4.19.

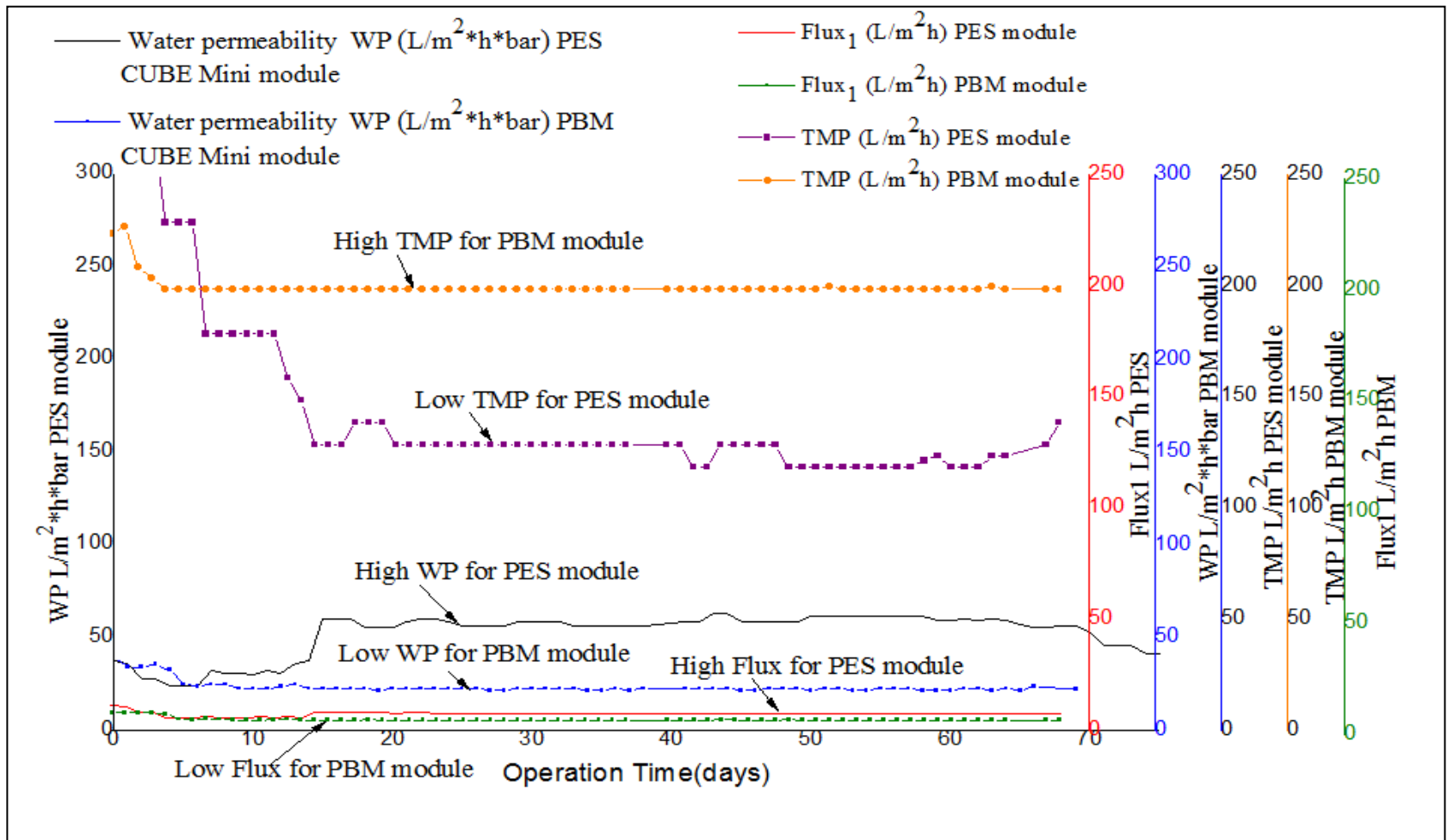


Figure 4.19: WP, flux and TMP for PES module and PBM module

As illustrated in Figure 4.19, both systems were operated separately at a relatively constant low flux with that of the PBM module varying from $4.4\text{L}/\text{m}^2 \cdot \text{h}$ - $4.9\text{L}/\text{m}^2 \cdot \text{h}$ (green line) in comparison to $5.6\text{L}/\text{m}^2 \cdot \text{h}$ - $7.8\text{L}/\text{m}^2 \cdot \text{h}$ (red line) observed for PES module. The PBM coated membrane had initial water permeability (WP) slightly higher at the start of the experiment varying between $34\text{-}39\text{L}/(\text{m}^2 \cdot \text{h} \cdot \text{bar})$ and thereafter was lowered to $22\text{-}24\text{L}/(\text{m}^2 \cdot \text{h} \cdot \text{bar})$ illustrated (blue line) in Figure 4.19. However, from day 10, WP for the PBM membrane was relatively constant with low fluctuations observed. The decrease in WP at the start of the experiment might have been caused by swelling of membrane pores when the membranes are immersed in water, a phenomenon that could make the pore size smaller thus increasing resistance to the flow of influent. A similar trend was also observed with the PES membrane as illustrated in Figure 4.19 (black line).

A comparison of the two tested membranes showed a large difference right from the acclimation period and with WP varying between $22\text{-}39\text{L}/(\text{m}^2 \cdot \text{h} \cdot \text{bar})$ (blue line) for the PBM module in comparison to $56\text{-}61\text{L}/(\text{m}^2 \cdot \text{h} \cdot \text{bar})$ observed for the PES module illustrated by (black line) respectively. TMP of the PBM coated module was in the range of $200 \pm 1\text{mbar}$ to $230 \pm 1\text{mbar}$ in comparison to $120 \pm 1\text{mbar}$ and $130 \pm 1\text{mbar}$ observed after acclimation with PES commercial module. These results are in agreement with the observations made from the WP experiment conducted using the cross flow test (illustrated in Section 4.4.4) where the PBM membrane exhibited low WP in comparison to the PES membrane.

Table 4.12: Comparison of TMP, flux and WP for PBM-coated and PES membrane module (One-way, paired t-test, n=0.05)

Parameter measured	Module	Mean and STDEV	t-test		
			Parameter	t calculated	t critical
TMP	PES	147.9±34.5	TMP	10.4	2.78
	PBM	204.0±9.3			
Flux	PES	7.2±0.7	Flux	3.5	2.78
	PBM	4.9±1.1			
WP	PES	57.6±4.7	WP	11.8	2.78
	PBM	24.7±4.8			

A comparison of the results in Table 4.12 showed a significant difference in the mean values for TMP, WP, and flux for the two tested modules as ($t_{\text{calculated}} > t_{\text{critical}}$) for paired T-test (at 95 % confidence level). This was attributed to the higher mass resistance created by the extra PBM layer on PES surface. Consequently, it was attributed to low WP and low flux observed for the PBM coated membrane. These observations have also been confirmed by (Deowan *et al.*, 2016; Francesco *et al.*, 2018).

4.5.2 Critical flux for PBM coated membrane module and PES membrane module

Critical flux measurement was conducted and the ability of PES and PBM modules to resist fouling obtained and recorded. These results are presented in Figure 4.20.

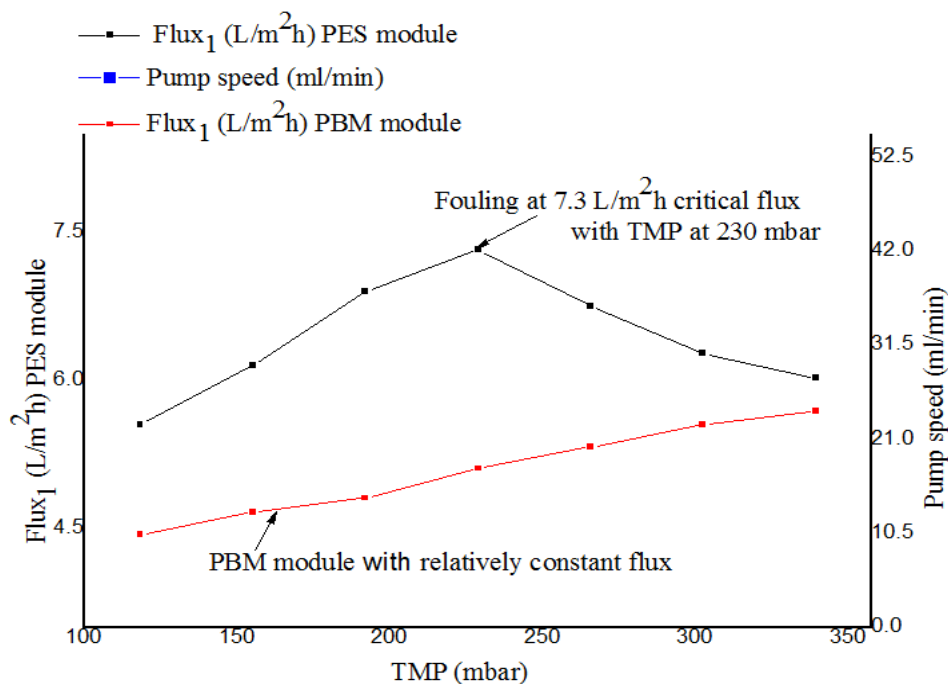


Figure 4.20: Critical flux measurements for PES module and PBM module

As illustrated in Figure 4.20, the MBR was operated by increasing the speed of the suction pump from 0.5V (25.3ml/minute) to 1.11 V (55.6ml/minute) with time intervals of 24hours (where 5000ml/minute = 99Volts). The initial flux for PES and PBM modules was 5.6L/m²h (black line) and 4.4L/m²*h (red line) respectively. The critical flux of the PES module was observed at 7.3L/m²*h with TMP of 230mbar. Above this point, a decrease in flux and the onset of fouling was observed. The PBM module, however, had a relatively constant flux during the experimental period and the critical flux was not achieved at TMP of up to 340mbar. From the experimental results, it might be expected to operate the PBM membrane module at higher flux (above 350mbar) than the commercial one without having achieved critical flux. However, this needs to be further studied. These findings are in line with what was reported the author (Deowan *et al.*, 2016) while studying on the critical flux for PES membranes and PBM membranes using model textile dye wastewater.

4.5.3 Comparison of COD removal efficiency for PES module and PBM-coated PES module

The COD removal efficiency for PES and PBM membrane module showed better performance for PBM module concentrations in permeate varying between 71.3±12 relative to 96.3±9.8 observed for PES modules. This might have resulted from longer residence time (HRT) (38.4 – 46.0h) for PBM module in comparison to (27-40h) observed with PES module. These results are discussed in this Section and presented in Figure 4.21.

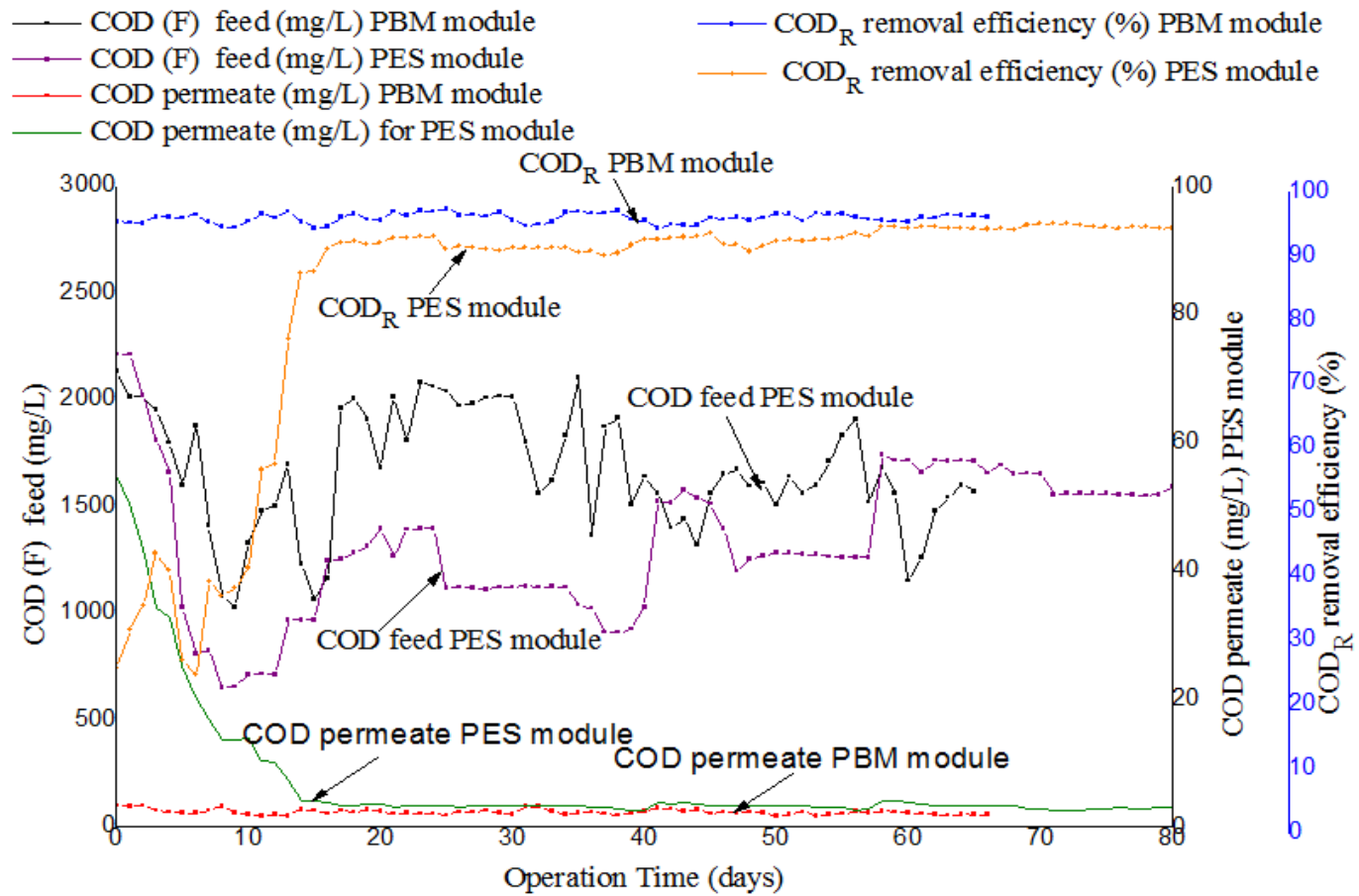


Figure 4.21: Comparison of COD removal efficiency for PES module and PBM module

Figure 4.21 indicates good biodegradation and better performance for the PBM membrane module with constant and high removal efficiency for COD varying from 95% - 97% from start phase and for the entire duration in comparison to 92% - 95% observed with the PES membrane module. Stable values for COD in permeate were noted varying from 100mg/L to 61.7mg/L for the PBM membrane module from the start and to the entire duration when the experiment was conducted. On the other hand, the PES module was characterized by fluctuations of permeate COD varying after acclimation from 78.0mg/L to 123mg/L. The better performance of the PBM module might have resulted from longer residence time (HRT) (38.4 – 46.0h) in the reactor in comparison to (27-40h) for the PES module. The COD concentration in permeate for both modules were mainly within the maximum allowable concentration of < 100mg/L as per the WHO guidelines for wastewater reuse for irrigation (WHO, 2006).

Table 4.13: Comparison of COD concentration in permeate for PES module and PBM module (One-way, paired t-test, n=0.05)

Module	Mean and STDEV permeate COD kg/L	t-test	
		t _{calculated}	t _{critical}
PES	96.3±9.8	4.42	2.78
PBM	71.3±12		

From Table 4.13, a comparison of the two tested PES and PBM modules were significantly different with ($t_{\text{calculated}} > t_{\text{critical}}$) for paired T-test (at 95 % confidence level). The better performance for the PBM module was attributed to longer residence time attributed to the higher mass resistance created by the extra PBM layer on PES surface thus resulting to lower flux for the system (Figure 4.21). Longer residence time (HRT) of the effluent in the reactor results to increased food to microorganism (F/M) ratio, higher biodegradation rate and improved COD removal efficiency (Figure 4.22). The author (Galiano *et al.*, 2015) made similar observation while working on treatment of textile dye wastewater using PBM coated membranes.

A comparison of COD removal efficiency, F/M ratio and HRT for the two tested modules was conducted. This results are presented in Figure 4.22.

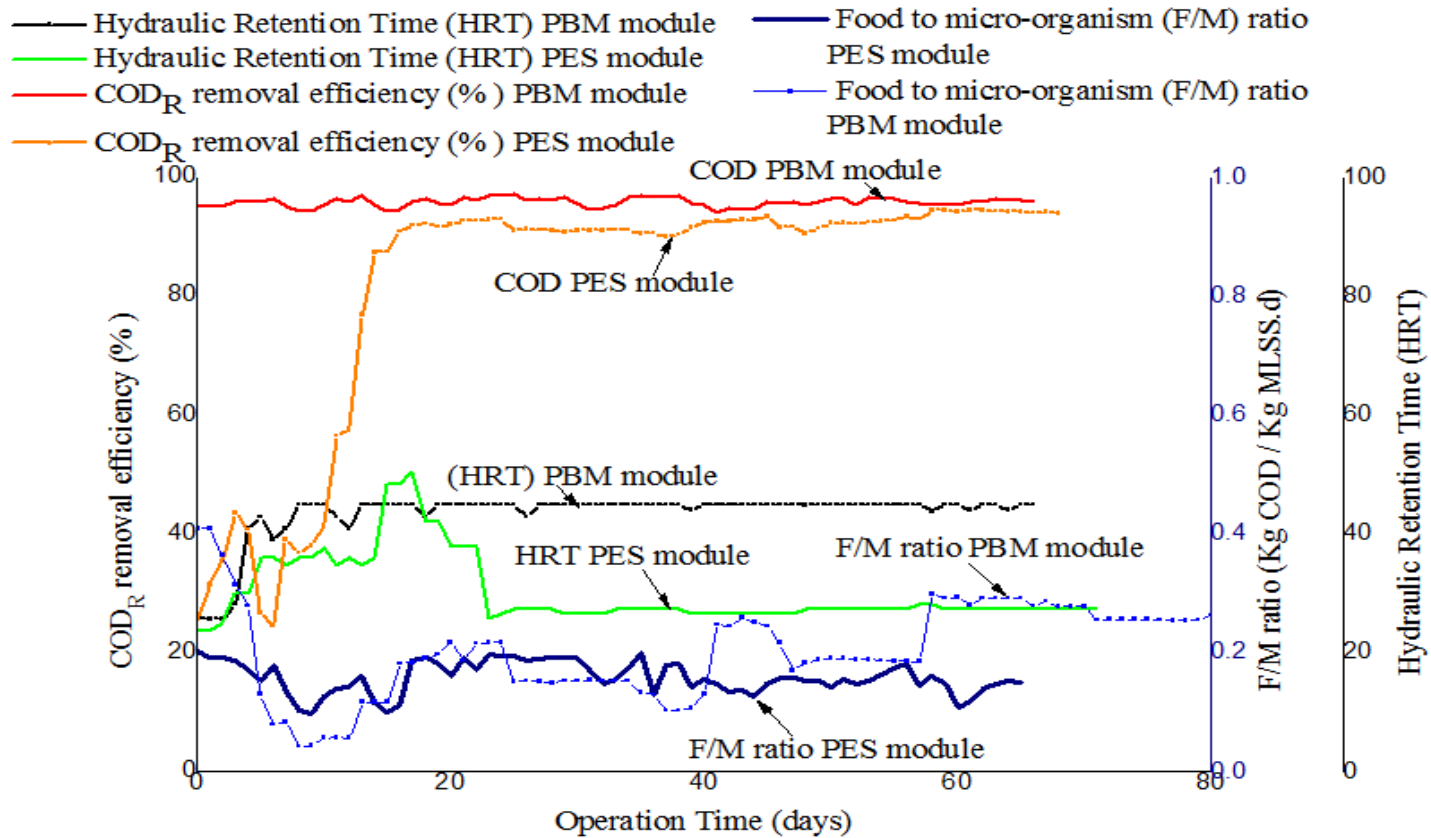


Figure 4.22: Comparison of HRT, F/M ratio and COD removal efficiency with operation time for PES and PBM membrane module

As can be seen in Figure 4.22, the PBM module exhibited a higher residence time varying between 38.4h -46.0h (black line) in comparison to the PES module whose residence time was low (green line) after day 16 and was in the range of 27.4h -31.7h. The COD removal efficiency of the PES membrane was at the beginning rather low and achieved 90% only after day 18 with an average F/M ratio of 0.16 ± 0.1 (Kg COD/ (Kg MLSS.d) and average HRT of 29 ± 2 h. The COD removal efficiency of the PBM membrane showed high values $>90\%$ right after start despite fluctuating HRT until day 10 (illustrated in Figure 4.22). The average F/M ratio after day 16 was in the range of 0.20 ± 0.1 (Kg COD/ (Kg MLSS.d). Based on these findings, PBM coated membrane module with longer residence time (HRT) and increased food to microorganism (F/M) ratio had higher COD removal efficiency compared to the commercial PES membrane.

4.4.4 Comparison of nitrogenous compounds removal in permeate using PES and PBM coated membrane

The results for removal of ammonium-nitrogen ($\text{NH}_4^+\text{-N}$) and nitrate-nitrogen ($\text{NO}_3^-\text{-N}$) in the treated effluent for PES and PBM-coated membrane module showed improved performance for the PBM module with the mean concentration of $\text{NO}_3^-\text{-N}$ and $\text{NH}_4^+\text{-N}$ varying between 0.9 ± 0.5 and 0.6 ± 0.2 relative to 3.3 ± 1.2 and 3.9 ± 1.8 for PES module respectively. The concentrations were all within the acceptable range of 5 to 30mg/L and $<5\text{mg/L}$ for $\text{NO}_3^-\text{-N}$ and $\text{NH}_4^+\text{-N}$ as per the WHO guidelines for wastewater reuse for irrigation (WHO., 2006). These results are presented in Figures 4.23 and 4.24 respectively.

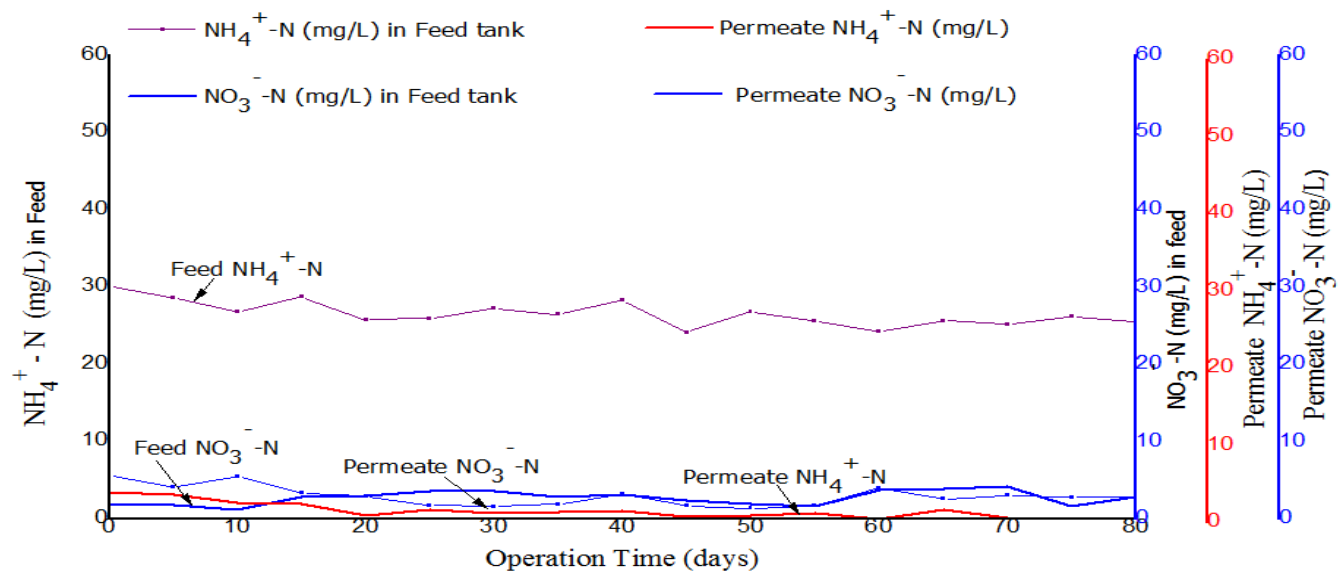


Figure 4.23: Comparison of NH₄⁺ -N and NO₃⁻ -N in the feed and in permeate for the PES module

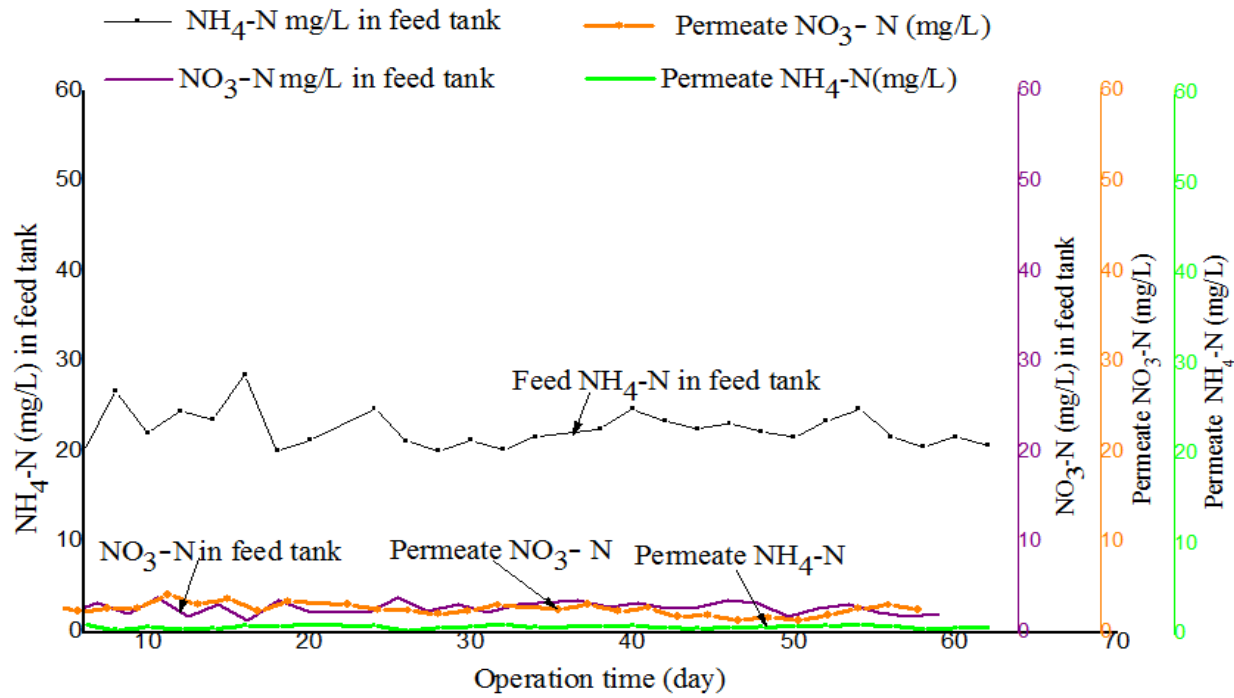


Figure 4.24: Comparison of $\text{NH}_4^+ \text{-N}$ and $\text{NO}_3^- \text{-N}$ in the feed and in permeate for the PBM-coated module

As presented in Figure 4.23 and 4.24, the concentration of $\text{NH}_4^+\text{-N}$ and $\text{NO}_3^-\text{-N}$ in the feed for the two systems was in the range of 24.2 to 28.7mg/L and 1.8 to 6.1mg/L respectively for PES module and from 22.3 to 27.1mg/L and 1.5 to 5.9mg/L respectively for the PBM module. The concentrations were lowered after treatment, with permeate $\text{NO}_3^-\text{-N}$ obtained in the range of 1.8mg/L – 3.3 mg/L illustrated in Figure 4.23 (blue line) for the PES module and 0.5mg/L- 2.9mg/L (orange line) illustrated in Figure 4.24 for the PBM module respectively. Permeate $\text{NH}_4^+\text{-N}$ was lowered to 0.9mg/L – 4.1mg/L after day 20 for PES module illustrated in Figure 4.23 (red line) and 0.2mg/L- 0.6mg/L for PBM module illustrated in Figure 4.23 (green line) respectively. The two tested membranes demonstrated good removal efficiency for $\text{NO}_3^-\text{-N}$ in permeate and was mainly within an acceptable range of 5 to 30mg/L as per the WHO guidelines for wastewater reuse for irrigation (WHO., 2006). Further, the PBM membrane had higher performance with average percentage removal efficiency for nitrogenous compounds in the range of $88\pm 1\%$ as compared to $85\pm 2\%$ observed with the PES membrane which might be due to longer HRT.

Table 4.14: Comparison of $\text{NH}_4^+\text{-N}$ and $\text{NO}_3^-\text{-N}$ in permeate for PES module and PBM module (One-way, paired t-test, $n=0.05$)

Membrane module	Parameter	Mean and STDEV	t-test	
			t _{calculated}	t _{critical}
PES	$\text{NH}_4^+\text{-N}$ (mg/L)	3.9±1.8	3.2	2.78
PBM		0.6±0.2		
PES	$\text{NO}_3^-\text{-N}$ (mg/L)	3.3±1.2	5.44	2.78
PBM		0.9±0.5		

A comparison of the performance of the two tested modules showed a significant difference in the mean values for $\text{NH}_4^+\text{-N}$ and $\text{NO}_3^-\text{-N}$ in permeate for PES and PBM modules with ($t_{\text{calculated}} > t_{\text{critical}}$) for paired T-test (at 95 % confidence level) as illustrated in Table 4.14. The better performance of the PBM module was attributed to longer HRT. Longer HRT allows the bacteria in the reactor to acclimate easily to the reactor conditions thus improve biodegradation rates.

4.4.2.6 Comparison of phosphates removal in permeate using PES and PBM membrane module

The result for reduction of phosphate ($\text{PO}_4^{3-}\text{-P}$) in the treated effluent showed improved performance for the PBM module with the mean concentration of $\text{PO}_4^{3-}\text{-P}$ varying between $1.9\pm 0.1\text{mg/L}$ relative to $3.5\pm 0.4\text{mg/L}$ observed with PES membrane. The concentrations for both were within the acceptable range of $<5\text{mg/L}$ as recommended by WHO guidelines for wastewater reuse for irrigation (WHO., 2006). These results are presented in Figure 4.25.

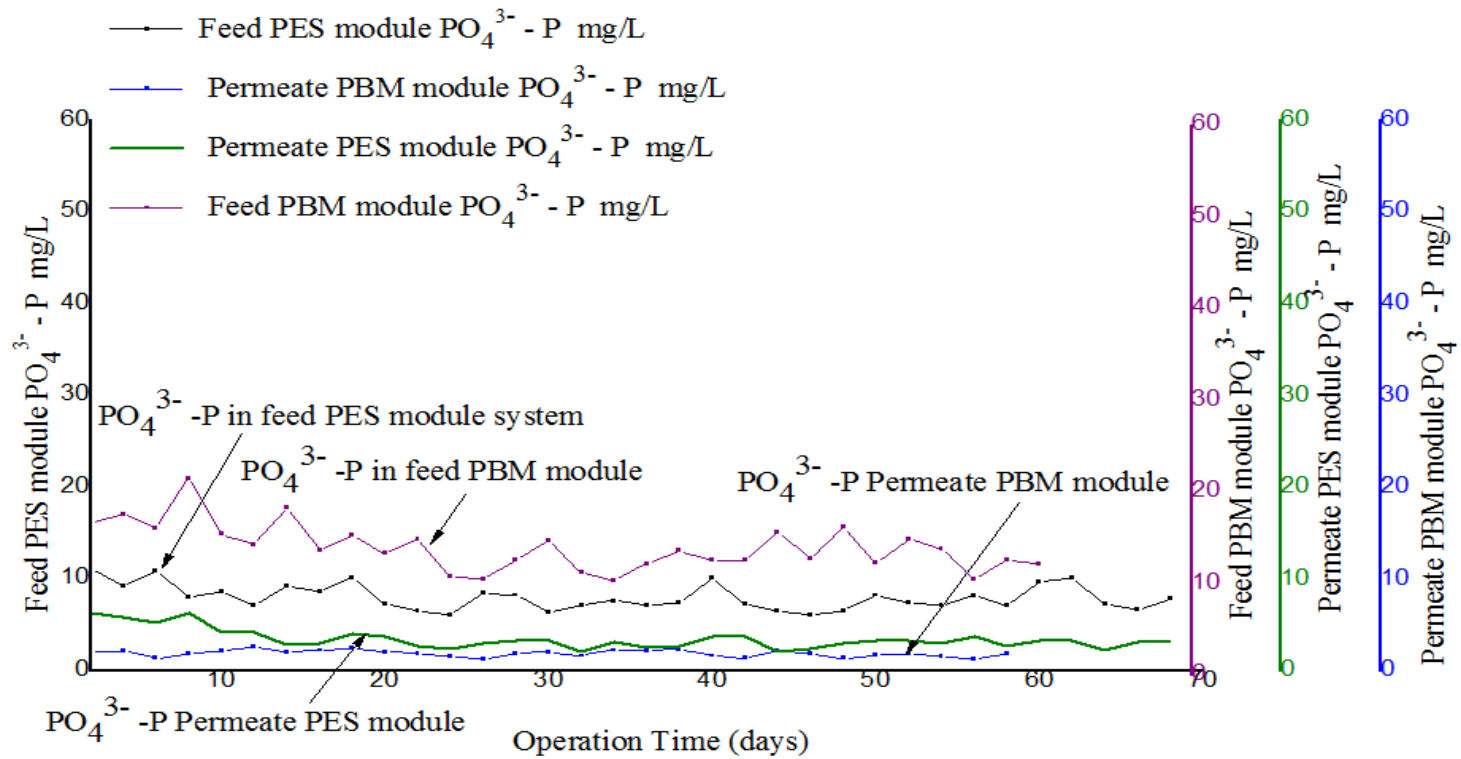


Figure 4.25: Comparison of PO_4^{3-} -P concentration in the feed and in permeate for PES and PBM-coated membrane modules

As illustrated in Figure 4.25, both systems were operated separately with $\text{PO}_4^{3-}\text{-P}$ concentration in feed varying between 6.4mg/L to 11.5mg/L illustrated by the (black line) for the PES module and from 10.3mg/L to 21.4mg/L (purple line) for the PBM module respectively. The level of $\text{PO}_4^{3-}\text{-P}$ in permeate was lowered to a range of 1.3mg/L to 2.6mg/L for PBM module (blue line) and 1.8mg/L to 5.0mg/L (green line) for PES module. The results showed good performance for both modules with permeate $\text{PO}_4^{3-}\text{-P}$ obtained within an acceptable range of $\leq 5\text{mg/L}$ as per the WHO guidelines for wastewater reuse for irrigation (WHO, 2006). The two tested modules had a $\text{PO}_4^{3-}\text{-P}$ percentage removal efficiency of $69\pm 3\%$ for the PES module and $84\pm 1\%$ for the PBM module. The higher removal efficiency observed with the PBM module might be due to long HRT as demonstrated in Figure 4.22.

4.5 Cost-benefit analysis for a containerized MBR system

The cost analysis for a small-scale MBR containerized system with a flow capacity of $10\text{m}^3/\text{d}$ and a lifetime of 25 years was obtained. These results are presented in the following section using tables and equations.

4.5.1 Calculation of CAPEX

The capital expenditure (CAPEX) for the MBR components and equipment was obtained and recorded as presented in Table 4.15.

Table 4.15: Total cost for MBR components and equipment

Energy consuming components	Description/ Quantity	Unit price	Total price ksh.
Permeate pump	1	22800	22800
MBR feed pump	1	38000	38000
Recirculation pump	1	8000	8000
Blower aeration	1	34200	34200
Blower membrane module	1	28500	28500
Stirrer		14820	14820
Sub total			146,262
Tanks	Quantity	Unit price	Total price ksh.
Denitrification tank	1000 L	6500	6500
Nitrification/ filtration tank	3000 L	12000	12000
Permeate collection tank	3000 L	12000	12000
Feed tank	3000 L	12000	12000
Sub total			42,408
Sensors	Quantity	Unit price	Total price ksh.
Dissolved oxygen sensor	1	57000	57,000
Pressure sensor permeate line	1	39900	39,900
Float switch intake tank/nitrification tank /permeate tank	3	1710	5,130
Volume flow sensor permeate line	1	5742	5,742
Sub total			107,772
Infrastructure and other components	Quantity	Unit price	Total price ksh.
Tubes and pipes	50m	600	30,000
Connectors	20	500	10,000
Drain valves	4	1500	6,000
Sampling valve for nitrification tank, and permeate tank	2	1500	3,000
Pre-filter (1mm mesh size)	1	34200	34,200
Electronic installation (fuses, residual current device (RCD), cables)	1	14000	14,000
Membrane Module	1 with flow capacity of 10m ³ per day	171000	171,000
Sub total			268,200
Total			564,642

Where components and equipment used are priced according to the supplier information provided by the various Companies

The capital cost (expenditure) was 565,711ksh. This is presented in equation 31

$$\text{CAPEX} = \left\{ \frac{564,642\text{ksh} + \left(\frac{171,000 \text{ ksh/m}^2}{20\text{m}^2} \right)}{(8 \text{ years})} \right\} = 565,711\text{ksh} \dots\dots\dots 30$$

The capital expenditure (CAPEX) per unit volume per day for a plant with a life time of 25 years was 6.22ksh/d. This is presented in equation 32

$$\text{CAPEX} = \frac{\{565,711\text{ksh}/10\text{m}^3\}}{25\text{years} \times 364\text{days}} = 6.22 \text{ ksh/m}^3\text{d} \dots\dots\dots 31$$

Total specific energy demand was calculated as illustrated in equation 33.

$$E_{\text{tot}} = \sum (0.8\text{kWh} \times 24\text{h}) / 10\text{m}^3\text{d} = \frac{1.92\text{kWh}}{\text{m}^3\text{d}} \dots\dots\dots 32$$

Specific energy cost obtained was 34.56ksh. This is presented in equation 34.

$$\text{Specific energy cost}(1.92\text{kWh/m}^3\text{d} \times \text{ksh}18) = 34.56\text{ksh} \dots\dots\dots 33$$

Where: 1 kWh = 18KSh.

Assumption was made that there were no energy losses and that all input energy was consumed

4.5.2 Calculation of OPEX

Operational expenditure (OPEX) was 185,329.4ksh. This is presented in equation 35.

$$\begin{aligned} \text{OPEX} &= 60388 + 107 + 8167.5 + 5850 + 60,000 + 169,393 = \\ &185,329.40\text{ksh} \dots \dots \dots 35 \end{aligned}$$

The operational expenditure (OPEX) per unit volume per day for a plant with a life time of 25 years was 2.03ksh/m³d⁻¹. This is presented in equation 36.

$$\text{OPEX} = \frac{(185,329.4 \text{ ksh}/10\text{m}^3)}{(364 \text{ days} \times 25 \text{ years})} = \frac{2.03\text{ksh}}{\text{m}^3\text{d}} \dots \dots \dots 36$$

The total expenditure (TOTEX) or total input was 82.5ksh/d. This is presented in equation 37.

$$\text{TOTEX} = \text{CAPEX } 10\text{m}^3 \left(\frac{6.22\text{ksh}}{\text{m}^3\text{d}} \right) + \text{OPEX } 10\text{m}^3 \left(\frac{2.03\text{ksh}}{\text{m}^3\text{d}} \right) = 82.5\text{ksh/d} \dots 37$$

374.5.3 Calculation of the total output

Total output obtained was 480ksh/m³d. This is presented in equation 38.

$$\begin{aligned} \text{Total output} &= \text{Treated water (48ksh/m}^3) \times \text{Total volume (10 m}^3/\text{d)} \\ &= 480\text{ksh/d} \dots \dots \dots 38 \end{aligned}$$

- Where 1m³ of treated water cost 48ksh as per the price offered by water service provider

The total cost benefit was 397.5ksh/d. This is presented in equation 39.

$$\text{Total Output (480 ksh/d)} - \text{Total Input (82.5 ksh/d)} = 397.5 \text{ ksh/d} \dots \dots \dots 39$$

Where the approach used is appropriate to small-scale MBRs with a net flow of approximately 10m³/d and with minimal cost for labor and land requirement.

Assuming that 10m³ of clean water produced per day sells for 480ksh (price for potable treated water); it is equated to 100% total output. Therefore, the CAPEX and OPEX for the MBR system were factored and, a benefit of approximately 397.5ksh/d was obtained, which is 82.8% cost-benefit per m³ of treated water. According to the author, the cost of treated water may be high for small volumes but significantly reduced with increasing volume for real-field industrial scale (Saadia *et al.*, 2015). It was evident despite the higher CAPEX required for installation and operation, the MBR system is economical over time as it allows reuse of high quality treated effluent in comparison to the cost of potable treated water obtained with no provision for reuse.

4.5.4 Comparative analysis for MBR, activated sludge process (ASP) and wastewater stabilization ponds (WSP)

A comparative analysis conducted with basic cost model equations showed high operational expenditure (OPEX) for MBR systems relative to activated sludge process (ASP) and wastewater stabilization ponds (WSP). However, capital expenditure (CAPEX) was dependent on the size of the treatment plant. These results are presented in Figures 4.26 and 4.27 respectively.

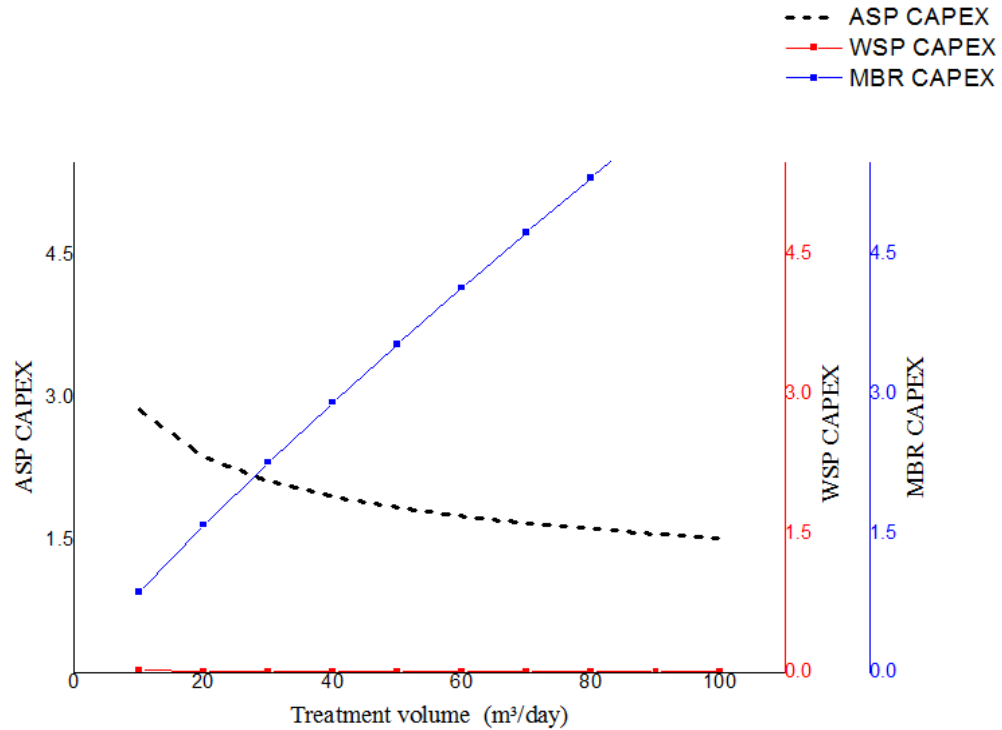


Figure 4.26: Correlation of CAPEX for ASP, WSP and MBR treatment systems with similar flow capacity

As can be seen in Figure 4.26, the MBR systems showed high capital expenditure per unit product water in comparison to ASP and WSP. Further, CAPEX for WSP was relatively low in comparison to ASP and MBR systems. However, it was demonstrated that small-scale MBR containerized systems with volume flow capacity within the range of $10\text{m}^3\text{d}^{-1}$ to $30\text{m}^3\text{d}^{-1}$ have lower CAPEX compared to ASP systems of similar size. This was expected as capital investment for ASP systems is driven high by the cost of land where huge areas of land are needed and site redesign requirements. Therefore, small ASP systems have high capital expenditure, with a low flow capacity. However, a decrease in cost per unit product water is expected with increasing treatment volume. The small-scale MBR containerized systems can be installed without construction or site redesign requirements that make the investment costs lower. The capital expenditure for these systems is therefore dependent on the size of the MBR equipment as smaller systems cost less compared to large systems with higher flow capacity.

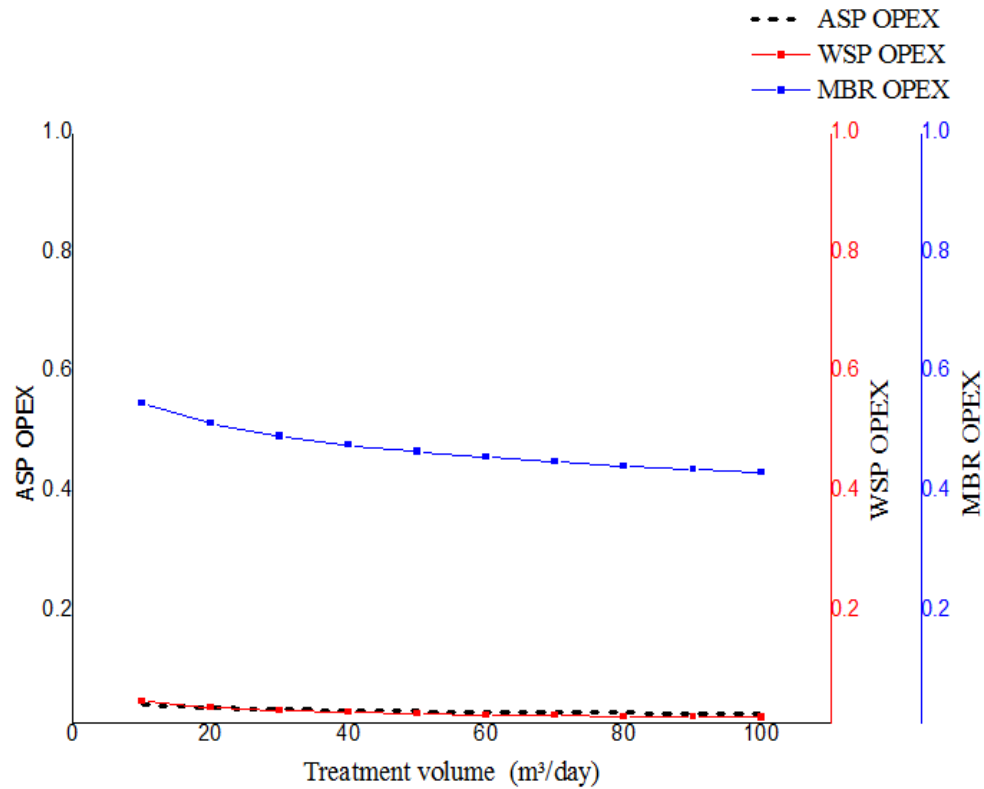


Figure 4.27: Correlation of OPEX for ASP, WS and MBR treatment systems with similar flow capacity (treatment volume)

As illustrated in Figure 4.27, a comparison of OPEX for the three treatment systems showed low OPEX for ASP and WSP systems in comparison to the MBR system. The high OPEX for MBR can be explained by the high energy demand requirement for operation unlike ASP and WSP treatment systems that have low energy requirements. However, as illustrates in Figure 4.27, all the three systems, showed a decrease in OPEX as a function of size and flow capacity. This was largely attributed to the higher returns for unit product water. Further, despite the higher operational energy demand required for MBR systems, it encourages reuse of highly clarified effluent for irrigation, washing and for other purposes thus making the system economical and a reliable source for clean water.

CHAPTER FIVE

CONCLUSIONS AND RECOMMENDATIONS

5.1 Conclusions

The fish processing wastewater used for the MBR lab-scale experiments was of higher strength with respect to high organic load with COD varying between 2349-509mg/L, thus responsible for causing fouling on the surface of the PES membranes.

An optimized process for MBR system was achieved using PES commercial membranes, with over 67%, 81% and 96% removal efficiency for phosphates, N-compounds and COD respectively. The two studied UF/PES membrane modules showed good performance with removal of COD, $\text{NH}_4^+\text{-N}$, $\text{NO}_3^-\text{-N}$, and $\text{PO}_4^{3-}\text{-P}$ within the acceptable range (WHO., 2006) However, the membranes showed significant fouling problem that caused a decrease in Water Permeability (WP) with mean reduction varying between 101 ± 27 to $21\pm 14\text{L/m}^2\text{ h*bar}$ which is a significantly difference where ($t_{\text{calculated}} > t_{\text{critical}}$) for paired T-test (at 95 % confidence level).

The two tested commercial UF/PES membrane modules had levels of COD, nitrogenous compounds, and soluble phosphates in permeate within an acceptable range of < 100 mg/L, 5 to 30 mg/L and ≤ 5 mg/L respectively as per the WHO guidelines for wastewater reuse for irrigation.

The two tested Microdyn-Nadir and CUBE Mini module showed fouling problem with mean WP reduction rate varying between 61 ± 10 to $24\pm 4\text{L/m}^2\text{ h*bar}$ which is a significantly difference with ($t_{\text{calculated}} > t_{\text{critical}}$) for paired T-test (at 95 % confidence level). A change of membrane module design therefore did not result in improved resistance to fouling.

A novel low-fouling membrane was successfully developed through a successful coating process as was demonstrated using IR spectrums that confirmed the presence of PBM coating on the coated membranes. The modified PBM membrane showed low contact angles (CA) with a reduction change of about 48% thus indicating that hydrophilic property was achieved.

The PBM coated membranes showed improved ability for foulant rejection and improved resistance to fouling attributed to the hydrophilic property of the modified PBM membrane. The probability of operating the PBM module at higher flux (above 350mbar) than the commercial one without causing fouling to the membrane pores was unveiled. This is a key point towards obtaining a technological breakthrough for the implementation of the MBR technology for use by fish industries in Kenya.

Further PBM-coated membrane module showed better performance for the removal of COD, nitrogenous compounds, and phosphates. with mean values for COD, $\text{NH}_4^+\text{-N}$, NO_3^- -N, and $\text{PO}_4^{3-}\text{-P}$ in permeate obtained as (4.42>2.78), (3.20>2.78), (5.4> 2.78) and (6.12> 2.78) where ($t_{\text{observed}} > t_{\text{critical}}$) respectively for paired T-test (at 95 % confidence level). We are therefore at a 95% confidence level convinced that the PBM module has better performance than the PES module, and thus reject the null hypothesis.

From the cost analysis calculations, a cost-benefit of about 82.8% per m^3 of treated water was realized for the a containerized MBR system with a flow capacity of $10\text{m}^3/\text{d}$. These findings confirmed the use of MBR is economical and thus reject the null hypothesis.

The results from the correlation cost curves demonstrated that CAPEX for MBR treatment systems with flow capacity between $10\text{m}^3/\text{d}$ and $30\text{m}^3/\text{d}$ are cost-effective in comparison to ASP whose capital cost is driven high by the cost of land procurement and construction.

Further, it was demonstrated that small-scale containerized systems could be an economic solution for small industries (such as fish processing industries) in the urban centers in

Kenya compared to WSP's and ASP that require huge capital investment driven high by the cost of land and construction.

5.2 Recommendations

The following recommendations were made from this study;

1. The MBR technique can be adopted for treatment of high strength wastewater by fish processing industries in urban centers thus ensure continued operation with minimal pollution and hygiene problems.
2. The MBR technique is recommended as a potentially economical option for treatment and reuse of fish processing wastewater by industries operating in the urban centers where land is scarce and expensive

5.2.1 Areas of further research

From the findings of this study, it might be expected to operate the PBM membrane module at higher flux (above 350mbar) than the commercial one without having achieved critical flux. However, this needs to be further studied.

REFERENCES

- Aloyce, W., Mayo, M., & Joel, N. (2018). Modeling nitrogen transformation and removal in mara river basin wetlands upstream of Lake Victoria. *Physics and Chemistry of the Earth, Parts A/B/C*, 105, 136-146.
- Alkudhiri, A., & Hilal, N. (2018). 3 - Membrane distillation Principles, applications, configurations, design, and implementation. *Emerging Technologies for Sustainable Desalination Handbook*, 55-106.
- Amir, R., Jaleh, M., & Vicki, C. (2011). The effect of chemical and mechanical modification of TiO₂ nanoparticles on the surface chemistry, structure and fouling performance of PES ultrafiltration membranes. *Journal of Membrane science*, 378(2), 73-84.
- Amanmyrat, A., Maged, F., Dorian, A., & Aleksander, G. (2019). Materials and Applications for Low-Cost Ceramic Membranes. *Membranes*, 9(9), 105.
- APHA. (2017). American Public Health Association American Water Works Association, & Water Environment Federation. (22 ed.). *Standard methods for the examination of water and wastewater*, Washington DC,
- Awangea, J., Saleem, A., Sukhadiya, R., Kexiang, H., and Oumab, Y. (2019). Physical dynamics of Lake Victoria over the past 34 years (1984–2018): Is the lake dying? *Science of the Total Environment*, 658(25), 199-218.
- Balster, J. (2015). Spiral Wound Membrane Module. In E. Drioli & L. Giorno (Eds.), *Encyclopedia of Membranes* (pp. 1-3). Berlin, Heidelberg: Springer Berlin Heidelberg.

- Bing, W., & Anthony, G. (2012). Microbial Relevant Fouling in Membrane Bioreactors, Influencing factors, Characterization and Fouling Control. *Membrane Basel*, 2(3), 565-584.
- BioNexGen, (2010). *www.bionexgen.eu*. accessed March 2, 2020.
- Bokhary, A., Tikka, A., Leitch, M., and Liao, B. (2018). Membrane Fouling Prevention and Control Strategies in Pulp and Paper Industry Applications: A Review. *Journal of Mebrane Science*, 4, 181-197.
- Bouhadjar, S., Deowan, S., Galiano, F., Figoli, A., Hoinkis, J., & Djennad, M. (2016). Performance of commercial membranes in a sidestream and submerged membrane bioreactor for model textile wastewater treatment. *Desalination Water Treatment*, 57, 5275–5285.
- Candau, F., & Ottewill, R. H. (2012). An introduction to polymer colloids *Springer Science & Business Media*, 303, 126-288. doi:10.1007/978-94-009-0521-4.
- Carolyne, N., Paul, N., Benson, K., & James, R. (2020). Performance of a Modified Trickling Filter Packed with Different Substrates in Polishing Aquaculture Wastewater. *Journal of Environmental Science and Engineering*, 9, 1-11.
- Charles, K., Simon, M., Zachary, M., Shadrach, S., & Josephine, K. (2011). The Impact of Land Use Activities on Vegetation Cover and Water Quality in the Lake Victoria Watershed. *Environmental Engineering Journal*, 4, 66-77.
- Charles, C., & Victor, M. (2014). Review of Estimation of Pollution Load to Lake Victoria. *Journal of Environment and Earth Science*, 4(1), 113-120.
- Cheruiyot, E. K., Mito, C., Menenti, M., Gorte, B., Koenders, R., & Akdim, N. (2014). Evaluating MERIS-based aquatic vegetation mapping in Lake Victoria. *Remote Sensing*, 6(8), 7762-7782.

- Corominas, L., Foley, J., Guest, J., Hospido, A., Larsen, H., Moreraa, S., & Shaw, A. (2013). Life cycle assessment applied to wastewater treatment: State of the art. *Water Research*, 47(15), 5480-5492.
- Dauglas, W., Hongtao, W., & Fengting, L. (2014). Impacts of population growth and economic development on water quality of a lake: Case study of Lake Victoria Kenya water. *Environmental Science and Pollution Research*, 21, 5737–5746.
- David, M., Sudip, C., Emily, W., Megan, H., Christopher, B., Savvina, L., Leila, K., Anne, M., Andrea, A., Abbas, G., Lokesh, P., Shane, A., Stefano, C., Chad, V., Hassan, A., & John, H. (2016). A review of polymeric membranes and processes for potable water reuse. *Program polymeric science*, 10(81), 209-237. doi: 10.1016/j.progpolymsci.2018.01.004.
- Deowan, S., Galiano, F., Hoinkis, J., Figoli, A., & Drioli, E. (2013). Submerged membrane bioreactor (SMBR) for treatment of textile dye Wastewatertowards developing novel MBR process. *APCBEE Procedia*, 5, 259-264.
- Deowan S., A., Francesco, G., Jan, H., Daniel, J., Sacide, A., Bartolo, G., & Alberto, F. (2016). Novel low-fouling membrane bioreactor (MBR) for industrial wastewater treatment. *Journal of Membrane science*, 510, 524-532.
- Dipu, S., Rita, S., & Rakesh, C. (2015). Performance Evaluation of Prevailing Biological Wastewater Treatment Systems in West Bengal, India. *Applied Ecology and Environmental Sciences*, 3(1), 1-4. doi: 10.12691/aees-3-1-1
- Eckenfelder, J., Wesley, C., & Cleary, J., (2014). Activated Sludge Technologies for Treating Industrial Wastewaters *DEStech Publications*, 1, 234.
- Ephraim, G., Talha, A., Julian, A., Kyra, H., Francesco, G., Alberto, F., Bartolo, G., Raffaella, M., Pauline, N., Francis, A., Robert, Otim., Bwambale, M., Susan, A., Daniel, L., Mutambala, M. and Jan, H. (2020). Membrane Bioreactor (MBR)

treated domestic wastewater for sustainable reuse in the Lake Victoria region. *Integrated Environmental Assessment and Management* 00, 1-13.

EMCA. (1999). The Environmental Management And Co-Ordination Act, 1999.

EMCA. (Ed.). (2006). *Environmental Management and Coordination Act (Water Quality) regulations, 2006 Kenya*.

Espinoza, S., Arbeitman, C., Clochard, M., & Grasselli, M. (2014). Functionalization of nanochannels by radio-induced grafting polymerization on PET track-etched membranes. *Radiation Physics and Chemistry*, 94, 72-75.

Fábio, H., & Liliana, P. (2019). Reuse alternatives for effluents from the fish processing industry through multi-criteria analysis. *Journal of Cleaner Production*, 227(1), 336-345. doi: <https://doi.org/10.1016/j.jclepro.2019.04.110>.

Figoli, A., Hoinkis, J., Gabriele, B., De Luca, G., Galiano, F., & Deowan, S. (2014). Bicontinuous Microemulsion Polymerized Coating for Water Treatment. *Patent Application, PCT/EP2014/070603* WO2014/EP070603.

Francesco, G., Stefan, A., Xiaoyun, Y., Rohit, K., Raffaella, M., & Efrem, C. (2018). UV-LED induced bicontinuous microemulsions polymerisation for surface modification of commercial membranes. Enhancing the antifouling properties. *Separation and Purification Technology*, 194, 149-160.

Galiano, F., Figoli, A., Deowan, S., Johnson, D., De Luca, G., Mankuso, R., & Gabriele, B. (2015). A step forward to a more efficient waste water treatment by membrane surface modification via polymerizable biocontinuous microemulsion. *Journal of Membrane Science*, 482, 103-114.

Galiano, F., Schmidt, S., Ye, X., & Kumar, R. (2018). Innovative UV-LED bicontinuous microemulsions polymerisation for surface modification of commercial

membranes- Enhancing the antifouling properties. *Separation and Purification Technology*, 194(3), 149-160.

Geoffrey, S. (2015). The treatment of brewery wastewater for reuse by integration of coagulation/flocculation and sedimentation with carbon nanotubes ‘sandwiched’ in a granular filter bed. *Journal of Industrial and Engineering Chemistry*, 21(25), 1277-1285

Gichuru, N., Nyamweya, C., Owili, M., Mboya, D., & Robert, W. (2017). Poor management of Lake Victoria fisheries (Kenya); a threat to sustainable fish supplies. *Nature and Faune Journal*, 32(2), 38-42.

Gidudu, A., Mugo, R., Letaru, L., Wanjohi, J., Nakibule, R., Adams, E., Flores, A., Page, B., & Okello, W. (2018). Evaluation of satellite retrievals of water quality parameters for Lake Victoria in East Africa. *African Journal of Aquatic Science*, 2, 141-151.

Gkotsis, P., Batsari, E., Peleka, E., Tolkou, A., & Zouboulis, A. (2017). Fouling control in a lab-scale MBR system: Comparison of several commercially applied coagulants. *Journal of Environmental Management*, 203, 838-846.

Goyal, A., & Ananthkrishnan, R. (2013). Biogas Production from a mixture of WaterHyacinth, Water Chestnut and Cow Dung. *International Journal of Science, Engineering and Technology Research (IJSETR)*, 2, 35-37.

Guirgis, A., Gay-de-Montella, R., & Faiz, R. (2015). Treatment of produced water streams in SAGD processes using tubular ceramic membranes. *Desalination*, 358, 27-32.

Halis, S., Murthy, K., Jae-Bom, O., Mark, B., & Eakalak, K. (2013). Bioavailable and biodegradable dissolved organic nitrogen in activated sludge and trickling filter wastewater treatment plants. *Water Research*, 47, 3201-3210.

- Hao, L., Liss, S., & Liao, B. (2016). Influence of COD:N ratio on sludge properties and their role in membrane fouling of a submerged membrane bioreactor. *Water Resources*, 89, 132-141.
- Hong, A., Tran, D., & Hung, D. (2017). Surface photochemical graft polymerization of acrylic acid onto polyamide thin film composite membranes. *Journal of Applied Polymer Science*, 134(5), 1- 9.
- Hongtao, W., Tao, W., Bingru, Z., Fengting, L., Brahima, T., Isaiah, B., Thomas, C., Mohamed, A., & Mahesh, P. (2014). Water and Wastewater Treatment in Africa, Current Practices and Challenges. *Soil, Air, Water*, 42(8), 1029-1035.
- Ibrahim, O., Paul, N., & Jared, N. (2015). Effects of Occupational Safety and Health Management Practices on Work Environment in the Water Service Industry within Kisumu County-Kenya. *International Journal of Science and Research (IJSR)*, 6(5), 566-571.
- Iffat, N., Devendra, P., Sadia, M., & Naeem, A. (2015). Assessment of biological trickling filter systems with various packing materials for improved wastewater treatment. *36*, 424-434
- Inne, V., Nicole, P., & Wim, T. (2018). Modelling the water balance of Lake Victoria (East Africa) *Hydrology and Earth System Science*, 22(10), 5509–5525.
- Iorhemen, O. T., Hamza, R. A., & Tay, J. H. (2016). Membrane bioreactor (MBR) technology for wastewater treatment and reclamation: membrane fouling. *Membranes*, 6(2), 33..
- Jane, M., Ephraim, G., Paul, M., Robert., K., Francesco, G., Raffaella, M., Bartolo, G.,Alberto, F., and Jan, H. (2020). Application of Novel Low-Fouling Membranes for Fish Processing WastewaterTreatment and Comparison to PES Commercial

- Membranes in a Lab Scale Membrane Bioreactor. *International Journal of Water and Wastewater Treatment*, 6, 1-12.
- Judd, S., Lo, C., & McAdam, E. (2015). The cost of a small membrane bioreactor. *Water Science and Technology*, 72(10), 1739-1746. doi: 10.2166/wst.2015.394.
- Kabenge, M., Wang, H., & Li, F. (2016). Urban eutrophication and its spurring conditions in the Murchison Bay of Lake Victoria. *Environmental Science and Pollution Research Interntional*, 23(1), 234-241. doi: 10.1007/s11356-015-5675-0
- Kevin, O., Richard, O., Murithi, J., Phillip, O., Raburu, A., Alfred, A., Rodrick, K., Erick, O., Jonathan, M., & Ted, L. (2015). The challenges of management: Recent experiences in implementing fisheries co-management in Lake Victoria, Kenya. *Lakes and Reservoirs, Science, policy and Management for Surstainable Use*, 20(3), 139-154.
- Khalid, K., & Kara, L. (2014). Sunlight mediated inactivation mechanisms of *Enterococcus faecalis* and *Escherichia coli* in clear water versus waste stabilization pond water. *Water Research*, 50, 307-317.
- Kim, J., Hamza, K., Morsi, M., Nassef, A., Metwalli, S., & Saitou, K. (2013). Design Optimization of a Solar-Powered Reverse Osmosis Desalination System for Small Communities. In *ASME 2013 International Design Engineering Technical Conferences and Computers and Information in Engineering*, 3, 1-10.
- Kochkodan, V., Johnson, D., & Hilal, N. (2014). Polymeric membranes: surface modification for minimizing (bio) colloidal fouling. *Advanced Colloid Interface Science*, 206, 116–140
- Kolding, J., Medard, M., Mkumbo, O., & Zwieten, P. (2014). Status, trends and management of the Lake Victoria fisheries. In: *Inland Fisheries Evolution and*

- Management – Case Studies From Four Continents. *Fisheries and Aquaculture*, 579, 1-19.
- Kumar, R., Goswami, L., Pakshirajan, K., & Pugazhenthii, G. (2016). Dairy wastewater treatment using a novel low cost tubular ceramic membrane and membrane fouling mechanism using pore blocking models. *Journal of Water Process Engineering*, 13, 168-175
- Liu, Y., Zhang, X., Ngo, H., Guo, W., Wen, H., Deng, L., & Guo, J. (2018). Specific approach for membrane fouling control and better treatment performance of an anaerobic submerged membrane bioreactor. *Bioresource technology*, 268, 658-664.
- Liumo, R., Shuili, Y., & Jianefeng, L. (2019). Pilot study on the effect of operating parameters on membrane fouling during ultrafiltration of alkali/surfactant/polymer flooding wastewater: optimiation and modeling. *Royal Society of chemistry*, 9, 11111-11122.
- Lo, C., McAdam, E., & Judd, S. (2015). The cost of a small membrane bioreactor. *Water Science and Technolology*, 72(10), 1739–1746.
- Luong, T., Schmidt, S., Deowan, S., Hoinkis, J., & Figoli, A. (2016). Membrane bioreactor and promising application for textile industry in Vietnam. *Procedia CIRP*, 40, 419-424.
- LVBC. (2017). Lake Victoria Basin Commission: Atlas of Our Changing Environment. *Lake Victoria Basin Commission and GRID-Arendal, Kisumu and Arendal*. <https://www.lvbcom.org>, 12-108.
- LVEMP. (2017). Lake Victoria Environment Management Project Phase 2 (LVEMP II) R. o. K. 2017 (Ed.) *Kisumu County Integrated Development Plan. Rehabilitation of Kisumu Sewage Treatment Plan*. info@lvemp2kenya.org, 25-45.

- Ma, W., Rahaman, M., & Therien-Aubin, H. (2015). Controlling biofouling of reverse osmosis membranes through surface modification via grafting patterned polymer brushes. *Journal of Water Reuse and Desalination*, 5(3), 326-334.
- Malik, M. A., Wani, M. Y., & Hashim, M. A. (2012). Microemulsion method: A novel route to synthesize organic and inorganic nanomaterials. *Arab J of Chemistry*, 5, 397-417.
- Mancuso, R., Amuso, R, Biagio, A., Grasso, G., Rago, V., Galiano, F., Figoli, A, De Luca G, Hoinkis, J, & Gabriele, B (2017). Synthesis and Antibacterial Activity of Polymerizable Acryloyloxyalkyltriethyl Ammonium Salts. *Chem Plus Chem*, 82, 1235 – 1244.
- Mara, D. (2013). Domestic wastewater treatment in developing countries, 1-293.
- Martin, K., Hongtao, W., & Fengting, L. (2016). Urban eutrophication and its spurring conditions in the Murchison Bay of Lake Victoria. *Environmental Science and Pollution Research*, 23, 234–241.
- Martin-membrane, (2020). www.martin-membrane.de Retrieved February 2, 2020
- Matindi, C., Njogu, P., Kinyua, R., & Nemoto, Y. (2014). Analysis of heavy metal content in water hyacinth (*Eichhornia crassipes*) from Lake Victoria, Kenya. *Proceedings of Sustainable Research and Innovation Conference*, (5), 196-199. ISSN 2079-6226.
- Mayerhöfer, T., Mutschke, H., & Popp, J. (2016). Employing Theories Far beyond Their Limits. The Case of the (Boguer) Beer–Lambert Law. *Chemical Physics and Physical Chemistry*, 17(13), 1948-1955.

- Meena, K., Anwar, K., & Absar, A. (2014). Modified septic tank-anaerobic filter unit as a two-stage onsite domestic wastewater treatment system. *Environmental Technology*, 35(17), 2183-2193
- Mehta, S., & Kaur, G. (2011). Microemulsions: Thermodynamic and Dynamic Properties, Thermodynamics, *In Technology and dynamic properties*, <http://www.intechopen.com/books/thermodynamics/microemulsionsthermodynamic> (Ed.)
- Meléndez-Ortiz, H., Varca, G., Lugão, A., & Bucio, E. (2015). Smart polymers and coatings obtained by ionizing radiation: synthesis and biomedical applications. *Open Journal of Polymer Chemistry*, 5(3), 17.
- Merckmillipore, (2014). www.merckmillipore.com. accessed March 2, 2020.
- Microdyn-Nadir. (2020). www.microdyn-nadir.com. Retrieved February 2, 2020
- Miyoshi, T., Yuasa, K., Ishigami, T., Rajabzadeh, S., Kamio, E., Ohmukai, Y., Saeki, D., Ni, J., & Matsuyama, H. (2015). Effect of membrane polymeric materials on relationship between surface pore size and membrane fouling in membrane bioreactors. *Applied Surface Science*, 330, 351-357.
- Moghimifar, V., Raisi, A., & Aroujalian, A. (2014). Surface modification of polyethersulfone ultrafiltration membranes by corona plasma-assisted coating TiO₂ nanoparticles. *Journal of Membrane Science*, 461, 69-80.
- Mondal, S., & Wickramasinghe, S. (2012). Photo-induced graft polymerization of N-isopropyl acrylamide on thin film composite membrane: Produced water treatment and antifouling properties. *Separation and purification technology*, 90, 231-238.

- Muthukumaran, S., & Baskaran, K. (2013). Organic and nutrient reduction in a fish processing facility a case study. *International Biodeterioration and Biodegradation*, 85, 563-570.
- Nagy, E. (2019). Chapter 2 - Membrane Materials, Structures, and Modules. In E. Nagy (Ed.), *Basic Equations of Mass Transport Through a Membrane Layer 2*, 11-19.
- Neena, S., & LekhaMathai, P. (2013). Physicochemical process for fish processing wastewater. *Journal of Environmental Science*,
- N.E.P. (2013). National Environment Policy. Ministry of Environment, Water and Natural resources R. HIF Building, Upper Hill P.O. BOX 30126 - 00100 Nairobi Website: www.environment.go.ke (Ed.)
- Nitin, K., Kazmi, A., & Starkl, M. (2015). A review on full-scale decentralized wastewater treatment systems: techno-economical approach. *Water Science and Technology*, 71(4), 468-478.
- Njenga, M., Sylvie, M., Johan, J., Van, B., Diederik, P., & Njogu, P. (2013). Performance comparison and economics analysis of waste stabilization ponds and horizontal subsurface flow constructed wetlands treating domestic wastewater: A case study of the Juja sewage treatment works. *Journal of Environmental Management*, 128(15), 220-225.
- Njogu, P., Kinyua, R., John, N., Muthoni, P., & Nemoto, Y. (2014). Biogas production using Water Hyacinth (*Echinoria Crassipes*) as the feedstock for electricity generation in Kenya. *Proceedings of Sustainable Research and Innovation Conference*, 79-81.
- Nobuyuki, S., Tsutomu, O., Takashi, O., Lalit, K., Akiyoshi, O., & Hideki, H. (2007). Economic evaluation of sewage treatment processes in India. *Journal of Environmental Management*, 84, 447-460. doi: 10.1016/j.jenvman.2006.06.019

- Norfamilabinti, C., Yuecun, L., & Glenn, L. (2014). Hollow fiber membrane modules. *Current Opinion in Chemical Engineering*, 4, 18-24.
- Oliver, T., Rania, A., & Joo, H. (2016). Membrane Bioreactor (MBR) Technology for Wastewater Treatment and Reclamation: Membrane Fouling. *Membranes* 6(2), 29-33.
- Pugazhenth, G. (2015). Elaboration of novel tubular ceramic membrane from inexpensive raw materials by extrusion method and its performance in microfiltration of synthetic oily wastewater treatment. *Journal of Membrane Science*, 490, 92-102.
- Qiang, L., Pan, Z., Qu, X., Zhao, Y., Jin, H., Dai, B., & Yang, X. (2013). Understanding the dependence of contact angles of commercially RO membranes on external conditions and surface features. *Desalination and Water Treatment*, 309, 38-45.
- Raffaella, M., Roberta, A., Biagio, A., Giuseppe, G., Vittoria, R., Anna, R., Francesco, G., Alberto, F., Giorgio, L., Jan, H. & Bartolo, G. (2017). Synthesis and Antibacterial Activity of Polymerizable Acryloyloxyalkyltriethyl Ammonium Salts. *ChemPlusChem*, 82, 1235 – 1244.
- Rahayu, S., & Hady, H. (2018). Estimating Environmental Impact Potential of Small Scale Fish Processing Using Life Cycle Assessment. *Journal of Ecological Engineering*, 19(6), 65-74.
- Ramadan, H., & Ponce, V. (2016). Design and Performance of Waste Stabilization Ponds". San Diego State University. Retrieved 2016-10-26. *San Diego State University*, 10, 26-30.
- Retailleau, M., Ibrahim, A., & Allonas, X. (2014). Dual-cure photochemical/thermal polymerization of acrylates: a photoassisted process at low light intensity. *Polymer Chemistry*, 5(22), 6503-6509.

- Robert, G., Anthony, M., Mugassa, S., Frank, K., & Amelia, K. (2009). Nile perch fish processing waste along Lake Victoria in East Africa: Auditing and characterization. *African Journal of Environmental Science and Technology*, 3 (1), 013-020.
- Rodrick, K., Christopher, M., Chrispine, N., Nyamweya, S., Simon, A., Lewis, S., Henry, B., Collins, O., Zachary, O., & Kenneth, W. (2017). Changes in pollution indicators in Lake Victoria, Kenya and their implications for lake and catchment management. *Lakes and Reservoirs, Science, policy and Management for Sustainable Use*, 22(3), 199-214.
- Ronald, L. (Ed.). (2018). *Fixed Biological Surfaces: Wastewater Treatment. The Rotating Biological Contactor* London New York: CRC PressTaylor & Francis Group
- Saadia, I., Shamim, A., Francesco, G., Alberto, F., & Jan, H. (2015). Performance of commercial membranes in a side-stream and submerged membrane bioreactor for model textile wastewater treatment. *Desalination and Water Treatment*, 57(12), 5275-5285.
- Salome, S., & Samwel, M. (2018). Nutrient release from sediments and biological nitrogen fixation: Advancing our understanding of eutrophication sources in Lake Victoria, Tanzania. *Lakes and Reservoirs, Science, policy and Management for Sustainable Use*, 23(4), 312-323.
- Sathishkumar, M., Jayabalan, R., Mun, S., & Yun, S. (2010). Role of bicontinuous microemulsion in the rapid enzymatic hydrolysis of (R,S)-ketoprofen ethyl ester in a micro-reactor. *Bioresource Technology*, 101, 7834-7840.
- Sayer, C., Máiz-Tomé, L., & Darwall, W. (2018). Freshwater biodiversity in the Lake Victoria Basin: Guidance for species conservation, site protection, climate resilience and sustainable livelihoods. *Cambridge, UK and Gland, Switzerland: IUCN*

- Serdarevic, A., Dzibur, A., & Muhibic, T. (2019). Role and Efficiency of MBR Technology for Wastewater Treatment. *Advanced Technologies, Systems, and Applications IV -Proceedings of the International Symposium on Innovative and Interdisciplinary Applications of Advanced Technologies (IAT 2019)*, 83, 229-237.
- Shao, L., Wang, Z., Zhang, Y., Jiang, Z., Liu, Y., & Key, S. (2014). A facile strategy to enhance PVDF ultrafiltration membrane performance via self-polymerized polydopamine followed by hydrolysis of ammonium fluotitanate. *Journal of Membrane Science*, 461, 10-21.
- Siddiqui, A., Farhat, N., Bucs, S., Linares, R., Piciooreanu, C., Kruithof, J., & Vrouwenvelder, J., 91, 55-67. (2016). Development and characterization of 3D-printed feed spacers for spiral wound membrane systems. *Water research*, 91, 55-67.
- Tan, V., Schmidt, S., Deowanb, S., Hoinkisb, J., Figolic, A., and Galiano, F. (2016). Membrane bioreactor and promising application for textile industry in Vietnam. *Science Direct* 40, 419-424.
- Thang, N., Felicity, A., & Linhua, F. (2012). Biofouling of Water Treatment Membranes: A Review of the Underlying Causes, Monitoring Techniques and Control Measures *Membrane* 2, 804-840.
- Tang, Long-Cheng & Zhao, Li & Guan, Li Zhi. (2017). *7 Graphene/Polymer Composite Materials: Processing, Properties and Applications*.
- Tim, M., Edward, H., & Joshua, E. (2015). Managing fisheries for human and food security. *Fish and Fisheries*, 16, 78-103.
- Ugya, A., & Fidelis, O. (2016). Convectonal and Advanced Method of Industrial Wastewater Treatment. In T. S. M. Ugya A.Y, Imam T.S, *Emerging Trends in the Remediation of Pollution* (Ed.) *Lulu Publishers*. ISBN: 9781365529177.

- Vanysacker, L., Declerck, P., Bilad, M., & Vankelecom, I. (2014). Biofouling on microfiltration membranes in MBRs: Role of membrane type and microbial community. *Journal of Membrane Science*, 453, 394–401.
- Vicinaqua. (2017). www.vicinaqua.eu (Design and feasibility study for an upscaled system). Retrieved August 20, 2020
- Vinay, K., Sahoo, B., Anwar, K., Kazmi, A., Ahmad, Z., & Chopra, A. (2010). Fate of cliforms and pathogenic parasite in four full-scale sewage treatment systems in India. *Environmental Monitoring and Assessment*, 181(1-4), 123-125.
- Wang, H., Pan, Q., & Rempel, G. (2011). Micellar nucleation differential microemulsion polymerization. *European polymer journal*, 47(5), 973-980. doi: 10.1016/j.eurpolymj.2010.11.009.
- WHO. (2006). WHO guidelines for the safe use of wastewater, excreta and greywater / World Health Organization (Vol. 2). 20 Avenue Appia, 1211 Geneva 27, Switzerland.
- Yanda, P. (2015). Climate Change Implications for Management and Use of Agricultural Biodiversity Resources in Africa. *Environment and Ecology Research*, 3(2), 35-43.
- Young, T., Smoot, S., Peeters, J., & Côté, P. (2013). When does building an MBR make sense? How variations of local construction and operating cost parameters impact overall project economics. *Procedia Water Environment Federation*, 8, 6354-6365.
- Yuan, L., Wang, Y., Pan, M., Rempel, G., & Pan, Q. (2013). Synthesis of poly (methyl methacrylate) nanoparticles via differential microemulsion polymerization. *European polymer journal*, 49(1), 41-48

Zhang, Y., Zhang, M., Fangyuan, W., Huachang, H., Aijun, W., Juan, W., Xuexiang, W., & Hongjun, L. (2014). Membrane fouling in a submerged membrane bioreactor: Effect of pH and its implications. *Bioresource Technology*, *152*, 7-14.

Zhu, Z., Wang, Y., Liu, Q., & Xie, J. (2012). Influence of Bond Numbers on Behaviors of Liquid Drops Deposited onto Solid Substrates. *Microgravity Science and Technology*, *24*, 181-188.

APPENDICES

Appendix I: Water Quality at The Vicinaqua Pilot Plant

Table 1: Wastewater quality wastewater at VicInAqua pilot site

Measured parameters	Mean values for water quality in 2017				
	February	March	April	May	June
COD(mg/L)	254±5.0	396±4.8	380±4.9	258±5.0	223±4.9
NH ₄ ⁺ -N (mg/l)	19.9.8±0.1	34.2±0.2	18.4±0.3	39.2±0.5	10.2±0.1
NO ₃ ⁻ -N (mg/l)	3.4±0.1	BDL	2.0±0.2	1.7±0.2	5.7±0.3
P-PO ₄ ⁻³ (mg/l)	12.2±0.3	10.8±0.5	22.5±0.1	10.3±0.1	12.3±0.1
pH	6.8±0.5	7.4±0.5	6.9±0.5	7.0±0.5	7.2±0.5
Conductivity (µS/cm)	464±0.2	759±0.4	433±0.5	456±0.2	428±0.3

Where: BDL = Below detection limit

Table 2: Wastewater quality at VicInAqua pilot site

Measured parameters	Mean values for water quality in 2018				
	January	February	March	April	May
COD(mg/L)	221±4.9	177±5.0	252±4.9	532±4.8	309±4.9
NH ₄ ⁺ -N (mg/l)	6.9±0.3	6.0±0.3	1.5±0.3	2.2±0.5	6.5±0.1
NO ₃ ⁻ -N (mg/l)	2.7±0.1	2.9±0.7	18.0±0.2	10.7±0.2	13.0±0.2
P-PO ₄ ⁻³ (mg/l)	6.1±0.2	2.8±0.9	12.5±0.7	16.3±0.1	6.5±0.2
pH	7.5±0.5	7.6±0.5	7.3±0.5	7.5±0.5	7.1±0.5
Conductivity (µS/cm)	585±0.5	606±0.9	722±0.5	556±0.4	518±0.5

Where: BDL = Below detection limit

Table 3: Wastewater quality at VicInAqua pilot site

Measured parameters	Mean values for water quality in 2018-2019				
	December	January	February	March	April
COD(mg/L)	239±4.9	438±5.0	380±4.9	283±4.9	323±5.0
NH ₄ ⁺ -N (mg/l)	21.8±0.3	36.0±0.3	18.4±0.3	9.2±0.5	46.5±0.1
NO ₃ ⁻ -N (mg/l)	6.7±0.4	0.9±0.7	2.5±0.3	4.7±0.2	BDL
P-PO ₄ ⁻³ (mg/l)	12.2±0.5	14.1±0.2	12.5±0.7	14.3±0.3	12.3±0.5
pH	7.0±0.5	6.9±0.5	6.8±0.5	7.0±0.5	7.2±0.5
Conductivity (µS/cm)	434±0.2	537±0.5	423±0.1	456±0.6	528±0.5

Mean ± std. deviation, where n=10

Where: BDL = Below detection limit